
UNIVERSIDAD NACIONAL AUTÓNOMA DE MÉXICO

POSGRADO EN CIECIAS DE LA TIERRA

INSTITUTO DE GEOFÍSICA, UNIDAD MICHOACÁN.

# FLUCTUACIÓN DE CAMPO MAGNÉTICO TERRESTRE DURANTE LOS ÚLTIMOS 5 MA EN MÉXICO: ADQUISICIÓN DE NUEVOS DATOS Y MODELACIÓN MATEMÁTICA.

TESIS

QUE PARA OPTAR POR EL GRADO DE:

**DOCTOR EN CIENCIAS DE LA TIERRA**

PRESENTA:

**RAFAEL GARCÍA RUIZ**

TUTOR

DR. AVTO GOGUITCHAISVILI (INSTITUTO DE GEOFÍSICA, UNAM)

CO-TUTOR

DR. F. JAVIER PAVÓN CARRASCO (DEPARTAMENTO DE FÍSICA DE LA TIERRA, UCM)

JURADO

DR. AVTO GOGUITCHAISVILI (INSTITUTO DE GEOFÍSICA, UNAM)

DR. F. JAVIER PAVÓN CARRASCO (DEPARTAMENTO DE FÍSICA DE LA TIERRA, UCM)

DR. LUIS M. ALVA VALDIVIA (INSTITUTO DE GEOFÍSICA, UNAM)

DR. MANUEL CALVO RATHERT (DPTO. DE FÍSICA, UNIVERSIDAD DE BURGOS)

DR. MARIO REBOLLEDO VIEYRA. (CENTRO DE INVESTIGACIÓN CIENTIFICA DE YUCATAN)

UNAM, UNIDAD MICHOACÁN, INTITUTO DE GEOFÍSICA, JULIO 2017.

## Agradecimientos.

El presente trabajo de tesis es el resultado del trabajo, apoyo, dirección y asesoría de diversas personas las cuales han contribuido de manera sustancial en mi crecimiento tanto profesional como personal.

Agradezco a la Universidad Nacional Autónoma de México al Posgrado en Ciencias de la Tierra y al Instituto de Geofísica unidad Michoacán, por todas las facilidades que me otorgaron a lo largo de estos cuatro años y las facilidades para desarrollar y ampliar mi formación profesional.

Agradezco al CONACYT, por el apoyo económico a lo largo de estos cuatro años, sin el cual hubiera sido muy difícil llevar acabo el presente proyecto de doctorado, así como a los proyectos de CONACYT Ciencia Básica (CB-2009-01-00131191), (00131191), CONACYT No. 252149, UNAM-DGAPA-PAPIIT IA104215, UNAM-PAPIIT IN101717, UNAM-PAPIIT-IA104215, UNAM-PAPIIT IN10524.

Quiero agradecer de manera muy especial al Dr. Avto Goguitchaisvili, por haberme proporcionado el tema correspondiente al presente trabajo de doctorado, por su asesoría, confianza, dirección y amistad. De la misma manera agradezco al Dr. F. Javier Pavón, por su asesoría en los temas de modelado, y en el compartir su conocimiento a lo largo de estos cuatro años así como por su tiempo y consejos. Agradezco al Dr. Juan Julio Morales Contreras, por su asesoría y atinados comentarios, así como por la accesibilidad en el préstamo de los equipos de laboratorio y su colaboración en los artículos que son el fruto del trabajo.

Agradezco en gran forma a mis compañeros, pero más importante mis amigos del instituto de geofísica, del LUGA, LIMNA, de la ENES, por sus consejos, apoyo incondicional y su gran amistad, gracias a él Dr. Rubén Cejudo, Dr. Anuar G. Terán, Dr. Miguel Cervantes, Ángela Alejo y a la Dra. Lisa Kapper, el conocerlos y contar con su amistad hizo que este periodo fuera muy grato y llevadero. De la misma

manera agradezco a Mtra. Adriana Briseño  y a Araceli Chaman por su apoyo y paciencia en cada uno de los tramites que llegue a realizar.

Agradezco de gran manera mi esposa e hijo  por su amor, apoyo y por ser mi motor a lo largo de él doctorado, por ser tan comprensivos en las tardes y noches cuando el trabajo no me permitía el poder disfrutar de su compañía, por los buenos deseos y su confianza en cada proyecto que he desarrollado, y por qué este doctorado no solo es mío sino de ellos también.

Agradezco a mis padres por su apoyo, amor y sus enseñanzas,  sin las cuales  no sería posible el día de hoy estar al final de este proyecto, así como a mis hermanos quienes siempre me han dado su amor y apoyo incondicional.

# Índice

## 1. Resumen.

En México se han realizado desde los años 70's diversos estudios de carácter paleomagnético y arqueomagnético y más recientemente, a partir del año 2000, ambas ramas del magnetismo antiguo han desarrollado consistentemente investigaciones que se realizan para esta región conformando así un amplia y creciente cantidad de registros de intensidades geomagnéticas absolutas que comprenden a los últimos 3 milenios, del mismo modo se ha visto un aumento considerable en los registros de paleodirecciones para los últimos 5 Ma. En virtud la creciente cantidad de datos, surge la necesidad de realizar una revisión sistemática en su calidad y confiabilidad, para con ellos examinar globalmente el comportamiento del CMT en esos periodos. El presente trabajo persigue dos objetivos primordiales: a) Obtener intensidades geomagnéticas absolutas correspondientes a la cultura Maya para los últimos dos milenios y generar una base de datos de arqueointensidades para crear, conjuntamente con los datos previos, una curva de referencia de variación paleosecular mediante el método computacional estadístico *Bootstrap* y el método de interpolación *P-Splines* (splines cúbicos) penalizados. Esta curva permitirá describir de manera continua el cambio de la intensidad absoluta durante los últimos 3000 años, permitirá también tanto obtener datos direccionales como ser una herramienta de datación para la región de Mesoamérica en dicha temporalidad. b) El segundo objetivo es obtener nuevas paleodirecciones de cuatro complejos volcánicos localizados en el sector central y el sector oeste de la Faja Volcánica TransMexicana. En específico el complejo Volcánico de Colima, el complejo volcánico de Mascota (localizado en el Bloque Jalisco), el complejo volcánico de Tancitaro y el complejo volcánico Los Azufres, estos dos últimos pertenecientes al complejo volcánico Michoacán-Guanajuato. Estas nuevas paleodirecciones en conjunto con las ya disponibles de la FVTM, permitirán realizar un análisis regional

detallado de la evolución del campo magnético de la Tierra para los últimos 5 Ma generando la primera curva paleodireccional que describa la variación de la inclinación y declinación magnética regional con un alcance temporal de millones de años.

## 2. Introducción.

El inicio del estudio del magnetismo tiene un origen incierto, pero posiblemente esté relacionado con el descubrimiento de los efectos que producen las rocas con un alto contenido de magnetita (un óxido de hierro) sobre algunos metales y que depende de la proporción de dicho mineral en la roca. Estos minerales se encuentran fácilmente en la naturaleza y sus propiedades se deben a un fenómeno físico llamado ferrimagnetismo el cual puede entenderse como el resultado de un ordenamiento a escala de los momentos magnéticos individuales de los cationes de hierro. El efecto combinado de estos cationes es el responsable de que algunos minerales, la magnetita, por ejemplo, produzcan un campo magnético vectorial a su alrededor que atrae a metales ferromagnéticos como lo son el cobalto, hierro, níquel y aleaciones, a dichos minerales se les denomina "imanes".

La magnetita debe su nombre a la ciudad griega de Magnesia de Tesalia, localizada en la actual prefectura de Magnesia en Grecia. Los filósofos griegos fueron los primeros en escribir sobre las propiedades de dicho mineral alrededor de 800 a.C., las propiedades que describen ya habían sido identificadas anteriormente por los chinos alrededor de ~300 a.C. Posteriormente los estudios de estos fenómenos cobraron mayor relevancia y se le comenzó a denominar como se le conoce actualmente, "magnetismo". Esta palabra proviene del latín "magneta", un término utilizado para referirse a los efectos de los "imanes" (Lowrie, 2007). Fue hasta el año 1600 que en el trabajo titulado "*De Magnete*" William Gilbert definió a la Tierra como un enorme imán, pero fue Henry Gellibrand (1635) mediante sus observaciones de la variación de la aguja magnética quien detectó que el campo magnético de la Tierra varía con respecto a el espacio y detectó también que la declinación magnética cambia al paso de los años (Van Helden and Burr, 1995). Gracias a los estudios anteriores, fue que Edmund Halley se interesó en el geomagnetismo, y en 1690 publicó su teoría del magnetismo terrestre en donde plantea que la Tierra es

un poderoso imán con cuatro planos magnéticos, distribuidos en el polo boreal y el polo austral, en 1692 desarrolló una ingeniosa teoría sobre el interior de la Tierra y cómo estaría compuesta por diversas capas magnéticas, así mismo Halley en 1698 comandó un viaje a bordo del buque Paramour con el objetivo de cartografiar el campo magnético del Océano Atlántico, estas observaciones permitieron desarrollar la primer carta magnética (Cook y Halley, 1997; Stern, 2001), posteriormente Friedrich Gauss instaló en 1873 el primer observatorio geomagnético en Alemania, lo que permitió que mediante el desarrollo de más de estos observatorios, se pudieran realizar estudios de la variación secular del campo geomagnético de manera continua vigentes hasta nuestros días.

La existencia de rocas con propiedades magnéticas a lo largo y ancho de la Tierra se debe primordialmente a que estas son producto de las erupciones volcánicas y, debido a su composición mineralógica la cual incluye a la magnetita o titianomagnetita, estas rocas registran las características del campo magnético de la Tierra presente en el momento de su formación por lo que constituyen una herramienta muy útil para el estudio de las variaciones del campo magnético terrestre en el pasado, siendo esta la base de los estudios paleomagnéticos enfocados en recuperar la información de estos registros. Mediante estos estudios se ha podio observar que el campo magnético de la Tierra ha presentado variaciones en su polaridad como lo descubrieron David en 1904 y Brunhes en 1906 (Caccavari, 2014). Más tarde Matuyama estableció con certeza que la magnetización inversa observada en ciertas rocas corresponde a un registro de la polaridad geomagnética invertida, es decir a una inversión de polaridad. Además de las inversiones de polaridad se ha registrado también en el pasado eventos denominados excursiones geomagnéticas y *jerks* que son manifestaciones de las constantes variaciones del Campo Magnético de la Tierra (CMT) (Bonhoment y Babkine, 1967; Smith y Foster, 1969).

El estudio de la variación paleosecular y las fluctuaciones finas del Campo Magnético de la Tierra en el pasado es decisivo para comprender los procesos geodinámicos internos responsables de generar el campo y comprender también cuáles son las condiciones que definen la ocurrencia de las inversiones de polaridad, las excursiones y los *jerks* que caracterizan y han estado presentes en la historia del CMT

Los cambios en las direcciones paleomagnéticas y en los valores de paleointensidad del CMT han estado presentes dese tiempos geológicos y pueden indicar cambios en la modulación de la acción del geodínamo en el núcleo por el estado convectivo del manto inferior (Glatzmaler et al., 1999). El desarrollo de metodologías más confiables y el incremento de estudios paleomagnéticos ha permitido el aumento en calidad y cantidad de los datos sin embargo su distribución espacial sigue siendo aún insuficiente concentrándose principalmente en Europa y Norte América, lo cual impide un análisis exacto de los cambios en escala fina de las características de la variación del vector completo del CMT.

Con la finalidad aportar nuevo conocimiento que resuelva esta problemática, el presente trabajo persigue dos objetivos principales:

- Ampliar y examinar la confiabilidad de los registros de la base de datos paleomagnéticos para estudiar la variación secular del CMT mediante el desarrollo de curvas regionales de variación paleosecular específicas. Una curva direccional (declinación e inclinación) paleomagnética para los últimos 5 Ma; y una curva de arqueointensidades y variación paleosecular de referencia la cuál será utilizada como herramienta para datación de materiales arqueológicos.

- Obtener nuevas direcciones e intensidades paleomagnéticas registradas en rocas volcánicas de los últimos 5 Ma y artefactos arqueológicos de los últimos tres milenios dentro del territorio mexicano.

Debido al gran acervo cultural del que dispone México existe una gran cantidad de artefactos y sitios arqueológicos disponibles para el desarrollo de estudios arqueomagnéticos por lo que representan papel muy importante en el estudio de la variación del campo magnético terrestre durante los últimos milenios y permiten conocer a detalle cómo se manifiestan estas variaciones a nivel regional. Gracias a los materiales arqueológicos se pueden obtener las características direccionales (arqueodirecciones) y la intensidad (arqueointensidad) del CMT presenta en el momento de su elaboración. La obtención de arqueodirecciones requiere que las estructuras u objetos se encuentren *in situ* lo que dificulta acceder a ellos por la protección a la que están sujetas las zonas arqueológicas. Por otro lado, a diferencia de la obtención de las arqueodirecciones, las arqueointensidades no requieren que los artefactos a estudiar se encuentren *in situ*, debido a que no se necesita la orientación de la muestra para la obtención de dicha arqueointensidad lo que facilita acceder a fragmentos cerámicos como ollas de barro utensilios de cocina, fragmentos de piso, paredes u hornos quemados. Sin embargo el proceso para obtener una arqueointensidad absoluta confiable es bastante más complejo que la obtención de las arqueodirecciones debido a que para su determinación se utilizan solamente materiales que posean una magnetización termorremanente completa o lo suficientemente grande para satisfacer ciertos criterios magnéticos específicos (Kosterov and Prévot 1998).

Aunque el conocimiento de la intensidad absoluta geomagnética es un elemento fundamental para el conocimiento de la morfología del CMT, los estudios realizados en Mesoamérica aún son esporádicos iniciándose en los 60's gracias a los trabajos realizados por Nagata *et al.,* (1965), posteriormente Coe (1967) desarrolló un estudio en San Lorenzo Veracruz y un poco después Bucha *et al.,* (1970), ambos autores son considerados como los pioneros del arqueomagnetismo en México. Posteriormente Wolfman (1973) realizó el primer levantamiento sistemático arqueomagnético, con lo cual se obtuvo una secuencia cronológica preliminar de Mesoamérica. Más tarde Carlson (1975), Malstrom (1976) y Urrutia *et al.,*

(1981, 1986) realizaron trabajos que proporcionaron nuevos datos arqueomagnéticos. El incremento de los estudios arqueomagnéticos sucedió recientemente a partir del año 2000 hasta el día de hoy, gracias a los trabajos realizados en el centro de Teotihuacán por Hueda (2000), Hueda y Soler (2001), Hueda *et al.,* (2004), Sánchez (2005), Romero-Hernández (2008), Saavedra-Cortes (2010), Hernández-Ávila (2010), así como los estudios realizados en Veracruz por López-Téllez *et al.,* (2008) y en Chiapas (Morales *et al.,* 2009). Desafortunadamente y a pesar del gran número de zonas arqueológicas de la cultura Maya existen pocos estudios arqueomagnéticos, hasta el momento solo existen los trabajos de Alva-Valdivia *et al.,* (2010) y Fanjat *et al.,* (2013). La realización de un estudio arqueomagnético en cerámicas provenientes de la cultura Maya, además de contribuir con uno de los objetivos de este trabajo, permitirá descubrir si una de las características observadas en estudios previos, el registro local de bajas intensidades geomagnéticas con respecto a intensidades globales, es una característica propia del CMT observado en Mesoamérica además que permitirá comparar los resultados con las curvas obtenidas por medio de modelos globales como lo es SHA.DIF.14k (Pavón-Carrasco *et al.,* 2014), y Cals3k.4 (Korte y Constable, 2011). El sitio de interés es la zona de Ichikaantijo, localizada en las cercanías de la ciudad de Mérida. La región de Ichikaantijo conocida como “el linaje de la serpiente” (Góngora y Ángel, 2015). Para desarrollar dicho trabajo se contó con siete fragmentos cerámicos de color gris, proporcionadas por arqueólogas a cargo de la zona de estudio y gracias a la campaña de excavación llevada a cabo por el “Instituto Nacional de Antropología e Historia” (INAH). La obtención de las arqueointensidades de cada fragmento se realizó mediante el protocolo Thellier y Thellier (1959) modificado por Coe (1967), los fragmentos tienen una distribución temporal entre 250 D.C y 1000 D.C.

Esta nuevas arqueointesnidades combinadas con resultados previos para el sur de Mesoamérica (México y Guatemala) con edades determinadas por métodos radiométricos, estratigráficos y arqueológicos confiables, generaron una base de datos. Con dicha base de datos se desarrolló la una curva de variación

arqueomagnética. Esta curva permite conocer las características finas de la fluctuación regional del campo magnético de la Tierra y puede ser utilizada como herramienta de datación regional. Si bien ya existen existe un número significativo de curvas de variación paleosecualar regionales bien definidas para (Cai et al., 2016, Genevey et al., 2016; Gómez-Paccard et al., 2016, Hervé et al., 2013, Tema y Kondopolou, 2011), la mayor parte de ellas son para Europa, esta nueva curva represnat un avance significativo ya que es la primer curva de variación regional arqueomagnética para Mesoamérica.

Como parte de los objetivos fue obtener nuevos datos paleomagnéticos registrados en rocas volcánicas de los últimos 5 Ma se realizaron diversos muestreos en distintos complejos volcánicos localizados dentro de la faja volcánica Transmexicana (FVTM), el complejo volcánico de Colima (CVC), el complejo volcánico de Mascota (CVM), el complejo volcánico de Tancitaro (CVT) y el complejo volcánico Los Azufres (CVLA).

El estudio realizado en el (CVC) tiene como objetivo contribuir a la base de datos global del campo promediado en el tiempo y al estudio de las inestabilidades geomagnéticas de polaridad a escalas temporales para los últimos 5 Ma. La zona de estudio está localizada en el complejo de Colima, la cual es una cadena volcánica orientada de N-S y está compuesta por tres estrato volcanes: El Cántaro, Nevado de Colima y el volcán Colima perteneciente a la porción oeste de la Faja Volcánica Trans-Mexicana (FVTM). Este estudio se basó en la recolección de especímenes correspondientes al volcán Colima y al Nevado de Colima, los cuales cuentan con edades asociadas por los métodos convencionales como lo son *Ar-Ar.* Según la descripción y localización realizada por Cortés (2015), existen hasta 30 flujos de lava distintos de los cuales de los cuales se tomaron muestras de 21 de ellos priorizando aquellos flujos que no presentaran alteración y de facíl acceso, sin evidencia de afectación tectónica y considerados sub-horizontales. Se recolectaron alrededor de 9 muestras por flujo mediante el uso de un taladro portátil y se orientaron mediante una brújula magnética y solar marca Brunton, pero debido a los factores

climáticos en la mayoría de los lugares no fue posible realizar la corrección magnética por medio de la declinación magnética local.

El segundo complejo volcánico que se estudió en este trabajo trabajo pertenece al bloque Jalisco (BJ), se obtuvieron diecinueve nuevas paleodirecciones con sus respectivas edades por métodos radiométricos (Ownby et al., 2008). Se trata del campo volcánico Mascota (CVM) el cual se localiza entre el bloque Jalisco (Oeste de México), la FVTM y La Sierra Cacome, se encuentra al sur-oeste del rift Tepic-Zacoalco con una longitud de 250 km y al noroeste de 65 km.

Estas nuevas determinaciones, en conjunto con las previamente reportadas Maillol y Bandy (1993) y Maillol et al. (1997) correspondientes al Plioceno hasta el Pleistocenos mediante el análisis de las características de la variación palosecular se examina evolución tectónica del oeste de la FVTM

El tercer complejo que se estudia es el volcán Tancitaro, localizado en el complejo volcánico de Michoacán-Guanajuato (CVMG), en donde se desarrolló un muestreo de ocho flujos entre los 70 kyr y los 957 kyr, El volcán Tancitaro es el único estratovolcán dentro del CVMG, siendo el volcán más alto dentro del complejo con 3840 mts de altura (Ownby et al., 2007) y el cual cuenta con una gran cantidad de flujos datados por métodos radiométrico gracias a los trabajos de Ownby et al., 2007 y Ownby et al., 2010. Se obtuvieron ocho nuevas determinaciones de paleodirecciones las cuales se combinaron con 11 determinaciones previas realizadas por Maciel et al. (2009) en el volcán Tancitaro y sus alrededores.

El cuarto y último complejo estudiado es el CVLA, dentro del complejo volcánico Michoacán-Guanajuato y pertenece a la zona central de la FVTM. Se trata de un complejo volcánico ácido, con un centro de silicio que incluye grandes calderas. Dicho centro volcánico es más conocido por su importancia como centro geotérmico en la generación de energía eléctrica para México.

Los cuatro muestreos realizados en el presente trabajo tienen como objetivo contribuir a la base de datos de paleodirecciones correspondientes a los últimos 5 Ma con edades radiométricas (e.g Ar-Ar, K-Ar) asociadas cada uno de los flujos correspondientes. La mayoría de las paleodirecciones están concentradas dentro de la FVTM, y los primeros trabajos que se realizaron fueron a partir de los años 70's. Comenzando por el trabajo desarrollado por Steele (1971), y Mooser (1972), posteriormente Herrero-Bervera y Pal (1978), junto Demant (1978). En los 80's comenzaron de Bönhel y Negendak (1981) realizaron estudios en lavas en la parte este de la FVTM, para el Plio-Pleistoceno, y más adelante se realizaron trabajos dentro de volcán Iztaccíhuatl por Steele (1985) y en la Sierra Chichinautzin por Herrero-Bervera *et al*., (1986). Pero los trabajos paleomagnéticos tuvieron continuidad e incrementaron en número después del año 2000 hasta ahora (e.g Blatter *et al.,* 2001; Bönhel y Molina-Garza, 2002; Conte-Fasano *et al.,* 2006; García-Ruiz *et al.,* 2016; García-Ruiz *et al.,* 2017a; García-Ruiz *et al.,* 2017b; Michalk et al., 2013; Morales et al., 2001; Ort and Carrasco-Nuñez, 2009; Ownby et al., 2011; Pretronille *et al.,* 2005, entre otros). Estos estudios proporcionan una mejor interpretación de la variación paleosecular de manera regional así como la evolución del campo geomagnético promediado en el tiempo. Se han realizado diversos estudios, con el objetivo de hacer un análisis de toda la FVTM (Ruiz-Martínez 2010; Mejía *et al*., 2005; Michalk *et al.*, 2013), así como estudios de movimiento de placa y rotación de bloque dentro de la FVTM, por lo cual el presente estudio contribuye en el conocimiento de la variación paleosecular así como examinar la posibilidad de que haya ocurrido un movimiento tectónico regional mediante la comparación de la dirección media con los polos de referencia.

Co estos nuevos datos paleodirecciones para los últimos 5 Ma, se desea obtener una curva de variación paleosecular a través de los últimos millones de años.

# 3. Last Two Millenia Earth's Magnetic Field Strength: New Archaeointensity Determinations From Ichkaantijo, Early to Late Maya Classic Period

## 3.1 Abstract

We report a detailed rock-magnetic and absolute geomagnetic intensity analysis performed on 48 samples belonging to eight pre-Columbian potteries from the Ichikaantijo area, near Merida city in the Yucatan Peninsula. Twenty six samples yielded reliable archaeointensity determinations which allowed estimating the geomagnetic field strength fluctuations for the central and northern Maya region during the Early to late Classic periods. The combined analysis of archaeointensity results obtained in this study with existing similar quality determinations indicate the persistence of substantially low geomagnetic field strength during the time interval involved, contrasting with the values predicted by the global geomagnetic field models. It seems that a large period of low geomagnetic field strength is accompanied by relatively dry climatic conditions just before the Maya Collapse.

*Keywords*: Geomagnetism,Archaeomagnetism, Maya Early-Late Classic Period, Paleosecular Variation, Paleoclimate.

## 3.2 Introduction

Burned archaeological artifacts retain reliable records of both directions and magnitude of the

Earth's Magnetic Field (EMF) during their manufacturing after heating and cooling. Oriented structures may offer full vector (declination, inclination and intensity), while displaced materials such as pottery may provide only intensities. The absolute geomagnetic intensity, however, is much more difficult to obtain than the directions since sophisticated and laborious sets of measurements are required.

Archaeomagnetic studies in Mesoamerica are still scarse and rather sporadic. They include the pioneering works of Nagata et al., (1965) and Bucha et al. (1970). First systematic archaeomagnetic survey was carried out by Wolfman (1973), who obtained a preliminary chronological sequence for the region. Carlson (1975), Malstrom (1976) and Urrutia et al. (1981, 1986) added new archaeomagnetic data to the incipient reference curve. These studies may be considered, however, as of only historical interest, since no rigorous experimental protocols were employed. At the beginning of the last century, archaeomagnetic investigations became the main goal for regional paleomagnetic laboratories, and consequently, the quality and quantity of reliable data significantly improved.

Recent archaeomagnetic studies in Mesoamerica were performed in the central Mexico, for the Teotihuacan center (Hueda 2000, Hueda and Soler 2001, Hueda et al., (2004), Sánchez (2005), RomeroHernández (2008), Saavedra-Cortes (2010), Hernández-Ávila, (2010) and other studies were carried out in Veracruz (López-Téllez et al. 2008) and Chiapas (Morales et al. 2009). Surprisingly, few studies are available from the Maya Area (Alva-Valdivia et al., 2010 and Fanjat et al., 2013).

This study is aimed to contribute high quality absolute archaeointensity determinations for the central and northern Maya area spanning the Early to late Classic periods. The analyzed pottery samples belong to the *Ichikaantijo* area, near Merida city. Reliable determinations were obtained from seven potsherd fragments which allowed estimating the geomagnetic field strength between 250 A.D and 1000 AD. The

combined analysis of the results obtained in this study with available determinations from southern Mesoamerica (sites from Mexico and Guatemala) permits resolving fine characteristics of the EFM fluctuations, with special emphasis on a possible link with the paleoclimate in the last two millennia.

### 3.3 Sampling

Eight potsherds analyzed in this study were obtained during several archaeological excavation campaigns carried out by the *Instituto Nacional de Antropología e Historia* (INAH). The samples belong to the pre-Hispanic style '*gray color potsherd'*, without any decoration, but with the particularity that the objects were bounded by *stucco*. These potsherds were elaborated with clay and carbonates from mines located close to the town where they were baked, at temperatures as high as 700°C. The samples where located in three different pre-Hispanic settlements from the *Ichkaantijoo* region (Figure 3.1), known as "The lineage of the snake" (Góngora and Ángel, 2015). The first settlement, with 6 pieces of potsherds (potsherds 8, 13, 14, 15, 16, and potsherd 17), is located to the northeast of the Yucatan Peninsula, near of the coastal strip. The other two potsherds were found near Merida city, one of them to the north (potsherd 19) while the other to the southeast (potsherds 23).

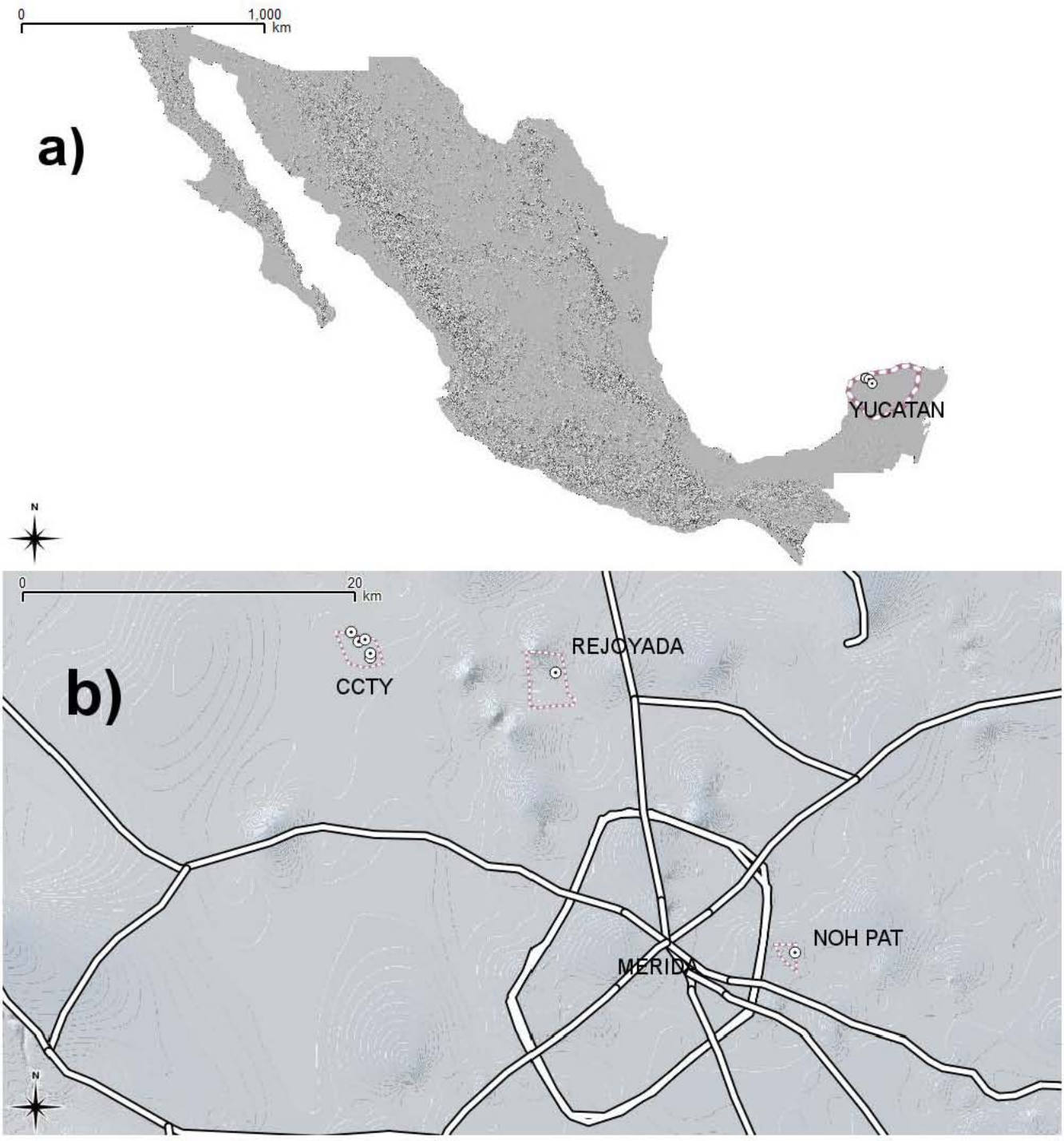


**Figure 3.1.** Schematic location of the archaeological sites involved in this study around of Merida city in Yucatán.

Analyzed pottery samples belong to distinct archaeological contexts, since four of them were unearthed from a single floor housing over the natural soil, while the other four come from the buildings which present more complex construction features. These potteries were mainly used for water and food storage. In general, the potsherds seem to be locally sourced and some of them could be related to the pottery found at the occidental region near to the Maxcanú area due to affinities observed (Figure 3.2).

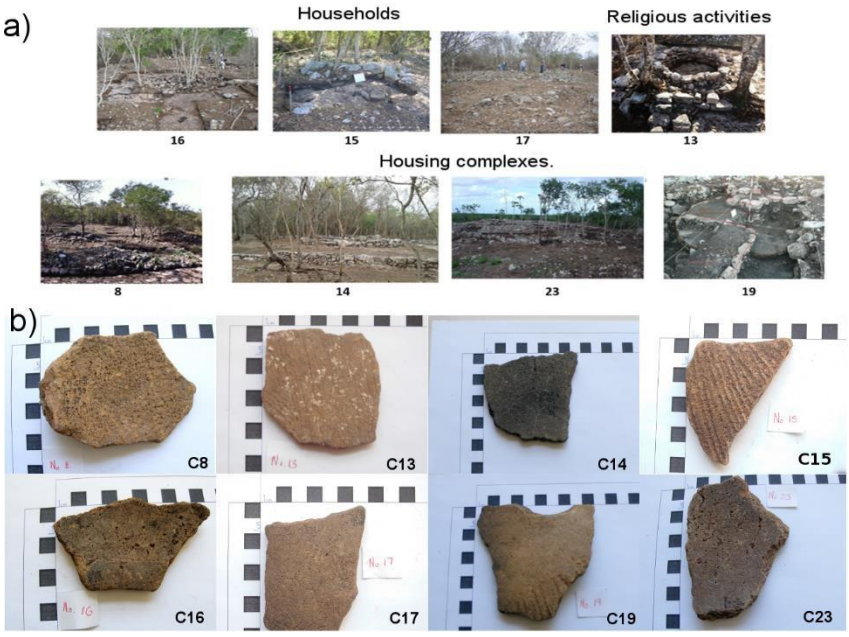


**Figure 3.2**. a) General view of sites of pottery provenance b) potsherds used in the present study.

The age estimation is rather well constrained (Table 3.1) thanks to the control provided by pottery style (Paz, 2010, Góngora et al., 2011, Paz, 2012 and Góngora et al., 2014). Fragments are assigned to the age interval between 250 AD-1000 AD. In order to check the reliability of archaeomagnetic dating based on intensity determinations, the global reference curves (Pavón-Carrasco et al. 2014) were used. Both archaeological and archaeomagnetic (tentative) age estimations are reported in Table 3.1.

### 3.4 Laboratory procedure

In order to evaluate the thermal stability and the magnetic mineralogy of samples, rock magnetic experiments were performed. These experiments also permitted the selection of the most suitable samples for Thellier-type archaeontensity experiments.

The potsherds were first demagnetized with peak alternating fields until 95 $mT$ as a first filter to reject those samples with multicomponent magnetization and/or chaotic behavior during the magnetic treatments. All eight fragments successfully passed this test since no evidence of strong secondary magnetization was observed.

The hysteresis curves, recorded using a Variable Field Translation Balance (VFTB), show a quite simple behavior (Figure 3.3), without any wasp-waisted or potbellied behavior (Roberts et al., 1995; Tauxe et al., 1996). Judging from associated isothermal remanence (IRM) acquisition curves, it seems that almost full saturation is reached at about 300 μT. The hysteresis ratios match to those of pseudo-single domain (PSD) grain size particles, as may be judged from the Day plot (Day et al. 1977). Continuous thermomagnetic curves (Ms-T) show stable, reasonably reversible behavior, indicating low-Ti to almost pure magnetite as the main ferrimagnetic phase. The presence of hematite is possible, but its contribution to total remanence seems negligible.

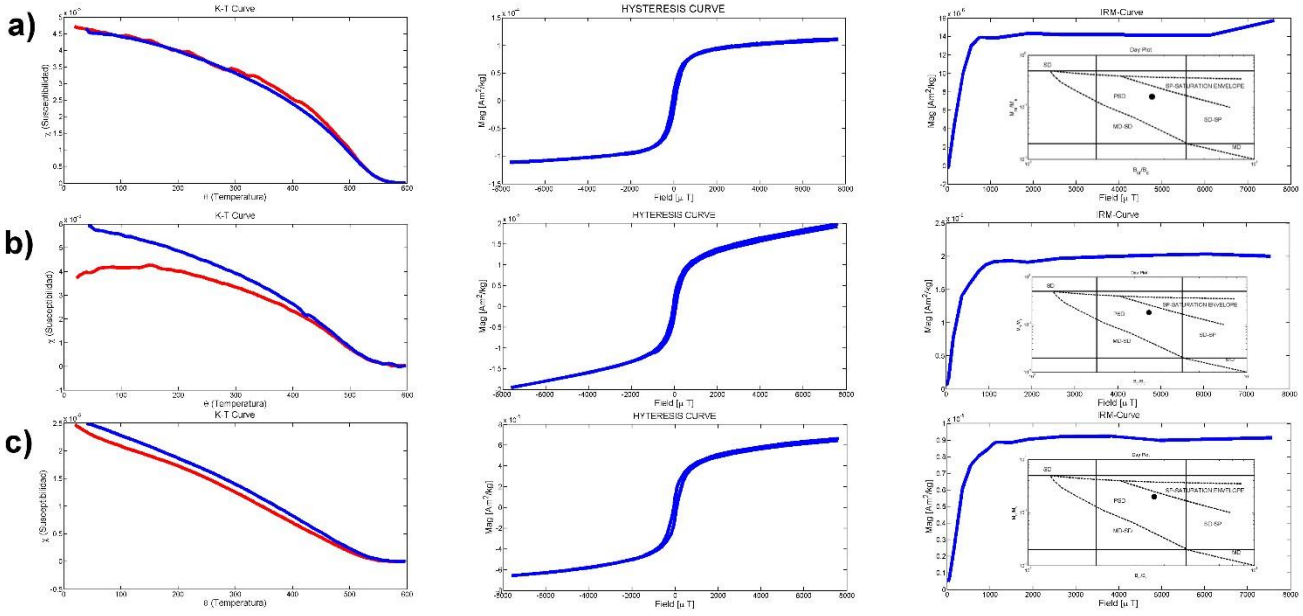


**Figure 3.3** Rock-magnetic results of representative samples including continuous thermomagnetic curves (Ms-T), hysteresis loops and associated isothermal remanent magnetization acquisition curves. Also shown is a Day Plot (Day et al. 1977) showing the relationship between specific hysteresis ratios (see text for more details).a) Sample 8, b) sample 13 and c) sample 16.

Once the thermal stability of the magnetic carriers was analyzed, the determination of the absolute intensity using the Thellier-Coe protocol (Thellier and Thellier1959, Coe 1967) was carried out. The laboratory magnetic field was set to 40 μT, with a precision of 0.1$\mu T$. An ASC TD-48 archaeointensity oven (thermal demagnetizer) and an AGICO JR6-A magnetometer were used for these experiments. In total 14 temperature steps, starting from 100°$C$ until 560°$C$, were distributed throughout the whole experiments. The eight potsherds were divided in six fragments and oriented into the salt pellets in six different positions ($\pm X$, $\pm Y$, $\pm Z$) to lessen the effect of magnetic anisotropy (Morales et al., 2012, 2013

and 2015). During the Thellier-Coe experiments the magnetic field was applied along the +Z direction. Cooling rate experiments were performed following a modified procedure to that described by Chauvin et al., 2000 (i.e., Morales et al. 2009). Three consecutive cooling's (fast, slow, fast) at the highest temperature step used allowed to estimate the cooling rate effect, and thus the correction of the absolute (raw) intensity values.

Some experimental conditions and specific criteria should be obeyed in order to consider archaeointensity determinations as reliable:

a) The so-called concave-up behavior should be rejected since it is most probably related to the fraction of remanence carried by multi-domain magnetic grains (Tauxe et al., 2010).

b) The associated orthogonal plot (Zijderveld diagram) must show a single and stable component during whole experiment, except at the very first steps, where some viscous remanent magnetization may be involved and thus tolerated.

c) Special attention was payed to the quality parameter (Coe et al., 1978) associated to the bestfitting line to the experimental data set, calculated by the mathematical procedure of York (1966): a NRM fraction $f > 0.3$, a gap factor $g \leq 1$ and a quality factor $q > 5$.

d) Estimation of the SCAT parameter, proposed by Shaar and Tauxe (2013), in order to reject all points which are significantly deviated from the best fit (Figure 3.4).

The archaeointensity determinations obtained in this study were classified into three types:

Type A : For this type, we accepted the specimens that have an almost linear behavior in both the Arai and associated Zijderveld plots, positive pTRM checks (control heating's) within the 10%.Small secondary viscous components may be present but easily removed at first temperature steps, between

250°$C$ to 350°$C$. The quality parameters match the above described criteria and the SCAT parameter is accomplished. The specimens that satisfied all these criteria were considered reliable and are accepted for mean archaeointensity determination.

Type B: These specimens show a more significant secondary (probably viscous origin) overprint, removed beyond 400°C. The NRM end points show erratic demagnetization steps, observed in the associated orthogonal plot. Although the SCAT parameter is almost the same of the Type A determinations, we rejected these samples for the calculation.

Type C: The Arai plots have a marked concavity shape and no linearity is observed on the associated Zijderveld plot. Moreover, no single segment points to the origin. The pTRM checks are clearly negative while significant mineralogical changes during the heating do not allow the cooling rate correction application.

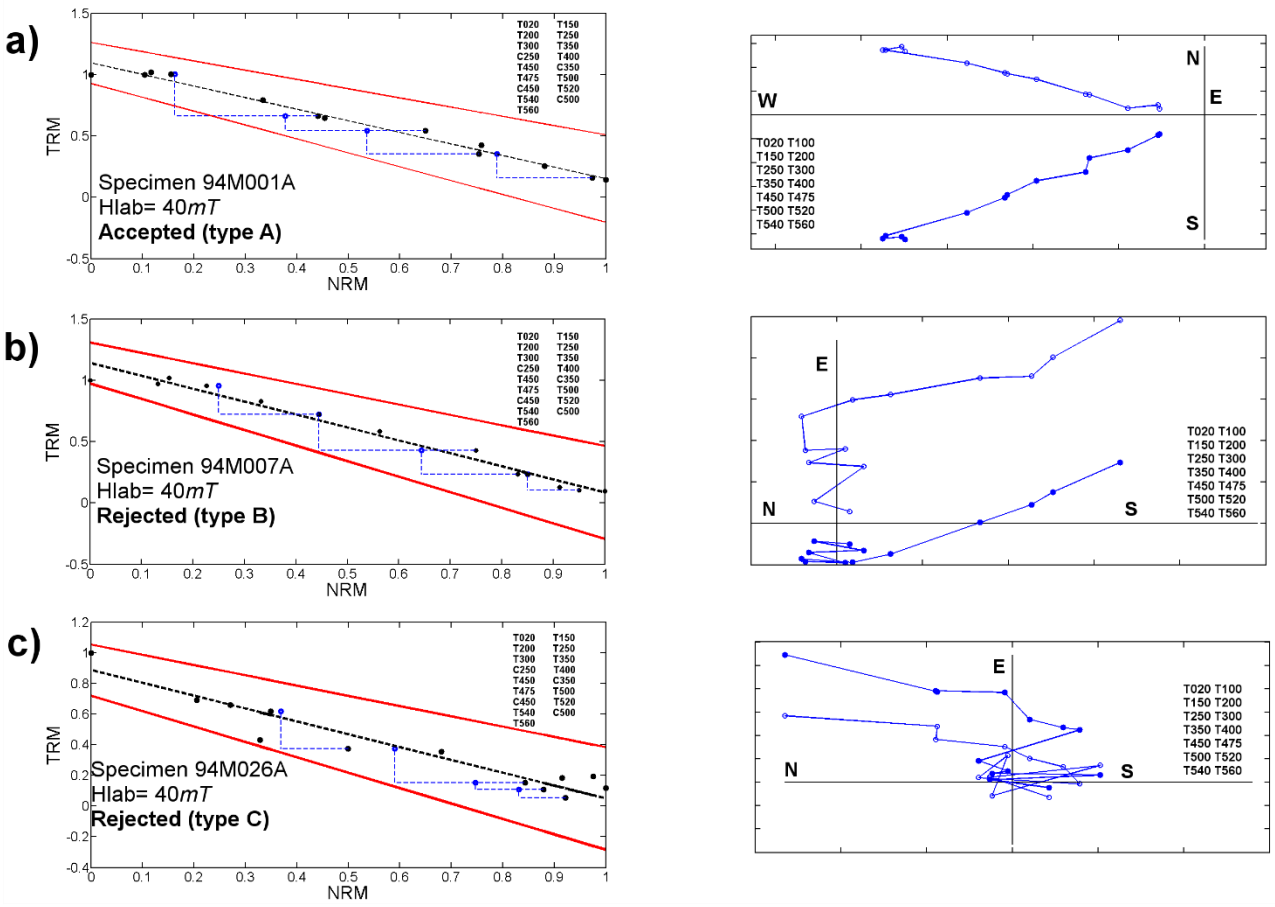


**Figure 3.4.** a) Summary of Thellier paleointensity experiments from three representative samples a) potsherd 8, b) potsherd 13 and c) potsherd 16 (see text for more details).

## 3.5 Discussion and concluding remarks

Absolute archaeointensity experiments indicate that 48 specimens yield acceptable quality parameters($q$, $f$, $g$) and 38 specimens meet to the SCAT criteria. Only 26 specimens belonging to seven out of eight pottery fragments (Table 3.1) yield type A determinations. Twelve specimens gave type B determinations, while the other ten specimens correspond to type C determinations.

| *Sample* | *Age estimation* | *Specimen* | *T1-T2* | *Hraw [μT]* | *f* | *g* | *q* | *n* | *Hcorr [μT]* | *VADM [A m²]* | *Type* | *An Intention of Archaeomagnetic dating* |
|---|---|---|---|---|---|---|---|---|---|---|---|---|
| Potsherd 8 | 300/400-550/700 A.D. | 94M001 | [200-560] | 41.92 | 0.478 | 0.848 | 15.195 | 11 | 41.24 | 9.05E+022 | A | 518-700 A.D. |
| CCTY 2011,2014 | | 94M002 | [0-560] | 37.23 | 0.857 | 0.853 | 14.022 | 13 | 35.94 | 7.88E+022 | A | 355-700 A.D. |
| 130/6-Ñ/I | | 94M003 | [25-560] | 37.89 | 0.806 | 0.847 | 17.369 | 12 | 36.96 | 8.11E+022 | A | |
| | | 94M004 | [0-560] | 34.00 | 0.804 | 0.848 | 13.983 | 13 | 32.81 | 7.20E+022 | A | |
| | | 94M005 | [25-560] | 33.58 | 0.937 | 0.843 | 10.158 | 12 | 31.29 | 6.86E+022 | A | |
| | | 94M006 | [25-560] | 32.25 | 0.793 | 0.849 | 7.914 | 12 | 30.27 | 6.64E+022 | A | |
| **Mean** | | | | **36.15** | | | | | **34.75** | **7.62E+022** | | |
| **S.d** | | | | **3.57** | | | | | **4.1** | **0.90** | | |

| | | | | | | | | | | | | |
|---|---|---|---|---|---|---|---|---|---|---|---|---|
| Potsherd 13 | 300/400-550/700 A.D. | 94M008 | [0-560] | 29.24 | 0.861 | 0.874 | 16.171 | 13 | 27.29 | 5.99E+022 | A | 651-700 A.D. |
| CCTY 2011,2014 | | 94M009 | [250-560] | 26.50 | 0.640 | 0.760 | 13.110 | 7 | 25.24 | 5.01E+022 | A | 617-738 A.D. |
| 128/PZ/1-II | | 94M010 | [150-560] | 32.27 | 0.790 | 0.810 | 20.320 | 8 | 30.71 | 6.38E+022 | A | |
| | | 94M011 | [200-560] | 26.17 | 0.770 | 0.820 | 24.130 | 10 | 24.56 | 5.10E+022 | A | |
| **Mean** | | | | **28.54** | | | | | **26.95** | **6.62E+022** | | |
| **S.d** | | | | **2.83** | | | | | **2.76** | **0.67** | | |
| Potsherd 15 | 550/600-900/1000 A.D. | 94M019 | [250-560] | 37.52 | 0.712 | 0.780 | 5.700 | 6 | 36.33 | 6.57E+022 | A | 550-797 A.D. |
| CCTY 2011,2014 | | 94M020 | [250-560] | 29.58 | 0.710 | 0.827 | 6.460 | 7 | 28.99 | 6.06E+022 | A | 398-758 A.D. |
| 231/PZ-1/I | | 94M021 | [200-560] | 28.68 | 0.782 | 0.844 | 8.895 | 11 | 28.16 | 6.18E+022 | A | |
| | | 94M022 | [25-560] | 28.74 | 0.821 | 0.871 | 9.029 | 12 | 28.08 | 6.17E+022 | A | |
| | | 94M024 | [100-520] | 31.08 | 0.784 | 0.811 | 23.187 | 9 | 29.08 | 6.38E+022 | A | |
| **Mean** | | | | **31.12** | | | | | **30.12** | **6.27E+022** | | |

| | | | | | | | | | | | | |
|---|---|---|---|---|---|---|---|---|---|---|---|---|
| **S.d** | | | | **3.70** | | | | | **3.49** | **0.22** | | |
| Potsherd 16 | 250-600 A.D. | 94M028 | [20-450] | 24.97 | 0.901 | 0.738 | 8.620 | 6 | 24.82 | 6.27E+022 | A | 541-600 A. D. |
| CCTY 2011,2014 115/H-9/I | | 94M030 | [150-475] | 19.71 | 0.553 | 0.771 | 5.820 | 6 | 18.64 | 4.29E+022 | A | 596-600 A.D. |
| **Mean** | | | | **22.34** | | | | | **21.73** | **5.28E+022** | | |
| **S.d** | | | | **3.71** | | | | | **4.36** | **1.40** | | |
| Potsherd 17 | 550/600-900/1000 A.D. | 94M031 | [20-500] | 21.42 | 0.840 | 0.750 | 20.110 | 6 | 21.18 | 5.31E+022 | A | 605-643 A.D |
| CCTY 2011,2014 139/PZ-1/I | | | | | | | | | | | | 653-701 A.D. |
| **Mean** | | | | **21.42** | | | | | **21.18** | **5.31E+022** | | |
| **S.d** | | | | **0.84** | | | | | **0.00** | **0.00** | | |
| Potsherd 19 | 550/600-900/1000 A.D. | 94M037 | [250-560] | 41.60 | 0.642 | 0.797 | 6.320 | 9 | 39.10 | 8.60E+022 | A | 550-816 A.D. |
| Rejoyada 2012 | | 94M038 | [25-560] | 33.07 | 0.755 | 0.872 | 12.924 | 12 | 31.07 | 6.82E+022 | A | 550-794 A.D. |

| | | | | | | | | | | | |
|---|---|---|---|---|---|---|---|---|---|---|---|
| 1/B-1/II | | 94M039 | [25-560] | 32.82 | 0.786 | 0.864 | 9.563 | 12 | 30.33 | 6.65E+022 | A | |
| | | 94M040 | [100-540] | 40.20 | 0.678 | 0.848 | 7.564 | 10 | 37.00 | 8.12E+022 | A | |
| | | 94M042 | [150-560] | 36.08 | 0.734 | 0.867 | 11.186 | 12 | 34.07 | 6.97E+022 | A | |
| **Mean** | | | | **36.75** | | | | | **34.31** | **7.43E+022** | | |
| **S.d** | | | | **4.02** | | | | | **3.76** | **0.87** | | |
| Potsherd 23 | 550/600-900/1000 A.D. | 94M043 | [150-560] | 19.42 | 0.759 | 0.806 | 7.120 | 7 | 17.79 | 3.91E+022 | A | 560-600 A.D. |
| Noh Path 2010. | | 94M045 | [25-560] | 20.34 | 0.835 | 0.824 | 11.255 | 12 | 18.40 | 4.04E+022 | A | 655-693 A.D. |
| 11/D-5, CL-3/II | | 94M047 | [100-540] | 19.37 | 0.330 | 0.758 | 10.280 | 10 | 17.62 | 2.76E+022 | A | |
| **Mean** | | | | **19.71** | | | | | **17.93** | **3.57E+022** | | |
| **S.d** | | | | **0.55** | | | | | **0.41** | **0.70** | | |

**Table 3.1.** Sample is the name with the specification provided by the archaeologist while *Specimen* refers to laboratory code. [T1-T2] is the interval of temperature involved in archaeointensity determination., Hraw, is the uncorrected intensity by the experiment, f, g, q are the Coe's (1978) quality factors, Mean is the fragment mean archaeointensity, s.d is the standard deviation, Hcor is the intensity corrected by the cooling rate, VADM is the virtual axial dipole

moment of each one of the intensities, Age estimation is the range of the age of each potsherd based on archaeological and stylistic considerations, Archaeomagnetic dating is the age estimated with the Matlab tool provided (PavónCarrasco et al., 2011) using Cals3k.4 model.

Archaeomagnetic dating of the pottery was carried out using the tool proposed by Pavón-Carrasco et al. (2011, 2014) in order to estimate whether the global reference curves may potentially be used for dating purposes in Mesoamerica, and also to know whether age estimations match with the intervals estimated from the archaeological and stylistic considerations. No single absolute intensity determination obtained in present study matches with the SHA.DIF.14k global model curve (Pavón-Carrasco et al. 2014). The Cals3k.4 model (Korte and Constable, 2011) seems to account better for the archaeointensities obtained (Figure 3.5). These age estimates are reported on the Table 3.1.

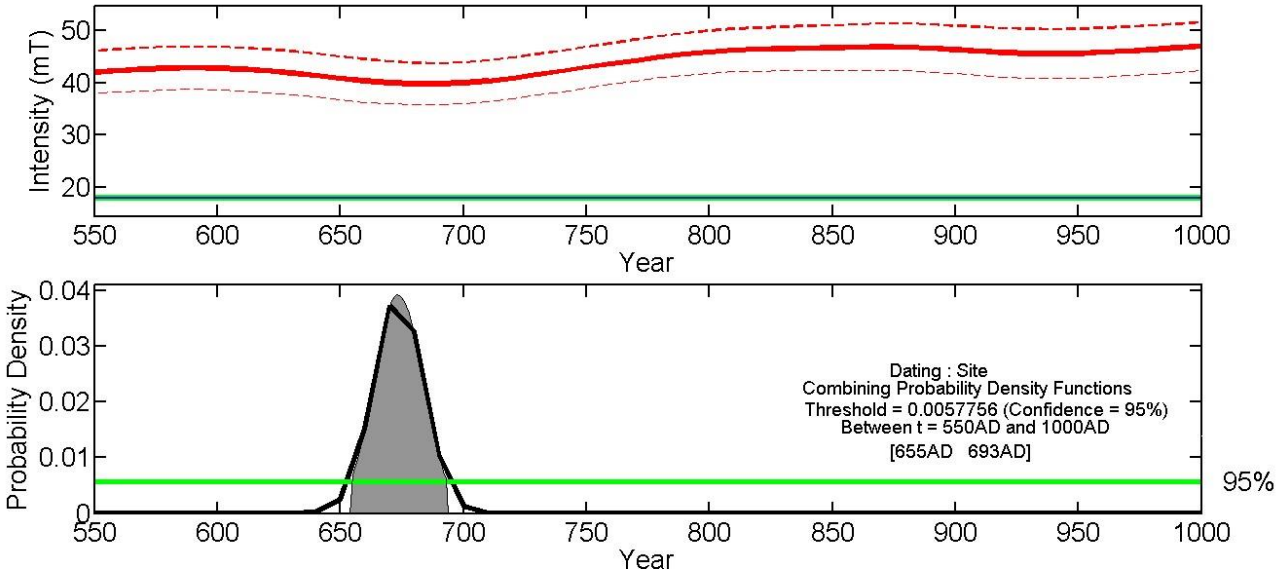


**Figure 3.5.** An intent to perform archaeomagnetic dating using global prediction model of Pavón-Carrasco et al. (2011) for the Holocene (see also Pavón-Carrasco et al., 2014).

In order to have a detailed perspective on the EMF strength variation through time for the Maya and surrounding areas, we compiled available similar technical quality determinations for the area, within the 12° and 22° North latitude and within the 262° and 274° West longitude using the GEOMAGIA50.v3 database (Brown et al., 2015). In total, 28 archaeointensity data were selected (Lee S., 1975, Morales et al., 2009; Fanjat et al., 2003). The reference models used are suitable for the time interval for the samples analyzed in the present work, as well for those of the study by Morales et al. (2009) and Fanjat et al. (2013). Worth noting is that the intensity values reported by Fanjat et al. (2013) are similar to the values presented in this study, and fall below the reference global models (Figure 3.6). Evidence of relatively high intensities comes from the studies reported by Lee S., 1975 (around 64 $\mu T$) and from Morales et al. (2009) who reported a value of 59.50$\mu T$ accompanied with a high uncertainty of 13.8 $\mu T$ (Morales et al., 2009). It should be noted that in the first case, the intensity is based on a single specimen and it cannot be ascertained that the value reported has geomagnetic significance. The low archaeointensities agree with the pioneering works by Nagata et al. (1965) and Bucha et al.(1970), pointing that the intensities for central and Southern part of Mexico were low, from 600 A.D. It is interesting to note that potsherds from the Mayan area yielded intensities even lower than 10$\mu T$. Thus, relatively low archaeointensities (Lee S. 1975, Morales et al., 2009 and Fanjat et al., 2013) are a general feature of this area during the time interval involved.

The changes of Earths' Magnetic Field strength through archaeological times may be related to paleoclimatic changes. The influence of the abrupt climatic changes in the evolution of ancestral cultures has received renewed importance (Gallet et al., 2005, 2006, 2008; Courtillot et al., 2007; Pétronille et al., 2012). Pétronille et al. (2012) remarked that this analysis is interesting since climatic and social changes are well documented for the Mesoamerican cultures, especially for the Maya area, as can be observed from the $\delta^{18}$O log obtained from the *Lake Punta Laguna*, in northeastern Yucatan Peninsula (Figure 3.6),

which provides an accurate record of paleoclimatic changes (Curtis et al., 1996; deMenocal, 2001, Rosenmeier et al., 2002)). As already noted by Petronile et al. (2012), the comparison between the $\delta^{18}O$ record (Figure 3.6b) and the predicted curves available from CALS3k.4 and SHA.DIF.14k (Figure 3.6a) indicates an inverse correlation over the millennial time scale. The trend in $\delta^{18}O$ values shows synchronous changes correlating with the main increments in predicted geomagnetic field intensities, and vice-versa. This correlation, basically supported with present dataset, contradicts the early hyphotesis of Gallet et al. (2006) and Courtillot et al. (2007) who suggested that the intensity fluctuations are correlated by climate changes over relatively long time scales. The warning (cooling) periods at North Atlantic are synchronous to the intensity decrease (increase) probably influenced by geomagnetic field trough the modulation of cosmic ray flux interacting with the atmosphere.

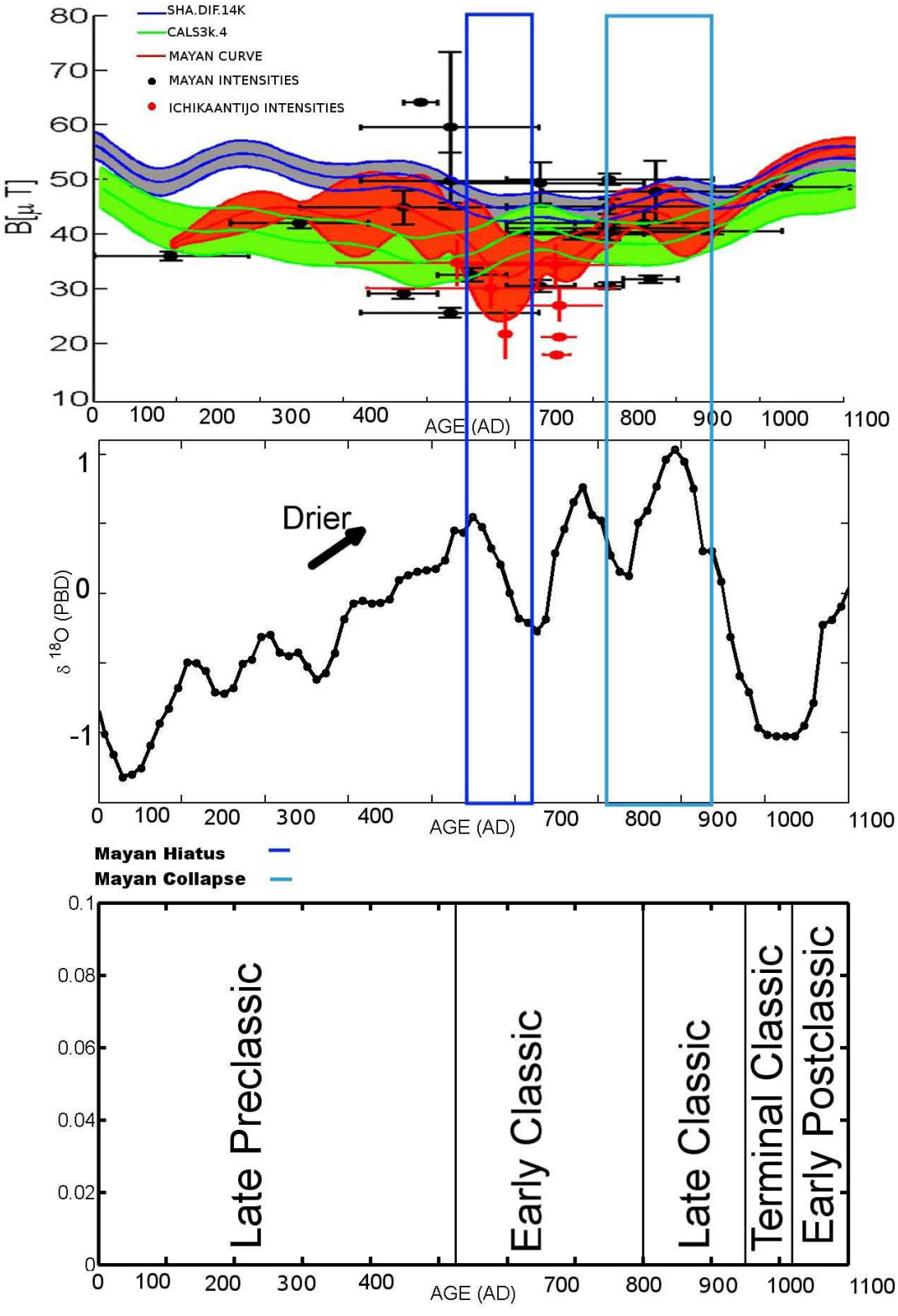
SHA.DIF.14K
CALS3k.4
MAYAN CURVE
MAYAN INTENSITIES
ICHIKAANTIJO INTENSITIES
B[μ T]
AGE (AD)
Drier
δ 18O (PBD)
Mayan Hiatus
Mayan Collapse
Late Preclassic
Early Classic
Late Classic
Terminal Classic
Early Postclassic

**Figure 3.6.** All available archaeointensity determinations from the Maya Area including the intensity values obtained in present study. Blue line denotes to the SHA.DIF.14k (Pavón-Carrasco et al., 2014) global model while green line refers to the Cals3k.4 (Korte and Constable, 2011).

The present study shows that low absolute geomagnetic intensity prevailed at the Maya area between at least 400A.D. and 750 A.D. accompanied by relatively dry climatic conditions just before so called Mayan Collapse. The persistence of low intensities (twice as low as present field strength) is not predicted by global models and thus a regional reference curve for the Maya area is needed.

**Acknowledgments**

The authors are thankful for the financial support provided by UNAM-PAPIIT IN101717 while some partial funds were provided by CONACYT n.° 252149.

**References**

Alva-Valdivia, L., Morales, J., Goguitchaichvili, A., de Hatch, M.P., Hernandez-Bernal, M., MarianoMatias, F., 2010, Absolute geomagnetic intensity data from preclassic Guatemala pottery. Phys. Earth Planet. Inter. v. 180, p. 41-51.

Bucha V., Tylor R. E., Berger R. and Haury E. W. 1970, Geomagnetic intensity: Changes during the past 3000 years in the Western Hemisphere, *Science,* v. 168, p. 111-114, doi: 10.1126/science.168.3927.111

Brown M. C., Donadini F., Nilsson A., Panovska S., Frank U., Korhonen K., Schuberth M., Korte M., and Constable G. C., 2015, GEOMAGIA50.v3: 2. A new paleomagnetic database for lake and marine sediments, Earth, Planet and Space.

Carlson J.B, 1975. Loadstone compass Chinese or Olmec primacy?,*Science*, v. 189, p. 753-760.

Chauvin A., Garcia Y., Lanos Ph., and Laubenheimer F., 2000, Archaeointensity of the geomagnetic field recovered on archaeomagnetic site from France, Physics of the Earth and Planetary Interiors, vo. 120, n. 1-2, p. 111-136.

Coe, R. S., Grommé S. and Mankinen E. A., 1978, Geomagneticpaleointensities from radiocarbon-dated lava flows on Hawaii and the question of the Pacific nondipole low, J. Geophys. Res., vo. 83, p. 17401756.

Courtillot, V., Gallet, Y., Le Mouël J.-L.Fluteau F., Genevey A., 2007, Are there connections between the Earth's magnetic field and climate? *Earth and Planetary Science Letters*, v. 253, p. 328-339.

Curtis, J. H., Hodell, D.A., Brenner, M., 1996. Climate variability on the Yucatan peninsula (Mexico) during the past 3500 years, and the implication for the Maya cultural evolution. Quaternary Research v. 46, p. 37-47.

deMenocal, P. B., 2001. Cultural responses to climate change during the Late Holocene. Science v. 292, p. 667-673.

Fanjat G., Camps P., Alva-Valdivia L. M., Sougrati M. T., Cuevas-García M., Perrin M., 2012. First archeointensity determinations on Maya incense burners from Palenque temples, Mexico: New data to constrain the Mesoamerica secular variation curve. Earth and Planet Science Letters, v. 363, p. 168-180.

Gallet, Y., Genevey, A., Fluteau, F., 2005. Does Earth's magnetic field secular variation control centennial climatic change? Earth and Planetary Science Letters v. 236, p. 339-3447.

Gallet, Y. Genevey, A., Le Goff, M., Fluteau, F., Eshraghi, S.A., 2006. Possible impact of the Earth's magnetic field on the history of the ancient civilizations, Earth and Planetary Science Letters v. 246, p. 17-26.

Gallet, Y., Le Goff, M. Genevey, A., Margueron, J., Matthiae, P., 2008. Geomagnetic field intensity behavior in the Middle East between 3000 BC and 1500 BC. GeophysicalResearchLetters v. 35.

Góngora S. A. G., Hernández G. C., Bolio Z. C. and Valencia B. M. 2011, Salvamento arqueológico ciudad científica y tecnológica de Yucatán 2010-2011. Tomo I. Registro, excavación, consolidación y restauración. Instituto Nacional de Antropología e Historía (INAH). Centro Yucatán. SEP. INCAY.

Góngora S. Á. G., Hernández G. C., Bolio C. Z., De la Cruz N. S., 2014. "Salvamento arqueológico ciudad científica y tecnológica de Yucatán Fase II". Tomo I. Registro, excavación y restauración de estructuras. Centro INAH Yucatán.

Góngora S. and Ángel G. JaaAjaulel. El reino de Joo, Ichkaantijo. Uniprint-Compañía tipográfia Yucateca S.A. de C.V.

Hernández-Ávila E. R., 2010. Control Cronométrico basado en arqueomagnetismo de Teopancazco, Estado de México, Tesis Licenciatura Física, Fac. Ciencias, UNAM, México 104 pp.

Hueda Y., 2000. Fechamientoarqueomagnéticos de estucos de los sitios de Teopancazco, Teotihuacan y Templo Mayor, Tenochtitlan. Tesis Licenciatura Arqueología, ENAH, México, 128 pp.

Hueda Y., Soler A. M., 2001. Fechamientoarqueomagnético de estucos en sitios de Teopancazco, Teotihuacan, Templo Mayor, Tenochtitlán. Informe presentado al Consejo de Arqueología. Agosto 2001.

Hueda Y., Soler-Arechalde A. M., Urrutia-Fucugauchi J., Barba L., Manzanilla L., Rebolledo M., Goguitchaishvili A., 2004. Archeomagnetic studies in central México-dating of Mesoamerican limeplasters. *Physics of the Earth and Planetary Interiors,* v. 147, p. 269-283.

Korte M., and Constable C., 2011. Improving geomagnetic field reconstructions for 0-3 ka, Physics of the Earth and Planetary Interiors, v. 188, no. 3-4, p. 247-259.

Lanos Ph., 2004. Bayesian inference of calibration curves: application to archaeomagnetism.In: Buck, C., Millard, A. (Eds.), Tools for Constructing Chronologies: Crossing Disciplinary Boundaries. SpringVerlag, London, v. 177, p. 43-82.

Lee S., 1975. Secular variation of the intensity of the geomagnetic field during the past 3,000 years in North, Central and South America., Ph. D. Thesis, University of Oklahoma.

López-Tellez, J. M., Aguilar-Reyes B., Morales J., Goguitchaichvili A., Calvo-Rathert M., Urrutia-

Fucugauchi J., 2008. Magnetic characteristics and archeointensity determination on Mesoamerican Pre-

Columbian Pottery from Quiahuiztlan, Veracruz, Mexico. GeofisicaInternacional, v. 47, no. (4), p. 329340.

Malstrom V., 1976. Knowledge of magnetism in pre-Columbian Mesoamérica, Nature, v. 259, p. 390391.

Morales J., Goguitchaichvili A., Acosta G., González-Morán T., Alva-Valdivia L. M., Robles-Camacho J., Hernández-Bernal M.S., 2009. Magnetic properties and archeointensity determination on Pre Columbian pottery from Chiapas, Mesoamerica. Earth Planets Space, v. 61, p. 83-91.

Nagata T., Kobayashi K., and Schwarz E. J., 1965. Archeomagnetic intensity studies of South and Central America. Journal of Geomagnetism and Geolectricity, vo. 17, p. 399-405.

Pavón-Carrasco F. J., Rodríguez-González J., Osete M. L., and Torta J. M., 2011, A Matlab tool for archaeomagnetic dating, *Journal for Archaeological Science.*, n. 38., p. 408-419.

Pavón-Carrasco F. J., Osete M. L., Miquel T. J. and De Santis A., 2014, A geomagnetic field model for the Holocene based on archaeomagnetic and lava flow data. Earth and Planetary Science Letters, v. 388, p. 98-109.

Paz R. D., 2010. "Informe personal del Salvamento Arqueológico Norte de Noth Pat". Centro INAH Yucatán.

Paz R. D. 2012. Informe personal del Salvamento Arqueológico La Rejoyada. Centro INAH Yucatán.

Pétronille, M., Goguitchaichvili, A., Morales, J., Carvallo, C., Hueda-Tanabe, Y., 2012, Absolute geomagnetic intensity determinations on Formative potsherds (1400-700 BC) from the Oaxaca Valley, Southwestern Mexico., Quaternary Research, v. 78, p. 442-453.

Roberts A. P., Cui Y., and Verosub K. L., 1995. Wasp-waisted hysteresis loops: mineral magnetic characteristics and discrimination of components in mixed magnetic systems. J. Geophys. Res. vo. 1000, p. 17909-17924.

Romero-Hernández E. 2008, FechamientosArqueomagnéticos de pisos con control estratigráfico de la excavación Teopancazco 2005, Teotihuacán. TesisLicenciaturaFísica, Fac. de Ciencias, UNAM, México 51 pp.

Rosenmeier, M. F., Hodell, D.A., Brenner M., and Curtis, J. H., 2002, A 4000-Year lacustrine record of environmental change in the Southern Maya Lowlands, Petén, Guatemala. QuaternaryResearch 57, 183-190.

Saavedra-Cortes S. P., 2010, Estudio arqueomagnético en el área de Tecamac, Estado de México, Tesis Licenciatura Física, Fac. Ciencias, UNAM, México, 85 pp.

Sánchez F., 2005. Nuevos fechamientosarqueomagnéticos en Xalla y Teopancazco, zonas habitacionales de Teotihuacán. Tesis Licenciatura Física, Fac. Ciencias , UNAM, México, 90 pp.

Shaar R., and Tauxe L. 2013, Thelliergui: An integrated tool for analyzing paleointensity data from thellier-type experiments, Geochem. Geophys. Geosyst., 14, 677–692, doi:10.1002/ggge. 20062.

Tauxe L., Mullender, T. A. T., and Pick, T., 1996. Potbellies, wasp-waists, and superparamagnetism in magnetic hysteresis, J. Geophys. Res. vol. 101, p. 571-583.

Tauxe L., Butler R. F., Van der Voo R., Banerjee S. K., 2010, Essentials of Paleomagnetism, University of California Press

Thellier E. and Thellier O., 1959. Sur l'intensité du champ magnétique terrestre dan le passé historique et géolique. Ann. Géophysique., vo. 15, p. 285-376.

Urrutia J., Maupome L., Brosche P., 1981. Archaeomagnetic research programme, I. An introduction to the knowledge of magnetism in pre-Columbian Mesoamerica. Int. Rep., Inst. Geofis., UNAM, Mexico & Obs. Hoher List der Univ. Sternwarte, Bonn, Germany, 25 pp.

Urrutia J., Maupome L., Brosche P., 1986. El compás magnético en China y Mesoamérica., Bol. GEOS, v. 6, no. (3), p. 5-7.

Wolfman D. 1973. A re-evaluation of Mesoamerica chronology: A.D. 1-1200, Ph.D. thesis, Univ. of Colo., Denver

# 4. Last Three Millennia Earth's Magnetic Field Strength in Mesoamerica and Southern United States


## 4.1 Abstract

The variation of the Earth's Magnetic Field strength may provide crucial information to understand the mechanism of geodynamo and elucidate the conditions on the physics of the Earth's deep interiors. Aimed to construct the first intensity paleosecular variation curve (PSVC) for Mesoamerica during the last three millennia, is analyzed the available absolute geomagnetic intensity, associated to absolute dates. This analysis is achieved using thermoremanent magnetization carried by volcanic lava flows and burned archeological artefacts. A total of 109 selected intensities from Mesoamerica and other 113 from the southern part of the United States represent the main core of the dataset to construct the reference curve using combined bootstrap and temporal P-spline methods. This first intensity PSVC for Mesoamerica generally disagree with the values predicted by the global geomagnetic field models and was compared by the virtual axial dipole moment with the PSVC of the east and west of Europe as with the PSVC of Asia to observe a non-synchronization and suggest a possible eastward drift. This PSVC be used as preferred dating tool for the region. The recent hypothesis about the relationship between the geomagnetic field strength and paleoclimate is also critically analyzed in lights of this new data compilation.



**Keywords:**

*Paleosecular Variation Curve, Mesoamerica, North America, Global Models, Eastward drift.*


## 4.2 Introduction.

Revealing the fine-scale variations of the Earth's magnetic field (EMF) is one of the major objectives of all geomagnetic studies[14]. These investigations may largely contribute to solve some critical issues about the origin and causes of the geomagnetic reversals, excursions and jerks. Present day observations of the geomagnetic field indicate that the dipolar contribution (about 90% of total field) is decreasing by about 10% since the eighteenth century[67]. On other hand, there is a general agreement among paleomagnetic community that during a geomagnetic reversal (or excursion) the absolute intensity may decrease up to 50% or even more[49] of its pre-transitional value. Korte and Constable[46] speculated that this behavior

may indicates a possible next large departure of the field (reversal or excursion). However, it is difficult to predict how these changes affects our planet[45]. Thus, it is crucial to reconstruct the past evolution of EMF elements. Another important question debated during the last decade is the possible influence of geomagnetic field variations on Earth's climate and biosphere. This still controversial hypothesis has gained a great interest during the last decade[21, 26, 33, 34].

Absolute geomagnetic intensity is a decisive element for a better knowledge of the geomagnetic field morphology. However, reliable absolute paleointensity values are generally much more difficult to obtain than directional data, because only objects carrying full thermoremanent magnetization and which satisfy some specific magnetic criteria may be used for paleointensity determination[48]. On other hand, the paleointensity determination has a great advantage because no *in situ* structures (very scare in Mesoamerica) and thus oriented samples are required. Well constrained intensity paleosecular variation curves (PSVC) already exist in Europe[13,38,40,43,72].

In Americas, no such reference curve is available in spite of the great cultural heritage. The first archeomagnetic survey was carried out in Cuicuilco, near to Mexico City by Nagata[61]. In 1967, Coe[17] developed a study in San Lorenzo (Veracruz) and three years later Bucha[12] performed archeointensity determinations on several pre-Columbian pottery samples from different archeological sites of central and southern Mexico.

A first chronology study of the past EMF based on Mesoamerican archeodirections was provided by Wolfman[80] that was complemented by indirect directional data coming from magnetically oriented buildings (first millennium BC) in Oaxaca and Tabasco[76, 77].

Almost two decades elapsed from these pioneering studies until late 90's, when numerous high quality determinations become available providing new information of the past evolution of the EMF coming from both lava flows and previously archeological sites[2,7,39,44,55,56].

The present study pretends to construct the first intensity PSVC for Mesoamerica during the last three millennia analyzing available absolute geomagnetic intensities carried out by volcanic lava flows and burned archeological artifacts, this PSVC may be used as preferred dating tool for the region in question. It want to compared this PSVC with global models to observe the proper characteristics of the variation of intensity in Mesoamerica, and following this idea, later it want to compare with the

regional PSVC for Europe and Asia by the use of VADM to try identify if it is possible some drift movement.

### 4.3 The database and Selection Criteria

All archeomagnetic and paleomagnetic (lava flows) data used in this study are distributed in the area which covering Mexico, Guatemala and the Salvador (Figure 4.1). Most of the archeointensities are available in the last version of GEOMAGIAv3[11] and ArcheoInt[37] while some volcanic data may be found in the most recent publications[10,31,54]. Remained archeointensity determinations comes from published papers since early eighties. Mesoamerican data consist of 109 intensities (Appendix 4.1) and spend the last 4000 years.


**Figure 4.1.** a) Schematic map of location of samples analyzed in this study. The blue color refers to the samples belonging to Mesoamerica, with a circular area with radios of 1200km, while intensities from southern United States are denoted in green. The map of this figure was produced with QGUIS 2.87 software (www.qgis.org)

The archeointensities were relocated to a common location in order to avoid spatial dependences and to provide a continuous temporal information of the EMF in the selected region. The relocation procedure is achieved assuming a geocentric axial dipole (GAD) field[50, 52], where the relocated intensities $F_R$, are calculated by the virtual axial dipole model (VADM) expression[5]:

$$F_R = F_S\sqrt{(1+3\cos^2\theta_R)/(1+3\cos^2\theta_S)},$$

where $F_s$ is the in situ intensity, $\theta_S$ is the site geographical colatitude, and $\theta_R$ is the colatitude of the reference point that was considered the downtown of Mexico City as the reference location, (Lat. 19° 25.17'N, Long. 99° 8.73'W). All sites within the radius of less than ~1200km from Mexico City were considered. The relocation of the intensity data introduces an error due non-dipole harmonic contributions of the EMF[5,23], which increases with the distance from the reference location (Mexico City). This error, called relocation error, was studied by Casas and Incoronato[15], for different spatial and temporal coverage. We have performed a similar study by using synthetic intensity data from the IGRF-12 model[74] covering our area of interest, i.e. a circular area centered in Mexico City with 1200 km (Figure 4.2)of radius. The maximum relocation error was less than 0.5 $\mu T$, a value lower than the average intensity uncertainty of our selected database ($\sim 4\mu T$)[Figure 4.2].

a)

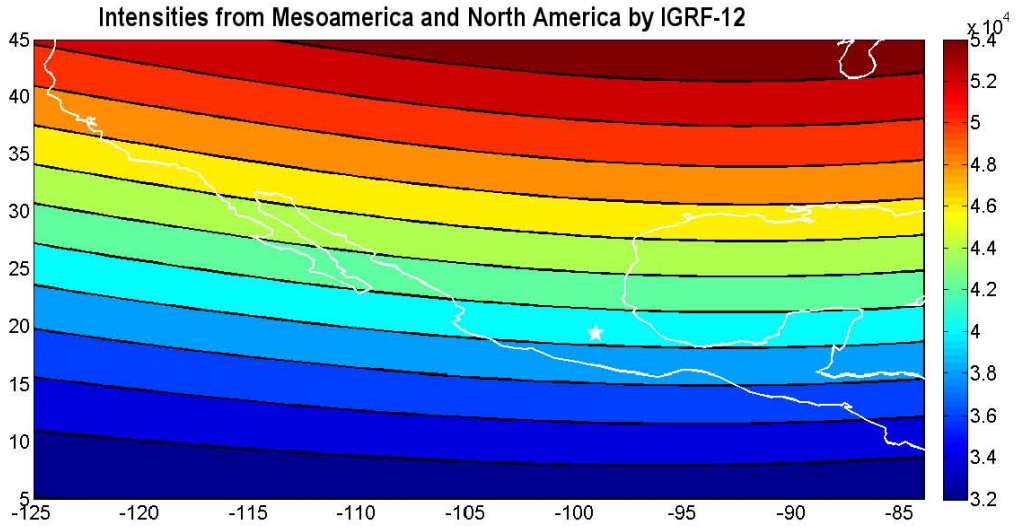
Intensities from Mesoamerica and North America by IGRF-12
x 10^4
5.4
5.2
5
4.8
4.6
4.4
4.2
4
3.8
3.6
3.4
3.2
45
40
35
30
25
20
15
10
5
-125
-120
-115
-110
-105
-100
-95
-90
-85

b)

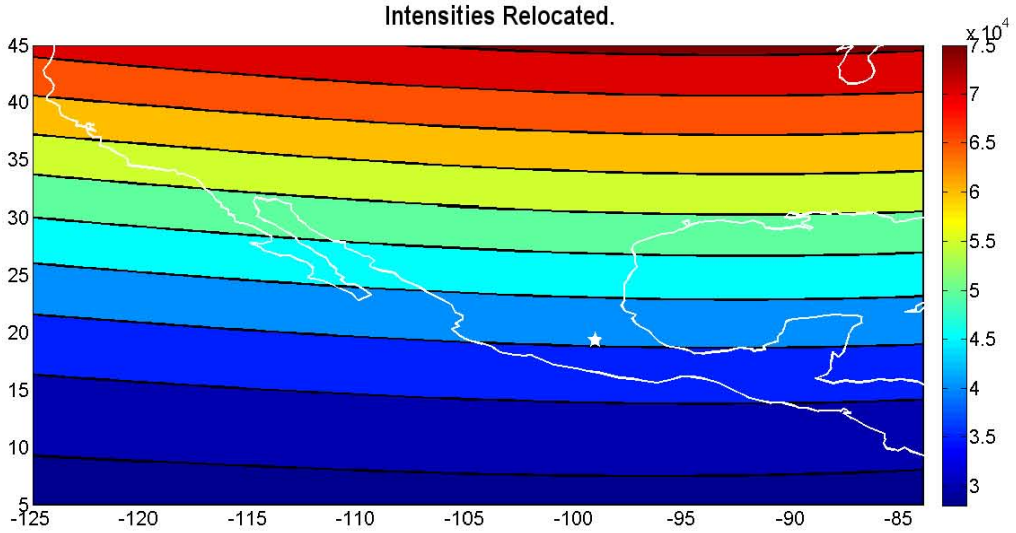
Intensities Relocated.
x 10^4
7.5
7
6.5
6
5.5
5
4.5
4
3.5
3
45
40
35
30
25
20
15
10
5
-125
-120
-115
-110
-105
-100
-95
-90
-85

c)

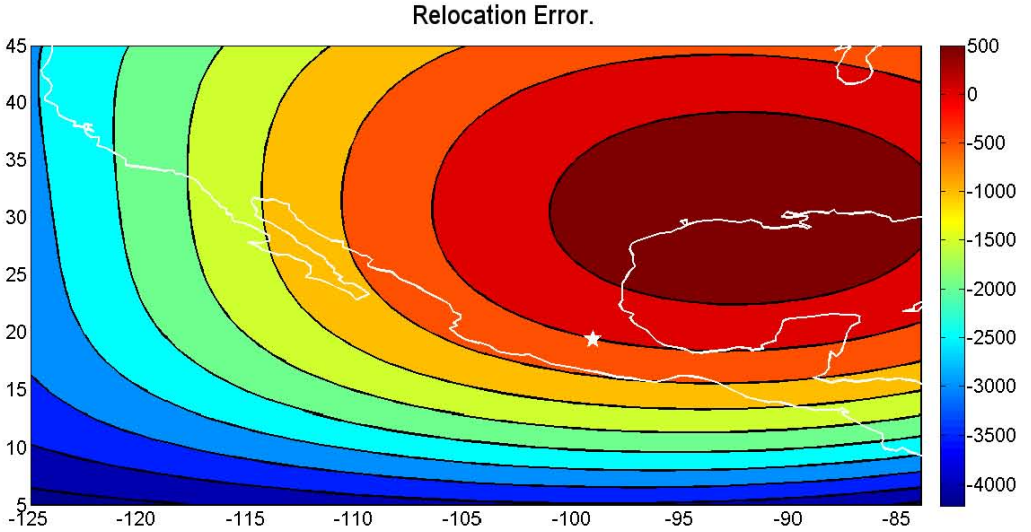
Relocation Error.
500
0
-500
-1000
-1500
-2000
-2500
-3000
-3500
-4000
45
40
35
30
25
20
15
10
5
-125
-120
-115
-110
-105
-100
-95
-90
-85

**Figure 4.2**. Analysis of relocation error a) Intensities for Mesoamerica and North America by using IGRF-12 model, b) Intensities relocated to the downtown of México City and c) Analysis of the relocated error (the bar of error is in $\eta T$).

The available archeointensity data for the last three millennia were classified in two categories based on statistical parameters and on the protocol followed in the laboratory measurements (such as the Thellier method[75]; and its modification by Coe[18]; the multispecimen method (of Dekkers and Böhnel[24]; the microwave technique (Walton[79]; Shaw[70]; among others).

1. The category A (the most reliable data) includes data with cooling rate and anisotropy corrected archeointensities derived from at least four specimens and with an intensity error ($1\sigma$) lower than $\sigma_E \leq 10\ \mu T$. Only 57 archeointensity data have been accepted out of 109 published archeointensities between 1000 B.C. and 2000 A.D. (Figure 4.3a).
2. The category B includes the rest of the data based on $N \leq 3$ specimens per fragment or site. The correction and dispersion parameters were not considered for this type of determinations. These category provided 21 archeointensities within the temporal range 900 B.C. to 1950 A.D (Figure 4.3b).

Both A and B category data are supported by radiometric age determinations. All these ages were calibrated for practical purposes of the present investigations.

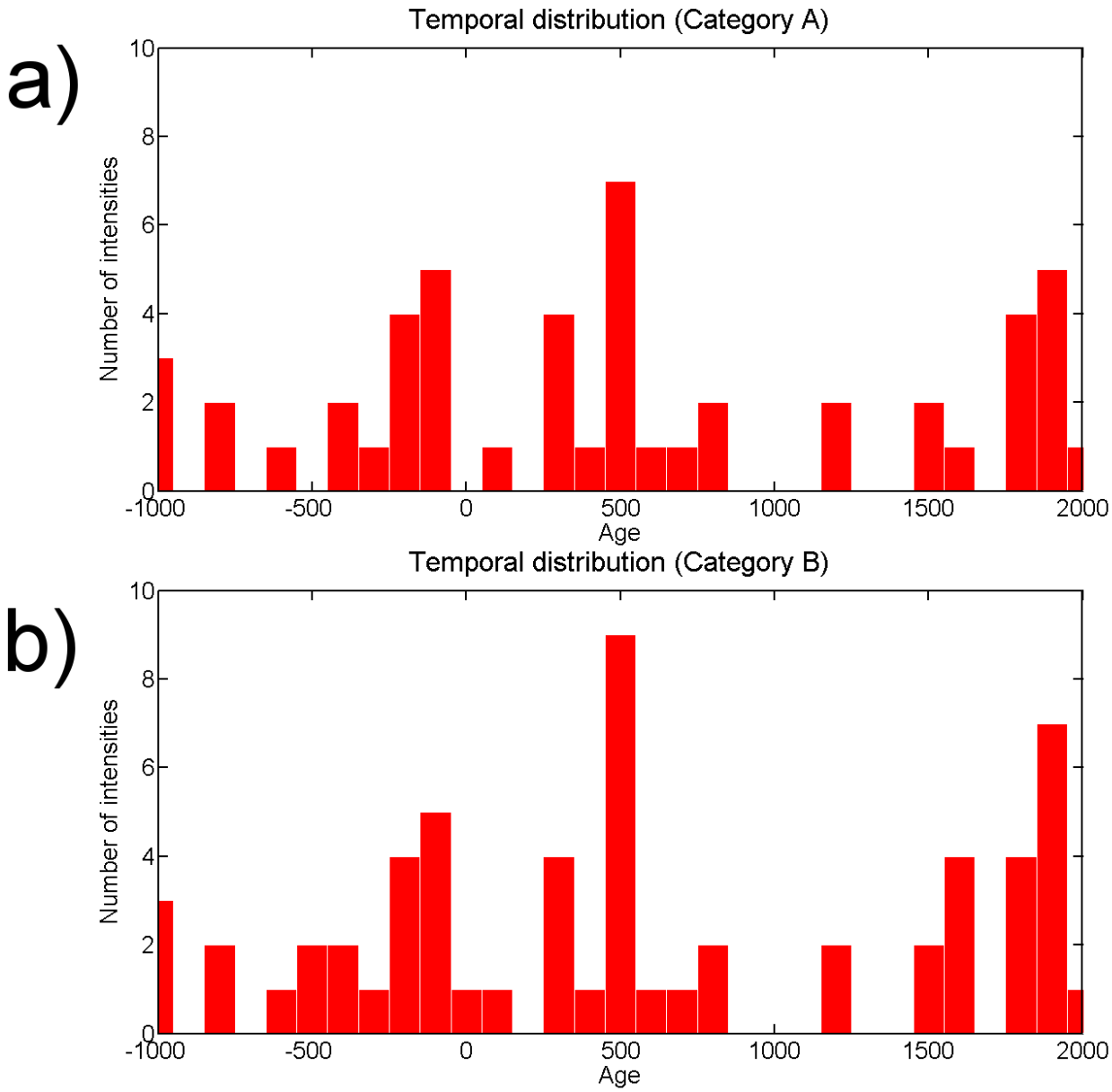


**Figure 4.3.** a) The number of intensity determinations vs. the age for the last three millennia in Mesoamerica for the category A, b). The number of intensity determinations vs. the age for the last three millennia in Mesoamerica for the category A+B.

The analysis of the relocation error shows that large areas of southern United States of America can be also included in our study (the maximum distance is 3639 km with respect to the reference point) due the relocation maximum error is 2.57$\mu$T, less than the established as maximum. For this reason, we have added a total of 144 archeointensity determinations coming from this country when only 17 of them correspond to the category A (from 775 AD to 1978 AD) and other 94 to the category B (from 150 BC

to 1930 AD). Summarizing, the global selected database consists of 74 reliable intensity estimations (category A, Figure 4.4a) and 122 intensities of category B (Figure 4.4b).

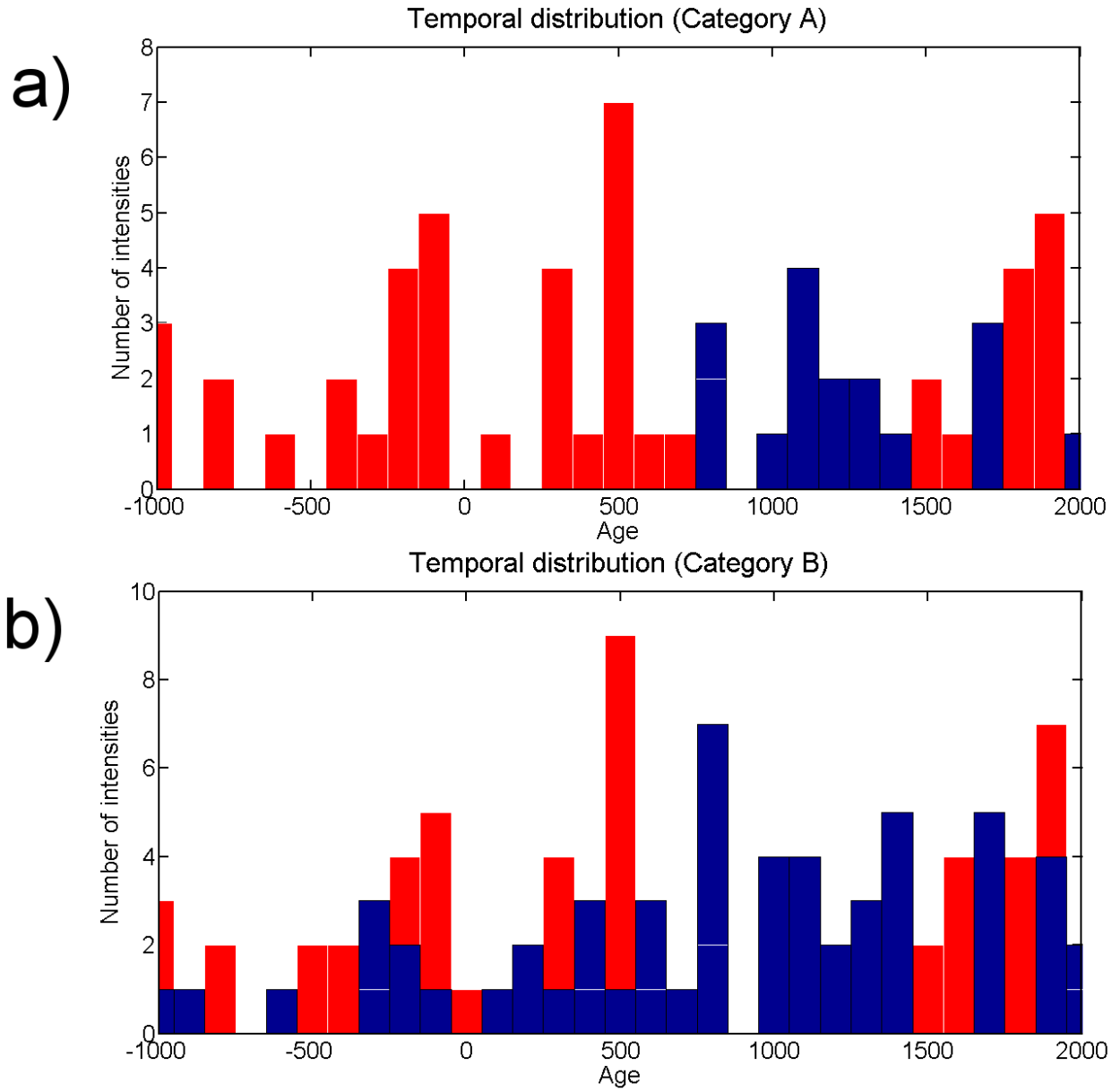


**Figure 4.4** Distribution of archaeointensities for Mesoamerica in red and the southern of the United States of America in blue a) Category A and b) Category B.

### 4.4 First intensity paleosecular variation curve for Mesoamerica and Southern United State of America.

The intensity PSVC has been built using a bootstrap method (following the approach of Thébault and Gallet[64]. The algorithm fits the data to a continuous temporal spline function (the PSVC) where each individual data is considered as the combination of two statistic distributions: 1) A Gaussian distribution with mean and standard deviation given by the intensity parameters. 2) A homogeneous distribution in time with minimum and maximum values delimited by the age uncertainties.

The approach requires several iterations where for each of them a PSVC, $\hat{\boldsymbol{f}}$, is generated by randomly picking up the data from the above detailed statistical functions and applying the next expression:

$$\hat{\boldsymbol{f}} = (\boldsymbol{A^T W A} + \boldsymbol{\lambda D})^{-1} \boldsymbol{A^T W^T f},$$

where $\boldsymbol{f}$ represents the intensity estimations which uncertainties are used to perform the diagonal weight matrix $\boldsymbol{W}$ with $\boldsymbol{w_{ii}} = 1/\sigma_F^2$. $\boldsymbol{A}$ is the parameter matrix based on a set of cubic b-splines with knot points every 50 yr. from 1000 BC to 2000 AD. The matrix $\boldsymbol{D}$ represents a penalty function that constrains the solution by means of the damping parameter $\boldsymbol{\lambda}$. The index $\boldsymbol{T}$ means the transpose matrix.

It is performed different test to estimate the damping parameter. The best compromise between data fitting and the root mean square (rms) error is found when this parameter if fixed as 10. A total of 1500 iterations provide an ensemble of PSVCs (Figure 4.5a)which mean value and standard deviation define the final intensity PSVC for the different datasets detailed in the previous section.

The PSVC of absolute intensity shows almost the same tendency when using Category A (Figure 4.5a) or both (A+B) data for some specific time intervals (Figure 4.5b). The pronounced maximum is observed at about 0 to 500 AD., accompanied with a well-defined minimum at about 550 AD. This tendency is based on high quality absolute archeointensity data from Southern Mexico (Maya Culture) and Guatemala[2,29,58]. The EMF strength variation for younger periods is rather similar since either A or A+B curve shows two maximum points located between 1000 AD and 1500 AD. Finally, the category A curve for the last 200 years show relatively low variation, with a smooth tendency at about 1900 AD.

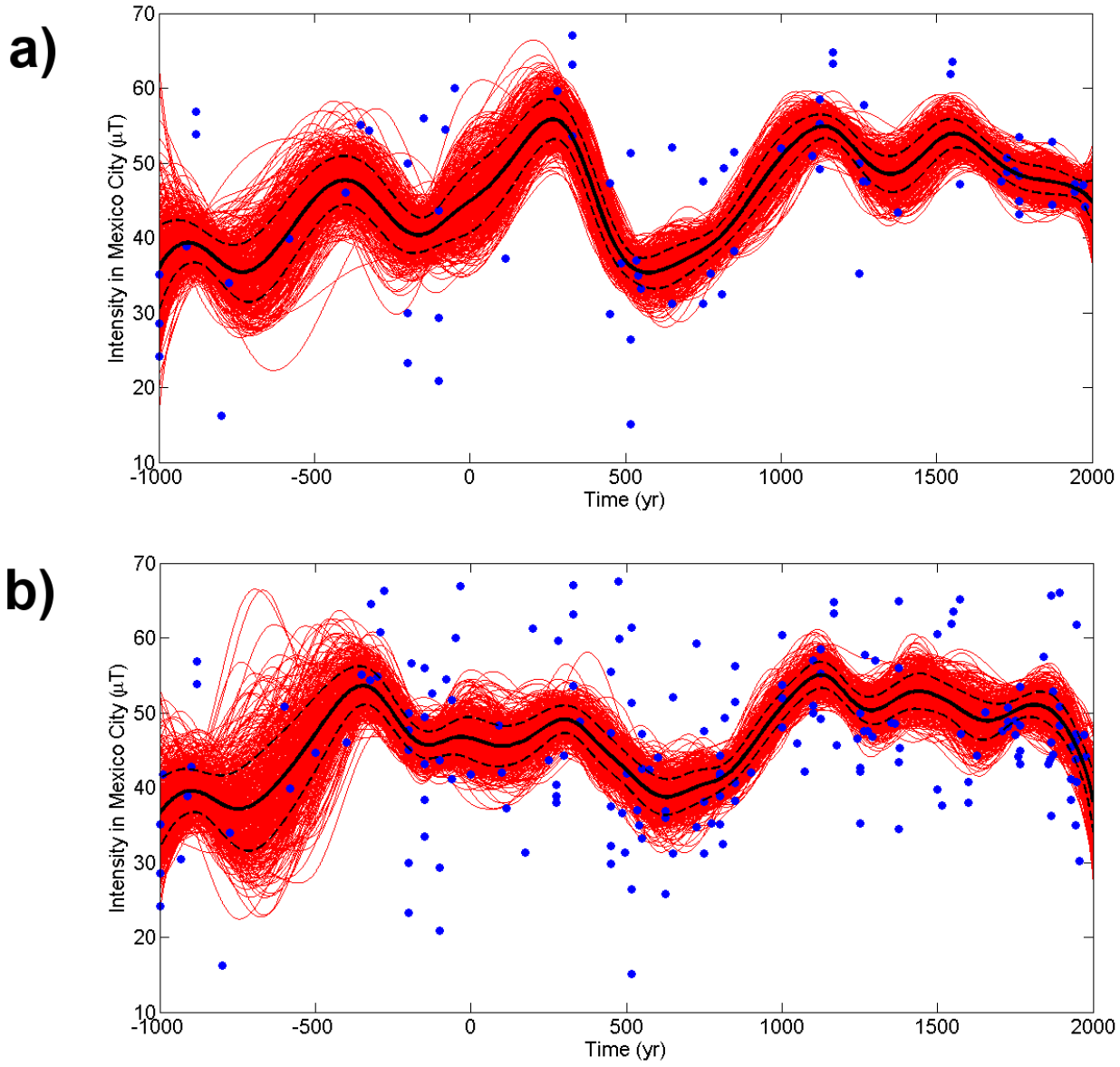


**Figure 4.5. a)** PSVC of reference for the category A (black line) with the data for Mesoamerica and Southern United States (blue dots), the red lines, represented all the synthetic curves after obtain the PSVC curve of reference, b) PSVC for both categories A+B.

### 4.5 Comparison previous local and global geomagnetic reconstructions.

The intensity PSVC of the present study was compared with two representative global model for the Holocene: CALS10k.2[19] and SHA.DIF.14k[63] (Figure 4.6). Both geomagnetic reconstructions were

developed using spatial spherical harmonics up to degree 10 and penalized cubic b-splines in time. The model CALS10k.2[19], was generated by a globally distributed paleomagnetic data from archaeological artifact and volcanic combined with sediments that provided the paleosecular variation of the EMF for the past $10\,000 yr$. The volcanic and archeomagnetic data involved in this model are available in GEOMAGIA50.v3[11]. The model SHA.DIF.14k[63] is a global model of the EMF that covers the last 14 millennial from 12000 BC to 1900 AD, and was developed using archeomagnetic and lava flow data from GEOMAGIA50v2[27,47] which was updated with new archeomagnetic and volcanic studies. No sedimentary data are involved in this field reconstruction.

The comparison (Figure 4.6a) shows how the model CALS10k.2[19] presents a similar but smoother variation for the last 3 millennia with respect to the PSVC of the present study without reaching the maxima and minima amplitudes recorded by the local PSVC. We assume that this effect falls on the use of sedimentary records since they may only provide smoother variations of the past EMF. The SHA.DIF.14k[63] model shows a wide fluctuation of the intensity and several maxima and minima which are not present in our curve. This is probably due to the fact that the SHA.DIF.14k[63] used several archeointensity determinations from Mexico which do not pass the selection criteria and thus were rejected in present study. In fact, the intensity PSVC obtained using all the available data (categories A and B, Figure 4.6b) better agrees with the model prediction but is less reliable due the high degree of uncertainty.

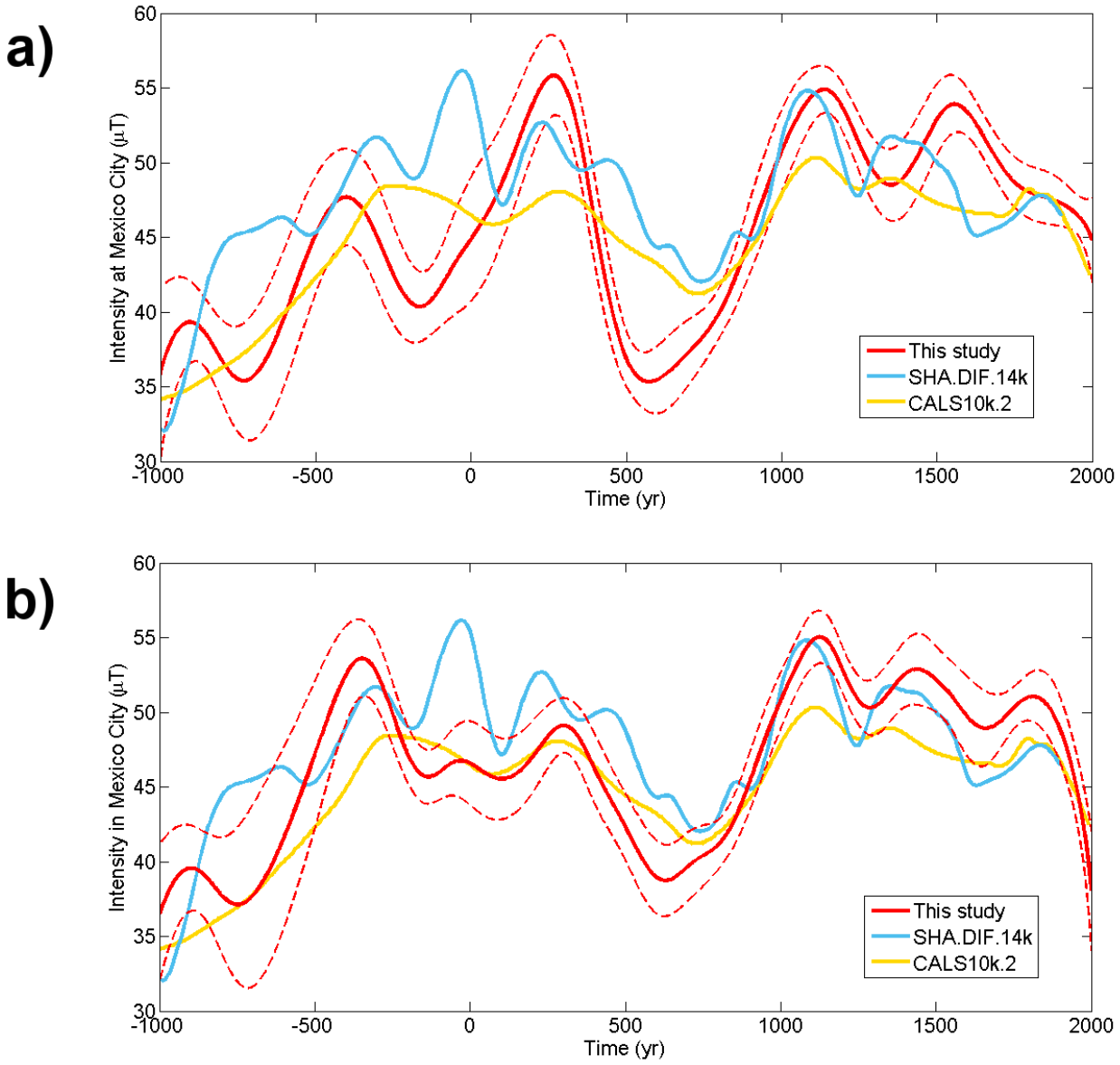


**Figure 4.6.** PSVC of reference for the present study (red line) compared with two geomagnetic global models: CALS10k.2 (green line) and SHA.DIF.14k (blue line). a) PSVC of the category A and b)PSVC of the category B.

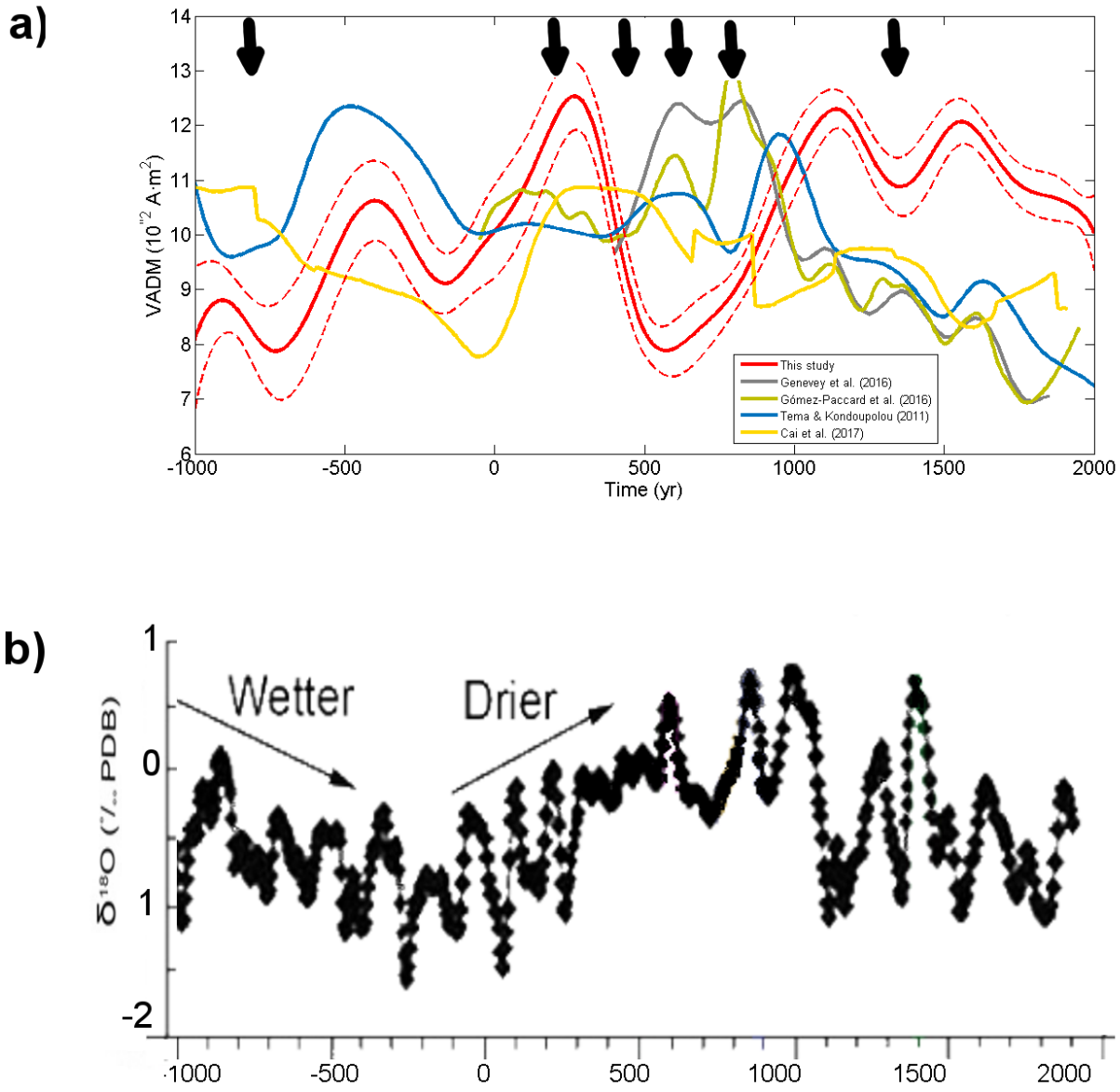


**Figure 4.7.** a) The variation of VADM for western of Europe (Genevey et al., 2016; Goméz-Paccard et al., 2016), eastern of Europe (Tema and Kondopolou et al., 2011), Asia (Cai et al., 2016) and the present study for the last three millennia with the evidence of six jerks detected in Europe together with b) $\delta^{18}$O log plot obtained from the *Lake Punta Laguna*, in northeastern Yucatan Peninsula (Southern Mesoamerica). Reprinted from Quaternary Research, 57, Rosenmeier M. F., Hodell D.A., Brenner M, Curtis J.H, & Guilderson P., A 4000-Year Lacustrine Record of Environmental Change in the Southern

Maya Lowlands, Petén, Guatemala, 183-190, Copyright 2002, permission in process of Elsevier.

Our regional PSVC curve also been compared with recent local PSVC from Europe and Asia trough the estimated virtual axial dipole moments (Figure 4.7). The PSVCs for Europe are:

- The PSVC of Genevey[38] for Western Europe is generated using the approach of Thébault and Gallet[64]. This PSVC considers archeointensities obtained with Thellier[75] and Shaw[70] methods and the criteria $N \geq 3$ and $\sigma_F \leq 15\mu T$ are used to select the most reliable intensities.
- The PSVC of Gómez-Paccard[40] is based on data of Belgium, France, Switzerland, Portugal and incorporated some new data from Spain spanning the last two millennia. Both the approach and the selection criteria in this case were basically similar to our study.
- The PSVC of Tema and Kondopolou[72] for the Eastern Europe (Balkan region) covers the last eight millennia. Archeointensity data comes mainly from Bulgaria but also from Greece, southern Hungary, Serbia and Italy. This PSVC was generated by the use of sliding moving window technique.

The PSVC for Asia:

- The PSVC of Cai[13] for Eastern China covers the last 6 millennia and is based on pottery and porcelain fragments from different locations like Shandong, Liaoning, Zhejiang and the Hebei providences. The PSVC was generated by a similar protocol of Gallet[36]
- The differences between the Central America PSVC and the PSVC from Europe and Asia (Figure 4.7) is notable. An important difference is observed around the last 1000 years when the present PSVC shows significantly higher values of VADM. A careful comparative analysis with the PSVC for the Eastern Europe[72] indicates a time lag between both curves of approximately 700 years, that could be associated with an eastward drift[28] observed $\sim 500$ BC for the azimuthal motion of a positive field feature detected for similar latitudes 20°N and longitudes $-120°$ as the coordinates of the intensities studied in the present work. In order to try to make a better analysis of this possible eastward drift detected in America it is essential to compare the dipole moments (DM) of the global models as SHA.DIF.14k[63] and CALS10k.2[19] with the VADM (Figure 4.8) of the present study in order to try to detect if some of the maxima points coincide.

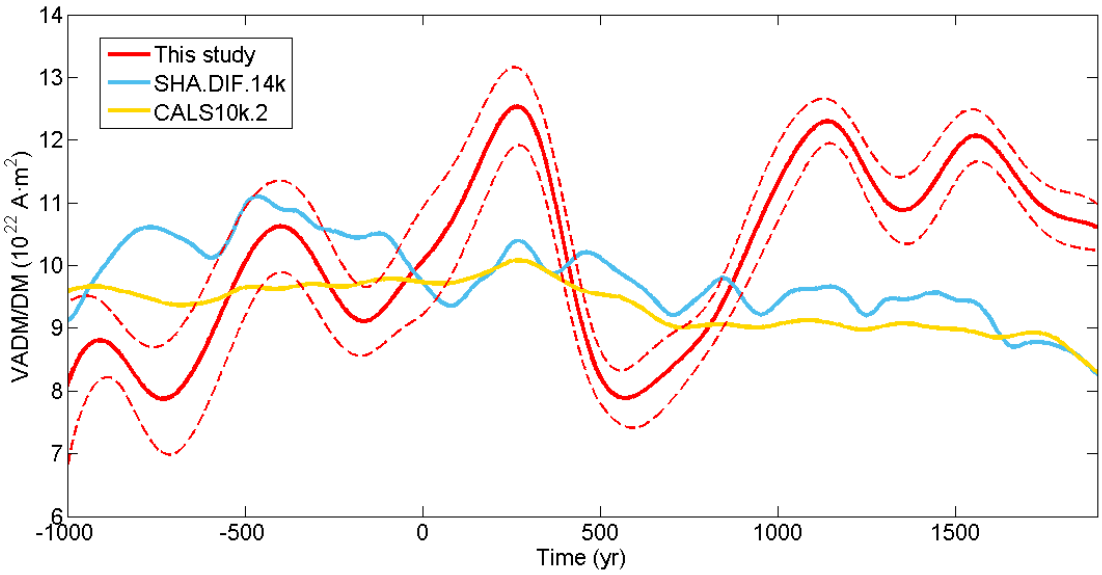


**Figure 4.8.** Comparison between Dipole moment of global model (SHA.DIF.14k and Cals10k.2) and the VADM of the present study.

However, this is difficult due to the low values presented by the DM of both models, but in essential if the PSVC goes through time approximately 700 years, some coincidence may be observed between 500 B.C and 1000 A. Many previous studies of the paleosecular variation provide important information of the rapid intensity changes known as *geomagnetic jerks*[32,35,63,73]. The origin of the geomagnetic jerks is not completely elucidated[28,35]. Gallet[33] proposed that a strongly inclined dipole may be the principal cause, while Dumberry[28] suggest a strong change in the direction of the dominant azimuthal flow near of the boundary of the core in the vicinity of the observed site as a principal mechanism to launch a geomagnetic jerk, and Gallet[35], relate said jerks with changes in the dipole eccentric. Exist several jerks detected by global model and for curves of reference from Europe for the time of interest and it is suppose that some of these anomalous variation may be present in the area of interest.

The Figure 4.7a illustrates six different jerks detected and largely confirmed on Europe(800BC, 200AD, 450AD, 600AD, 800AD, 1400AD)[35,63,72]. The present study speculatively associates two of these jerks with possible climatic changes detected in Punta Laguna[22,69], where the best estimation of the regional paleoclimate changes is reached. Curtis[22], De Menocal[25] and Rosenmeier[69] provide an isotope $\delta^{18}O$ variation for the Holocene (Figure 4.7b) which is linked to the climatic variation, specifically to the dry and wet events. Pétronille[66] reported an inverse correlation over the millennial time scale between the absolute geomagnetic intensity and climate. They suggest that three climatic events are associated with some major cultural discontinuities for the Maya culture. Climatic conditions indicated by the global decrease of $\delta^{18}O$ values are synchronous to the main increases in predicted geomagnetic field and vice-versa. One of these events is associated with the Mayan Hiatus with an increase of the $\delta^{18}O$ between 500 and 550 A.D. corresponding to the minimum in the PSVC of Mesoamerica. *The Mayan collapse* is another important event correlated to the strong aridity period between 850 and 900 A.D., which may be associated with another jerk reported by Gallet[35] around $\sim$800A.D.

### 4.6 Concluding remarks

The principal objective of the present study was to develop the first local intensity PSVC for Mesoamerica, through the compilation of a current database. The relocation error analysis allowed to incorporate some high quality determinations belonging to the sites located at the Southern United States of America.

The PSVC presented a specific behavior to the area of interest for the last 3 millennia's and substantial differences are observed when was compared with global models, as CALS10k.2[19] and SHA.DIF.14k[63], with CALS10k.2[19] due the low reliability of the sedimentary records and with SHA.DIF.14k[63] a less variation due the way was been selected the archeointensities, and the proper properties of the construction of such global model.

Six archeomagnetic jerks reported in the literature may tentatively associated for the temporality of interest and the area in question. These jerks when was related with the present PSVC suggest that could be associated with the slopes of changes after achieve the maximum and minima in contrast to what

report for the regional curve from Europe, where report that such jerks occur in the maximum and minima peaks of the PSVC. Two of them can be correlated to some climatic changes and major cultural discontinuities, especially for the Mayan Culture. The early hypothesis about the link between the fluctuations of the geomagnetic field strength and climate changes over multi-decadal time scales needs further investigations.

The present study suggest the presence of an eastward drift and opens the discussion to news studies with archeodirections to confirm this assumption.

**References.**


1. Aitken M. J., Pesonen, L. J. &Leino, M.A.H., The Thellier paleointensity technique: minisamples versus standard size. J.Geomag. Geoelectr. **43,** 325-331(1991).
2. Alva-Valdivia, L.M., Comprehensive paleomagnetic study of a succession of Holocene olivine basalt flow: Xitle Volcano, Mexico, revisted, *Earth. Planet. Sp.***57,** 839-853, doi:10.1186/BF03351862(2005)
3. Alva-Valdivia, L. M., et al. Absolute geomagnetic intensity data from preclassic Guatemala pottery, *Phys. Earth Planet. Inter*. **180**, 41-51, doi:10.1016/j.pepi.2010.03.002 (2010).
4. Aguilar-Reyes, B., et al. An Integraded archaeomagnetic and $C^{14}$ study on pre-Columbian potsherds and associated charcoals intercalated between Holocene lacustrine sediments in Western Mexico: Geomagnetic implications, *J. Geophy. Res. Solid Earth*, **118**, 2753-2763, doi:10.1002/jgrb.50196(2013).
5. Barton, C.E., Merrill, R. T. & Barbetti, M., Intensity of the Earth's magnetic field over the last 10 000 years, *Phys. Earth Planet. Inter*. **20**, 96-110, doi:10.1016/0031-9201 (1979).
6. Batt, C. M., The British Archaeomagnetic calibration curve: An objective treatment, *Achaeometry*, **39**, 153-168, doi:10.1111/j.1475-4754.1997.tb00795.x (1997).
7. Böhnel, H., Morales J., Caballero, C., Alva L., McIntosh, G., González S., & Sherwood, G. Variation of rock magnetic parameters and paleointensities over a single holocene lava flow. *J. Geomag. Geoelectr.* **49**, 523–542(1997).

8. Böhnel, H. & Molina, R. Secular Variation in Mexico during the last 40,000 years. *Phys. Earth and the Planet. Inter.*, **133**, 99-109 (2002).

9. Bönel, H. Biggin, A. J., Walton, D., Shaw, J., & Share, J. A., Microwave palaeointensities a recent Mexican lava flow baked sediments and reheated poterry. *Earth Planet. Sci. Lett.*, **214**, 221-236(2003)

10. Böhnel, H., Pavón-Carrasco, F. J., Sieron, K., & Mahgoub, A. N., Palaeomagnetic dating of two recent lava flows from Ceboruco volcano, western Mexico, *Geophys. J. Int.*, **207**, 1203-1215, doi:10.1093/gji/ggw310(2016).

11. Brown, M. C, et al. GEOMAGIA50.v3: 2.A new paleomagnetic database for lake and marine sediments, *Earth, Planets and Sp.*, **67**, 70, doi: 10.1186/s40623-015-0233-z(2015).

12. Bucha, V., Taylor, R. E., Berger, R. & Haury, W. E. Geomagnetic intensity: Changes during the past 3000 years in the western hemisphere, *Science*, **168**, 111-114 (1970).

13. Cai S., et al. Archaeointensity results spanning the past 6 kiloyears from eastern China and implications for extreme behaviour of the geomagnetic field, PNAS, **114**, 39-44, doi: 10.1073/pnas.1616976114 (2016).

14. Carrancho Á., et al. Full-Vector Archaeomagnetic Dating of Medieval Limekiln at Pinilla del Valle Site (Madrin, Spain), *Archaeometry*, **59**, 373-294, doi:10.1111/arcm.12245(2016).

15. Casas, Ll., & Incoronato, A., Distribution analysis of errors due to relocation of geomagnetic data using the 'Conversion via Pole' (CVP) method: implications on archaeomagnetic data. *Geophys. J. Int.*, **169**, 448-454, doi: 10.1111/j.1365-246X.2007.03346.x(2007).

16. Chauvin, A., Garcia, Y., Lanos, Ph., & Lauberheimer, F. Paleointensity of the geomagnetic field recovered on archaeomagnetic sites from France. Phys. *Earth. Planet. Inter.*, **120**, 111-136, doi:10.1016/S0031-9201(00)00148-5(2000).

17. Coe, M. D. Olmec civilization, Veracruz, Mexico: Dating of San Lorenzo Phase, *Science*, **155**, 1399-1401 (1967a).

18. Coe, R.S., Paleo-intensities of the Earth's magnetic field determined from Tertiary and Quaternary rocks. J. Geophys. Res. **72(12),** 3247-3262 (1967b)

19. Constable, C., Korte, M., & Panovska, S., Persistent high paleosecular variation activity in

southern hemisphere for at least 10 000 years, Earth Planet. Sci. Lett., **453**, 78-86, doi:10.1016/j.epsl.2016.08.015(2016).

20. Conte-Fasano, G., Urrutia-Fucugauchi, J., Goguitchaichvili, A., Icoronato, A., & Tiano, P., Lava identification by paleomagnetism: a case study and some problems surrounding the 1631 eruption of Mount Vesuvius, Italy. *Earth Planet. Sp.***58,** 1061-1069, doi:10.1186/BF03352611 (2006)

21. Courtillot, V., Gallet Y., Le Mouel, J.L. Flateau, F., & Genevey A. Are there connections between the Earth's magnetic field and climate?, *Earth Planet. Sci. Lett*. **253**, 328-339, doi: 10.1016/j.epsl.2006.10.032(2007).

22. Curtis, J.H., Hodell, D. A., & Brenner, M. Climate variation on the Yucatan Peninsula(México) during the past 3500 years, and implications for the Maya cultural evolution. Quaternay Research, **46**, 37-47, doi: 10.1006/qres.1996. 0042 (1996).

23. Daly, L., & Le Goff M. 1996. An updated and homogeneous world secular variation data base. Smoothing of the Archaeomagnetic results. Phys. Earth and Planet. Int., **93**, 159-190, (1996).

24. Dekkers, M.J., & Bonhël, H.N. Reliable absolute palaeointensities independent of magnetic domain state. *Earth Planet. Sci. Lett.* **248**, 508-517, doi:10.1016/j.epsl.2006.05.040(2006).

25. De Menocal, P.B. Cultural responses to climate change during the Late Holocene. *Science*, **292**, 667-673, doi: 10.1126/science.1059287(2001).

26. Dergachev, V. A., Raspopov, O. M., Vasiliev, S. S., & Jungner, H., Connection between the Earth's Climate Change and Variations in the Geomagnetic Field and Cosmic Ray Fluxes During the Past Ten Thousands of Years, Global Perspectives on Geography, 1, 47-57 (2013).

27. Donadini, F., Korhonen, K. Riisager, P., & Pesonen, L. Database for Holocene geomagnetic Intensity information. Eos Trans AGU, **87**, 137-143, doi:10.1029/2006EO140002(2006).

28. Dumberry, M., & Finlay, C. C. Eastward and westward of the Earth's magnetic field for the last three millennia, Earth Planet. Sci. Lett., **254**, 146-157, doi:10.1016/j.epsl.2006.11.026(2007).

29. Fanjat, G. et al. First archaeointensity determinations on Maya incense burners from Palenque temples, Mexico: new data to constrain Mesoamerica secular variation curve. *Earth Planet. Sci. Lett.* **363**, 168-180, doi:10.1016/j.epsl.2012.12.035(2013).

30. Finlay, C.C., et al. International Geomagnetic Reference Field: the eleventh generation, *Geophys.*

*J. Int.* **183**, 1216-1230, doi: 10.1111/j.1365-246X.2010.04804.x(2010).

31. García-Quintana, A. et al. Datación magnética de rocas volcánicas formadas durante el Holoceno: caso de flujos de lava alrededor de Lago de Pátzcuaro (campo volcánico Michoacán-Guanajuato), *Revista Mexicana de Ciencias Geológicas*, **33**, 209-220, (2016).

32. Gallet, Y., Genevey, A., & Courtillot, V., On the possible occurrence of 'archaeomagnetic jerk' in the geomagnetic field over the past three millennia, *Earth Planet. Sci. Lett.* **214,** 237-242 (2003).

33. Gallet, Y., Genevey, A., & Fluteau, F., Does Earth's magnetic field secular variation control centennial climate change?, *Earth Planet. Sci. Lett.* **236 (1-2)**, 339-347, doi:10.1016/j.epsl.2005.04.045(2005).

34. Gallet, Y., Genevey, A., Le Goff, M., Flutea, F., & Eshraghi S. A. Possible impact of the Earth's magnetic field on the history of ancient civilizations, *Earth Planet. Sci. Lett.*, **246**, 17-26, doi: 10.1016/j.epsl.2006.04.001(2006).

35. Gallet, Y., Hulot, G. Chulliat A., & Genevey, A. Geomagnetic field hemispheric asymmetry and archeomagnetic jerks, *Earth Planet. Sci. Lett.* **284,** 179-186 doi:10.1016/j.epsl.2009.04.028(2009).

36. Gallet, Y., et al. New Late Neolithic (c. 7000–5000 BC) archeointensity data from Syria. Reconstructing 9000 years of archeomagnetic field intensity variations in the Middle East, *Phys. Earth Planet. Inter.*, **238**, 89-103, doi:10.1016/j.pepi.2014.11.003 (2015).

37. Genevey, A., Gallet, Y., Constable, G. C., Korte, M., & Hulot, G. ArcheoInt: An upgrade compilation of geomagnetic field Intensity data for the past ten millenia and its application to the recovery of the past dipole moment. *Geochem. Geophys. Geosyst.* **9,** doi:10.1029./2007GC001881 (2008).

38. Genevey, A. et al. New archeointensity data from French Early Medieval pottery production ($6^{th}$-$10^{th}$ century AD). Tracing 1500 years of geomagnetic field intensity variations in Western Europe, Physics of the Earth and Planetary Interiors, **257**, 205-219, doi:10.1016/j.pepi.2016.06.001(2016).

39. Goguitchaichvili, A., et al. Microwave paleointensity analysis of historic lavas from Paricutín

volcano, Mexico, *Geof. Int.* **44**, 231-240(2005).

40. Gómez-Paccard M., et al. New constraints on the most significant paleointensity change in Western Europe over the last two millennia. A non-dipolar origin?, Earth Planet. Sci. Lett., **454,** 55-64, doi: 10.1016/j.epsl.2016.08.024(2016).
41. Gonzalez S., Sherwood G., Böhnel H., and Schnepp E., Palaeosecular variation in Central Mexico over the last 30000 years: the record from lavas, **130**, 201-219, doi: 10.1111/j.1365-246X.1997.tb00999.x(1997).
42. Gratton, M. N., Goguitchaichvili A., Conte, G., Shaw, J., & Urrutia-Fucugauchi J., Microwave palaeointensity study of the Jorullo volcano (Central Mexico), *Geophys. J. Int*, **161(3),**627-634, doi:10.1111/j.1365-246X.2005.02619.x
43. Hervé, G., Chauvin, A., & Lanos, P. Geomagnetic field variations in Western Europe from 1500 BC to 200AD. Part II: New intensity secular variation curve, *Phys. Earth Planet. Int.* **218,** 51-65, doi:10.1016/j.pepi.2013.02.003 (2013).
44. Hueda, Y., et al. Fechamiento arqueomagnéticos de estucos de los sitios de Teopancazo, Teotihucan, Templo Mayor, Tenochtitlan. *Tesis Licenciatura Arqueología, ENAH, México,* 128 (2000).
45. Jackson, A., Jonkers, A. R. T., & Walker, M. R., Four centuries of geomagnetic secular variation from historical records, *The Royal Society*, **358**, 1768, doi: 10.1098/rsta.2000.0569(2015).
46. Korte, M. & Constable, C.G. Spatial and temporal resolution of millennial scale geomagnetic field models, *ASR*, v. **41**, 57-69, doi:10.1016/j.asr.2007.03.094(2008).
47. Korhonen, K., Donadini, F., Riisager, P., & Pesonen, L., GEOMAGIA50: An archaeointensity database with PHP and MySQL. *Geochem. Geophys. Geosyst*, v.9 doi:10.1029/2007GC001893(2008).
48. Kosterov, A., & Prévot, M., Possible mechanism causing failure of Thellier paleointensity experiments in some basalts, *Geophys. J. Int.* 134, 554-572, (1998).
49. Laj, C., & Channell, J.E.T., , Geomagnetic excursions, (Elsevier B.V., 2007)
50. Lanos, P., Le Goff M., Kovacheva, M. & Schnepp, E., Hierarchical modelling of archeomagnetic data and curve estimation by moving average technique, *Geophys. J. Int.*, **160**, 440–476, doi:10.1111/j.1365-246X.2005.02490.x(2005).

51. Lee, S. S., Secular variation of the intensity of the geomagnetic field during the past 3, 000 years in North, Central and South America, *Ph.D. Thesis, Univ. of Okla.,* Norman (1975).
52. Le Goff, M., Gallet, Y., Genevey, A. & Warmé, N., On archeomagnetic secular variation curves and archeomagnetic dating, *Phys. Earth. Planet. Inter.,* **134**, 201–203(2002).
53. Michalk, D.M, Muxworthy A. R., Böhnel H. N., Maclennan J., & Nowaczyk N., Evaluation of the multispecimen parallel differential pTRM method: A test on historical lavas from Iceland and Mexico, **173(2),** 409-420, doi:10.1111/j.1365-246X.2008.03740.x(2008)
54. Michalk, D. M., et al. M., Application of the multispecimen palaeointensity method to Pleistocene lava flows from the Trans-Mexican Volcanic Belt, Phys. Earth Planet. Int., **179**, 139-156, doi:10.1016/j.pepi.2010.01.005 (2010).
55. Morales, J., Determinación de paleointensidades del campo geomagnético para el Cuaternario en la Sierra de Chichinautzin. M.Sc. *thesis*, *UNAM, Mexico City*, p. 80(1995).
56. Morales, J., Goguitchaichvili, A., & Urrutia-Fucugauchi, J., A rock-magnetic and paleointensity study of some Mexican volcanic lava flows during the Latest Pleistocene to the Holocene. *Earth Planet and Sp*, **53**, 893-902, doi:10.1186/BF03351686(2001).
57. Morales J., Alva-Valdivia L.M., Goguitchaichvili A., & Urrutia-Fucugauchi, J., Cooling rate corrected paleointensities from the Xitle lava flow: Evaluation of within-site scatter for single spot-reading cooling units, *Earth Planet. Sp.,* **58,** 1341-1347 (2006)
58. Morales J. et al., Magnetic properties and acheointensity determination on Pre-Columbian pottery from Chiapas, Mesoamerica, *Earth Planet Sp.,* **61**, 83-91, doi: 10.1186/BF03352887 (2009).
59. Morales, J. et al. Are ceramics and bricks reliable absolute geomagnetic intensity carriers?, Phys. *Earth Planet. Inter.,* **187**, 310-321, doi:10.1016/j.pepi.2011.06.007(2011).
60. Morales, J., Goguitchaishvili A., Olay-Barrientos, M. A., Carvallo, C., & Aguilar-Reyes, B., Archeointensity investigation on pottery vestiges from Puertas de Rolón, Capacha Culture: In search for affinity with other Mesoamerican pre-Hispanic cultures, *Stud. Geophys. Geod.,* **57**, 605-626, doi: 10.1007/s11200-012-0878-z(2013).
61. Nagata, T., Kobayashi, K., & Schwarz, E. J., Archaeomagnetic intensity studies of South and Central America. *J. Geomag. Geoelec.,* **17 (3-4)**, 399-405 doi: 10.5636/jgg.17.399(1965).
62. Néel, L. Some theorical aspects of rock-magnetism, *Adv. Phys*. **4**, 191-243(1955).

63. Pavón-Carrasco, F. J., Osete, M. L., & De Santis, A. Geomagnetic Field Model for the Holocene based on archeomagnetic and lava flow data. *Earth Planet. Sci. Lett.*, **388C**, p.98-109(2014a).

64. Pavón-Carrasco, F.J., Gómez-Paccard, M., Hervé G., Osete, M.L., & Chauvin, A., Intensity of the geomagnetic field in Europe for the last 3 ka: Influence of data quality on geomagnetic field modelling, *Geochem. Geophys. Geosyst.*, **15**, doi: 10.1002/ 2014GC005311(2014b).

65. Pineda, D. M., et al. Magnetic Properties and archeointensity of the Earth's magnetic field recovered from El Opeño, earliest funeral architecture known in western Mesoamerica, *Stud. Geophys. Geod.*, **54**, 575-593, doi:10.1007/s11200-010-0035-5 (2010).

66. Pétronille, M., Goguitchaichvili, Morales, J. Carvallo, C. and Hueda-Tanabe Y., Absolute geomagnetic intensity determinations on Formative potsherds (1400-700) from the Oaxaca Valley, Southwestern Mexico, *Quaternary Research*, **78**, 442-453, doi:10.1016/j.yqres.2012.07.011(2012).

67. Poletti, W., Trinidade, R. I. F., Hartmann G., A., Damiani N., Rech, R. M., Archeomagnetic of Jesuit Missions in South Brazil(1657-1706), *Earth Planet. Sci. Lett.* **455,** 36-47, doi:10.1016/j.epsl.2016.04.006(2016).

68. Rodriguez-Ceja M., et al. Integrated archeomagnetic and micro-Raman spectroscopy study of pre-Columbian ceramics from the Mesoamerican formative village of Cuanalan, Teotihucan Valley, Mexico, J. Geophys. R. **114**, doi: 10.1029/2008JB006106(2009).

69. Rosenmeier, M. F., Hodell, D.A., Brenner M., & Curtis, J. H. A 4000-Year lacustrine record of environmental change in the Southern Maya Lowlands, Petén, Guatemala. *Quaternary Research* **57**, 183-190, doi:10.1006/qres.2001.2305(2002).

70. Shaw, J., A new method of determining the magnitude of the paleomagnetic field applications to 5 historic lavas and five archeological samples, Geophys. *J. R. Astron. Soc.*, **39**, 133-141(1974)

71. Shaw, J., Walton, D., Yang S., Rolph, T., & Share J. A., Microwave archaeointensities from Peruvian ceramics. *Geophys. J. Int.*, **124(1)**, 241-244, doi: 10.1111/j.1365-246X.1996.tb06367.x (1996).

72. Tema, E. & Kondopoulou, D., Secular variation of the Earth's magnetic field in the Balkan region during the last eight millennia based on archaeomagnetic data, *Geophys. J. Int.*, **186**, 603-614,

doi:10.1111/j.1365-246X.2011.05088.x(2011).

73. Thébault, E. & Gallet Y., A bootstrap algorithm for deriving the archeomagnetic field intensity variation curve in the Middle East over the past 4 millennia BC, *Geophys R. Lett.*, **37**, doi:10.1029/2010GL044788(2010).

74. Thébault E., et al. International Geomagnetic Reference Field: the 12th generation, *Earth Planet. Sp.*, **67**, 67, doi:10.1186/s40623-015-0228-9(2015)

75. Thellier, E. & Thellier, O., Sur l'Intesité du champ magnétique terrestre dans le passé historique et géologique, *Ann Géophys.*, **15**, 285-376(1959).

76. Urrutia, J., Maupome, L., & Brosche, P., Archaeomagnetic research programme, I., An introduction to the knowledge of magnetism in pre-Columbian Mesoamerica. Int. Rep., Inst. Geofis., UNAM, Mexico and Obs. Hoher List der Univ. Sternwarte, Bonn, Germany, 25(1981).

77. Urrutia J., Maupome L., & Brosche P., El compás magnético en China y Mesoamérica. *Bol. GEOS*, **6**, 5-7(1986).

78. Urrutia-Fucugauchi, J., Alva-Valdivia, L.M., Goguitchaichvili A., Rivas M. L., & Morales J., Palaeomagnetic, rock-magnetic and microscopy studies of historic lava flows from Paricutin volcano, Mexico: implications for the deflection of palaeomagnetic directions. *Geophys. J. Int.* 156(3), 431-442, doi:10.1111/j.1365-246X.2004.02166.x(2004).

79. Walton, D. A new technique for determining paleomagnetic intensities. *J. Geomag. Geoelectr.* **43**, 333-339doi:10.5636/jgg.43.333(1991).

80. Wolfman, D., Mesoamerican chronology and archaeomagnetic dating, AD 1-1200. *Archaeomagnetic dating Eghmy, J. L. And R. S. Sternberg editors, University of Arizona Press, Tucson* (1990).

## Appendix 1

| N | Ba (mT) | ErBa (mT) | Age | ErAg | Site Lat. (°) | Site Lon. (°) | Archaeo/Volcanic | Method | Ref |
|---|---|---|---|---|---|---|---|---|---|
| 8 | 34.21 | 11.99 | -2962 | 79 | 19.95 | 282.3 | Archaeo | TTCoe | 65 |
| 5 | 52.9 | 4.2 | -2750 | 200 | 19.57 | 257.99 | Volcanic | TTCoe | 41 |
| 5 | 30.28 | 6.26 | -2190 | 85 | 19.69 | 278.84 | Archaeo | TTCoe | 68 |
| 7 | 32.37 | 0.76 | -2120 | 150 | 19.14 | 260.83 | Volcanic | TTCoe | 41 |
| 7 | 75.92 | 10.73 | -2120 | 150 | 19.14 | 260.83 | Volcanic | TTCoe | 41 |
| 8 | 25.9 | 8.8 | -2120 | 150 | 19.18 | 260.83 | Volcanic | TTCoe | 56 |
| 3 | 28.9 | 5.5 | -1880 | 150 | 19.45 | 257.89 | Volcanic | TT and Shaw | 41 |
| 6 | 35.3 | 3.4 | -1373 | 108 | 19.25 | 283.76 | Archaeo | TTCoe | 60 |
| 5 | 35.9 | 4 | -1275 | 125 | 17.08 | 263.25 | Archaeo | TTCoe* | 66 |
| 4 | 24.7 | 2.5 | -1275 | 125 | 17.08 | 263.25 | Archaeo | TTCoe* | 66 |
| 3 | 28 | 5.5 | -1275 | 125 | 17.08 | 263.25 | Archaeo | TTCoe* | 66 |
| 6 | 40.1 | 4.4 | -1260 | 30 | 19.456 | 281.55 | Volcanic | TTCoe | 31 |

| | | | | | | | | | |
|---|---|---|---|---|---|---|---|---|---|
| 8 | 39.2 | 1.4 | -1191 | 215 | 19.95 | 257.7 | Archaeo | TTCoe* | 65 |
| 8 | 38.1 | 2.5 | -1191 | 215 | 19.95 | 257.7 | Archaeo | TTCoe* | 65 |
| 6 | 35.3 | 8 | -1191 | 215 | 19.95 | 257.7 | Archaeo | TTCoe* | 65 |
| 6 | 25 | 2.3 | -1191 | 215 | 19.95 | 257.7 | Archaeo | TTCoe* | 65 |
| 8 | 29.4 | 6.5 | -1191 | 215 | 19.95 | 257.7 | Archaeo | TTCoe* | 65 |
| 6 | 33.8 | 4.8 | -1191 | 215 | 19.95 | 257.7 | Archaeo | TTCoe* | 65 |
| 3 | 40.2 | 3 | -1191 | 215 | 19.95 | 257.7 | Archaeo | TTCoe* | 65 |
| 4 | 35.6 | 1.6 | -1191 | 215 | 19.95 | 257.7 | Archaeo | TTCoe* | 65 |
| 4 | 35.1 | 1.8 | -1191 | 215 | 19.95 | 257.7 | Archaeo | TTCoe* | 65 |
| 3 | 34.9 | 5.7 | -1191 | 215 | 19.95 | 257.7 | Archaeo | TTCoe* | 65 |
| 2 | 32.5 | 1 | -1191 | 215 | 19.95 | 257.7 | Archaeo | TTCoe* | 65 |
| 3 | 33.8 | 1.7 | -1191 | 215 | 19.95 | 257.7 | Archaeo | TTCoe* | 65 |
| 2 | 33.2 | 3 | -1191 | 215 | 19.95 | 257.7 | Archaeo | TTCoe* | 65 |
| 4 | 29.6 | 5.6 | -1191 | 215 | 19.95 | 257.7 | Archaeo | TTCoe* | 65 |
| 4 | 27.8 | 5.3 | -1000 | 150 | 17.15 | 263.2 | Archaeo | TTCoe* | 66 |
| 6 | 23.5 | 2.3 | -1000 | 150 | 17.15 | 263.2 | Archaeo | TTCoe* | 66 |
| 5 | 34.1 | 2.8 | -1000 | 150 | 17.15 | 263.2 | Archaeo | TTCoe* | 66 |
| 9 | 39 | 4 | -910 | 50 | 19.624 | 276.9873 | Volcanic | MulSp | 54 |

| | | | | | | | | | |
|---|---|---|---|---|---|---|---|---|---|
| 2 | 40.5 | 14.4 | -900 | 100 | 14.61 | 270.53 | Archaeo | TTCoe | 3 |
| 7 | 54 | 5 | -880 | 40 | 19.624 | 277.0317 | Volcanic | MulSp | 54 |
| 8 | 57 | 2 | -880 | 40 | 19.6223 | 277.0679 | Volcanic | MulSp | 54 |
| 7 | 15.3 | 2.8 | -800 | 100 | 14.61 | 270.53 | Archaeo | TTCoe | 3 |
| 4 | 33 | 3.1 | -775 | 75 | 17.15 | 263.2 | Archaeo | TTCoe* | 66 |
| 4 | 39.95 | 6.54 | -580 | 50 | 19.62 | 281.57 | Archaeo | TTCoe* | 58 |
| 3 | 42.2 | 7 | -500 | 100 | 14.61 | 270.53 | Archaeo | TTCoe | 3 |
| 3 | 42.2 | 7 | -500 | 100 | 14.61 | 270.53 | Archaeo | TTCoe | 3 |
| 7 | 43.5 | 3.9 | -400 | 100 | 14.61 | 270.53 | Archaeo | TTCoe | 3 |
| 4 | 53.3 | 5.1 | -350 | 75 | 16.7 | 266.8 | Archaeo | TT and Shaw | 51 |
| 7 | 52.6 | 7.2 | -325 | 217 | 16.73 | 266.74 | Archaeo | TTCoe* | 58 |
| 1 | 55 | 0 | -300 | 0 | 19.6 | 267.3 | Volcanic | TT and Shaw | 51 |
| 5 | 28.3 | 2.3 | -200 | 100 | 14.61 | 270.53 | Archaeo | TTCoe | 3 |
| 5 | 22 | 2.4 | -200 | 100 | 14.61 | 270.53 | Archaeo | TTCoe | 3 |
| 4 | 48.3 | 1.3 | -200 | 75 | 16.6 | 266.5 | Archaeo | TT and Shaw | 51 |
| 2 | 43.5 | 0.5 | -200 | 75 | 16.6 | 266.5 | Archaeo | TT and Shaw | 51 |
| 1 | 46.1 | 0 | -200 | 75 | 16.7 | 266.7 | Archaeo | TT and Shaw | 51 |
| 8 | 55.9 | 5.4 | -150 | 150 | 19.35 | 260.84 | Volcanic | TT and Shaw | 61 |

| | | | | | | | | | |
|---|---|---|---|---|---|---|---|---|---|
| 1 | 36.3 | 2.6 | -150 | 100 | 14.61 | 270.53 | Archaeo | TTCoe | 68 |
| 8 | 41.3 | 4.7 | -100 | 100 | 14.61 | 270.53 | Archaeo | TTCoe | 3 |
| 6 | 27.7 | 6 | -100 | 100 | 14.61 | 270.53 | Archaeo | TTCoe | 3 |
| 6 | 19.7 | 3.8 | -100 | 100 | 14.61 | 270.53 | Archaeo | TTCoe | 3 |
| 13 | 54.8 | 6.6 | -80 | 60 | 19.93 | 260.82 | Volcanic | TTCoe | 53 |
| 2 | 39.8 | 0.8 | -62 | 63 | 16.7 | 266.8 | Archaeo | TT and Shaw | 51 |
| 2 | 50 | 0.1 | -62 | 63 | 16.7 | 266.8 | Archaeo | TT and Shaw | 51 |
| 9 | 59.9 | 7.7 | -50 | 0 | 19.3 | 260.82 | Volcanic | TTCoe | 2 |
| 9 | 66.8 | 10.1 | -35 | 55 | 19.32 | 260.82 | Volcanic | TT and Shaw | 41 |
| 4 | 36 | 0.8 | 113 | 112 | 16.7 | 266.8 | Archaeo | TT and Shaw | 51 |
| 17 | 59.6 | 3.5 | 280 | 0 | 19.3 | 260.8 | Volcanic | TTCoe | 57 |
| 2 | 42 | 1 | 300 | 100 | 15 | 267.8 | Archaeo | TT and Shaw | 51 |
| 9 | 53.4 | 4.2 | 330 | 50 | 19.08 | 260.87 | Volcanic | Microwave | 9 |
| 14 | 66.8 | 7.1 | 330 | 50 | 19.08 | 260.87 | Archaeo | Microwave | 9 |
| 15 | 62.9 | 2.7 | 330 | 50 | 19.08 | 260.87 | Volcanic | TTCoe | 7 |
| 2 | 49 | 0.1 | 350 | 0 | 19.7 | 261.2 | Archaeo | TTCoe | 12 |
| 4 | 44.8 | 3.1 | 450 | 150 | 14.7 | 269.5 | Archaeo | TTCoe | 12 |
| 14 | 29.1 | 0.9 | 450 | 50 | 17.48 | 267.96 | Archaeo | TTCoe* | 29 |

| | | | | | | | | | |
|---|---|---|---|---|---|---|---|---|---|
| 6 | 36.8 | 1.6 | 485 | 85 | 19.85 | 259.25 | Archaeo | TTCoe | 4 |
| 1 | 64 | 0 | 475 | 25 | 14.7 | 269.5 | Archaeo | TTCoe | 12 |
| 11 | 44.3 | 17 | 500 | 50 | 23.7 | 258 | Archaeo | TT* | 1 |
| 6 | 59.5 | 13.8 | 518 | 130 | 16.73 | 266.74 | Archaeo | TTCoe* | 58 |
| 7 | 14.6 | 1.5 | 518 | 130 | 16.73 | 266.74 | Archaeo | TTCoe* | 58 |
| 6 | 49.7 | 5.2 | 518 | 130 | 16.73 | 266.74 | Archaeo | TTCoe* | 58 |
| 7 | 25.6 | 0.9 | 518 | 130 | 16.73 | 266.74 | Archaeo | TTCoe* | 58 |
| 7 | 37.2 | 3.4 | 535 | 105 | 19.85 | 259.25 | Archaeo | TTCoe | 4 |
| 5 | 35.2 | 1.3 | 542 | 107 | 19.85 | 259.25 | Archaeo | TTCoe | 4 |
| 10 | 32.5 | 1.2 | 550 | 50 | 17.48 | 267.96 | Archaeo | TTCoe* | 29 |
| 4 | 49.3 | 3.8 | 650 | 150 | 14.7 | 269.5 | Archaeo | TTCoe | 12 |
| 8 | 30.5 | 1.1 | 650 | 50 | 17.48 | 267.96 | Archaeo | TTCoe* | 29 |
| 4 | 45 | 1.4 | 750 | 150 | 14.7 | 269.5 | Archaeo | TTCoe | 12 |
| 8 | 30.5 | 0.6 | 750 | 20 | 17.48 | 267.96 | Archaeo | TTCoe* | 29 |
| 2 | 42 | 2 | 800 | 100 | 15 | 267.8 | Archaeo | TT and Shaw | 51 |
| 15 | 31.7 | 0.7 | 810 | 40 | 17.48 | 267.96 | Archaeo | TTCoe* | 29 |
| 7 | 47.8 | 5.5 | 817 | 164 | 16.73 | 266.74 | Archaeo | TTCoe* | 58 |
| 2 | 40.5 | 0.5 | 900 | 100 | 16.4 | 267.3 | Archaeo | TT and Shaw | 51 |

| | | | | | | | | | |
|---|---|---|---|---|---|---|---|---|---|
| 4 | 63.8 | 1 | 1168 | 0 | 20 | 260.7 | Archaeo | TT and Shaw | 51 |
| 4 | 65.3 | 3.9 | 1168 | 0 | 20 | 260.7 | Archaeo | TT and Shaw | 51 |
| 6 | 58.96 | 5.82 | 1266 | 261 | 21.1 | 284.58 | Volcanic | MulSp | 10 |
| 2 | 48.5 | 0.5 | 1350 | 150 | 19 | 261.7 | Archaeo | TT and Shaw | 51 |
| 9 | 61.6 | 1.3 | 1545 | 5 | 19.01 | 262.71 | Volcanic | MulSp* | 54 |
| 9 | 65 | 6 | 1550 | 5 | 21.18 | 255.47 | Volcanic | MulSp* | 54 |
| 4 | 47 | 1.2 | 1575 | 75 | 19 | 261.7 | Archaeo | TT and Shaw | 51 |
| 1 | 43 | 16.8 | 1600 | 50 | 23.7 | 258 | Archaeo | TT* | 1 |
| 2 | 40.1 | 16.2 | 1600 | 50 | 23.7 | 258 | Archaeo | TT* | 1 |
| 2 | 46.7 | 17.5 | 1625 | 75 | 23.7 | 258 | Archaeo | TT* | 1 |
| 4 | 45 | 3.8 | 1708 | 8 | 14.7 | 269.5 | Archaeo | TTCoe | 12 |
| 2 | 43 | 1 | 1761 | 211 | 17.3 | 263.2 | Archaeo | TT and Shaw | 51 |
| 21 | 45 | 0 | 1766 | 7 | 19.5 | 258 | Volcanic | MulSp | 24 |
| 7 | 48.03 | 5.71 | 1766 | 7 | 19 | 258.25 | Volcanic | TTCoe | 20 |
| 5 | 53.5 | 9.2 | 1766 | 7 | 19.48 | 257.75 | Volcanic | TTCoe and Microwave | 42 |
| 6 | 43.2 | 3.5 | 1766 | 7 | 19.48 | 257.75 | Volcanic | TTCoe and Microwave | 42 |
| 9 | 45.42 | 6.28 | 1870 | 5 | 21.124 | 104.54 | Volcanic | MulSp | 10 |

| | | | | | | | | | |
|---|---|---|---|---|---|---|---|---|---|
| 8 | 54 | 6 | 1870 | 1 | 21.1 | 255.41 | Volcanic | MulSp* | 54 |
| 8 | 47.1 | 1.4 | 1943 | 1 | 19.32 | 257.86 | Volcanic | MulSp* | 54 |
| 21 | 45.9 | 1.25 | 1943 | 0 | 19 | 258 | Volcanic | MulSp | 24 |
| 12 | 43.8 | 19.8 | 1945 | 5 | 19.47 | 257.75 | Volcanic | TTCoe | 76 |
| 6 | 35 | 19 | 1945 | 1 | 19.47 | 257.75 | Volcanic | Microwave | 38 |
| 2 | 61.85 | 8.17 | 1948 | 5 | 19.5 | 257.8 | Volcanic | TT and Shaw | 41 |
| 3 | 40.75 | 4.79 | 1948 | 5 | 19.5 | 257.8 | Volcanic | TT and Shaw | 41 |
| 4 | 46.8 | 1.3 | 1971 | 0 | 19 | 261.7 | Archaeo | TT and Shaw | 51 |

**Appendix 4. 1.** Available archaeointensity data from Mesoamerica, N: Number of specimens used, Ba: Archaeointensities, ErBa: Uncertainty associated, Age: Associated age to each one of the intensities, ErAg: Age Uncertainty, SiteLat: Latitude site., SiteLon: Longitude of site, Archaeo/Volcanic: Type of material used, Method: Method used to determine absolute intensity, Ref: References, *Anisotropy correction (For more information see the reference).

# 5. Secular Variation and Excursions of the Earth Magnetic Field during the Plio-Quaternary: New Paleomagnetic Data from Radiometrically Dated Lava Flows of the Colima Volcanic Complex (Western Mexico)

## 5.1 Abstract

Detailed rockmagnetic and paleomagnetic investigations were performed on selected lava flows from the Colima Volcanic Complex (CVC) estimated in the western sector of the Trans-Mexican Volcanic Belt. Reliable paleomagnetic directions were obtained from 21 Ar-Ar dated lava flows (205 standard paleomagnetic cores) within the time interval from 372 to 34 ka. Ti-poor titanomagnetite is the main magnetic carrier in most of the samples, while some of them exhibit Curie temperatures ranging from 300 to 340°C, pointing to high Ti content in agreement with scanning electron microscopy observations. Nineteen sites yielded normal polarity magnetization as expected from Bruhnes Chron lavas, while two remaining lava flows show clearly defined transitional paleomagnetic directions. The mean direction excluding the transitional data is D=1.2°, I=38.2° (k=39.5, $\alpha_{95}$=5.5°). The corresponding paleomagnetic poles yield a longitude φ=270.1° and a latitude λ=87.6° (K=35.9, $A_{95}$=5.3°). This paleodirection is practically undistinguishable from the one expected for Pleistocene, as derived from the references poles for the stable North America. This suggests that no major tectonic rotation occurred in the studied area. The paleosecular variation is analyzed through the scatter of virtual geomagnetic poles (VGP) using the traditional cut-off angles and the cut-off angle of Vandamme. The dispersion estimated through the parameter $S_F$=13.0, with an upper confidence limit $S_U$=15.2 and a lower confidence limit $S_L$=12.7 is consistent with the recent geomagnetic field models for the last 5 My. The present study yields the

evidence of two "transitional" lava flows, whose age likely correspond to the Mono Lake or Laschamp excursion and to the Calabrian Ridge 1 or Portuguese Margin excursion, respectively.

Keywords: Paleomagnetism, Paleosecular Variation, Excursion, Colima Volcano, Trans-Mexican Volcanic Belt

## 5.2 Introduction

The current configuration of the Earth's Magnetic Field (EMF) is well known from the data of the global magnetic observatories and satellite missions, describing both dipolar and non-dipolar components and their fluctuations. The reconstruction of the geomagnetic field is made for different periods in the time after the obtention of direct measurement from the records of the magnetic carriers. These represent one of the principal topics of the modern paleomagnetic research. Different types of variations can be distinguished regarding their magnitude, duration and the global or regional character. Apart from obtaining new and reliable paleomagnetic records from different geological times, it is also necessary to develop mathematical models of the behavior of the ancient geomagnetic field, which help to understand the fine characteristics of the EMF.

The geomagnetic excursions and reversals are of particular interest in modern geo- and paleomagnetism research. Polarity transition are generally considered as an event of relatively short duration, usually spanning $10^3$ - $10^4$ years (e.g, Merrill and McFadden 2003). Excursions are defined in terms of very brief ($<10^3$ years) deviation of virtual geomagnetic pole (VGP) positions from the geocentric axial dipole (GAD) that lies outside the range of secular variation for a particular population of VGP (Laj. and Channell, 2007).

The geomagnetic polarity time scale, obtained from numerous studies conducted around the world, is mostly based on marine and lacustrine sediments (Laj and Channell, 2007). The paleomagnetic excursions are considered as a regional event that provide invaluable information on the behaviour of the geodynamo during the transitional state. It is particularly important for the late Pleistocene because the refinements related with extinction events and human evolution during some critical periods. Secular variation and field reversal rate are strongly influenced by the variations at the core-mantle boundary (Glatzmaier et al., 1997). Volcanic rocks are considered as reliable paleomagnetic recorders because of the high stability of the thermoremanent magnetization that provides instantaneous record of the ancient EMF (e.g, Prévot et al., 1985), but the records are discontinuous in the time, because they are strictly tied to volcanic eruptions. For these reason is important fill the gaps of the current database of the area of interest and globally.

The present study is aimed to contribute to the time-averaged field global database and geomagnetic polarity instability time scale for the last 5 My. For this purpose, we collected recently Ar-Ar dated lava flows associated to the Colima Volcano.

---

## 5.3 Geological setting and sampling

The Colima Volcanic Complex (CVC) is a volcanic chain oriented N-S, and is composed by three andesitic stratovolcanoes: El Cantaro, Nevado de Colima and Colima volcano. The CVC is located in the central part of Colima Graben and belongs to the western portion of the Trans-Mexican Volcanic Field (TMVF), one of the largest continental volcanic arcs on the American continent with more than 1000 km

of length (Luhr et al., 1990a.). This volcanic plateau approximately 1000-2000mts high, roughly extends from the Pacific Ocean to the Gulf of Mexico (Figure 5.1).

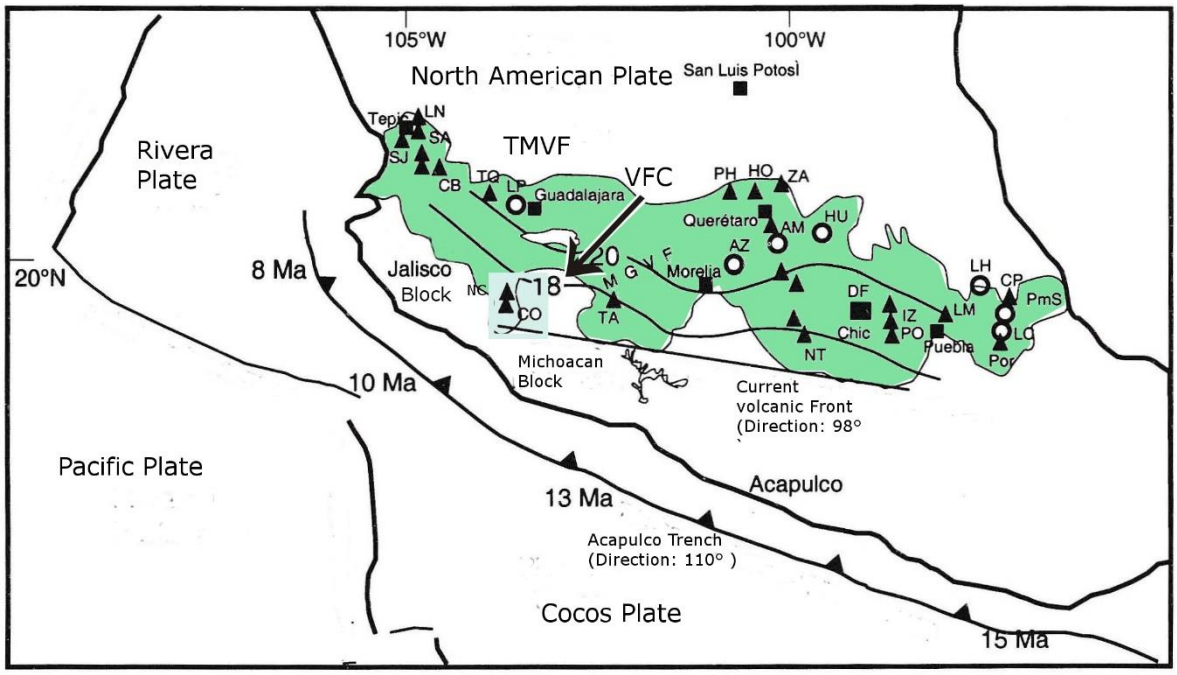


**Figure 5.1**. Location of the Trans-Mexican Volcanic Field (TMVF, selected area green). Tectonic environment and principal volcanic centers of TMVB. The ages in Trench refers to the plate entering the subduction zone. Triangles indicate the main stratovolcanoes belong TMVF: The Navajas (LN); Sangagüey (SA); San Juan (SJ); Ceboruco (CB); Tequila (TQ); Volcano Colima (VC); Tancitaro (TA); Palo Huerfano (PH); The Joya (HO); The Zamorano (ZA); Nevado of Toluca (NT); Iztaccíhuatl (IZ); Popocatépetl (PO); The Malinche (LM); Cofre of Perote (CP); Pico of Orizaba (Por); The blue box represent the area covered by Volcanic Field of Colima (VFC) with its two main structures, Nevado of Colima and Colima volcano. The circles indicate volcanic calderas: The Primavera (LP); The Azufres (Al); Amealco (AM); Huichapan (HU); The Humeros (LH); MGVF is one of the principal field volcanos: Michoacan Guanajuato Volcanic Field, Chic is the Sierra Chichinautzin; Pms Chiconquaco-Palma Sola.

The Colima volcano has a large historical volcanology recorded due to its intense activity (Cortes et al., 2010). The formation of CVC main buildings started about 1.5 My ago, with the building of the Cantaro volcano; and its relatively intense activity continued until approximately 1 My ago (Allan et al., 1986). Later, the volcanic activity moved about 15 km to the south, with the formation of Nevado de Colima, which involves three periods of eruptive activities between 0.53 and 0.15 My (Robien et al,. 1987). The next important event took place at about 50 kys, 5 km to the south, with the formation of the Colima volcano. That started by the building of the Paleofueogo (Robin et al, 1987), where several consecutive collapses occurred (Luhr et al,. 1988; Robin et al., 1987; Komoroswki et al., 1997, Cortes et al., 2005, 2010).

Due the large and permanent activity of the Colima volcano until now, it has been the center of the recent studies and for that reason it account with many historical records and 11 K-Ar absolute dating were first available (Allan et al., 1986; Robien et al., 1987). Cortes (2015) reported recently of 30 new absolute Ar-Ar radiometric dating. In contrast, the eruptive history of the El Cantaro and Nevado de Colima volcanoes is still poorly constrained.

Our sampling strategy was based on the Cortes (2015) investigation (Figure 5.2A). We sampled 21 out of the 30 sites (Figure 5.2B) reported in this work for the Colima volcano, prioritizing fresh outcrops with no alteration and relatively easy access. In total, 205 standard paleomagnetic cores were obtained with a portable drill and were oriented using both magnetic (Brunton) and solar compasses. In few cases, however only magnetic orientation was possible and local magnetic declination is considered as the correction factor.

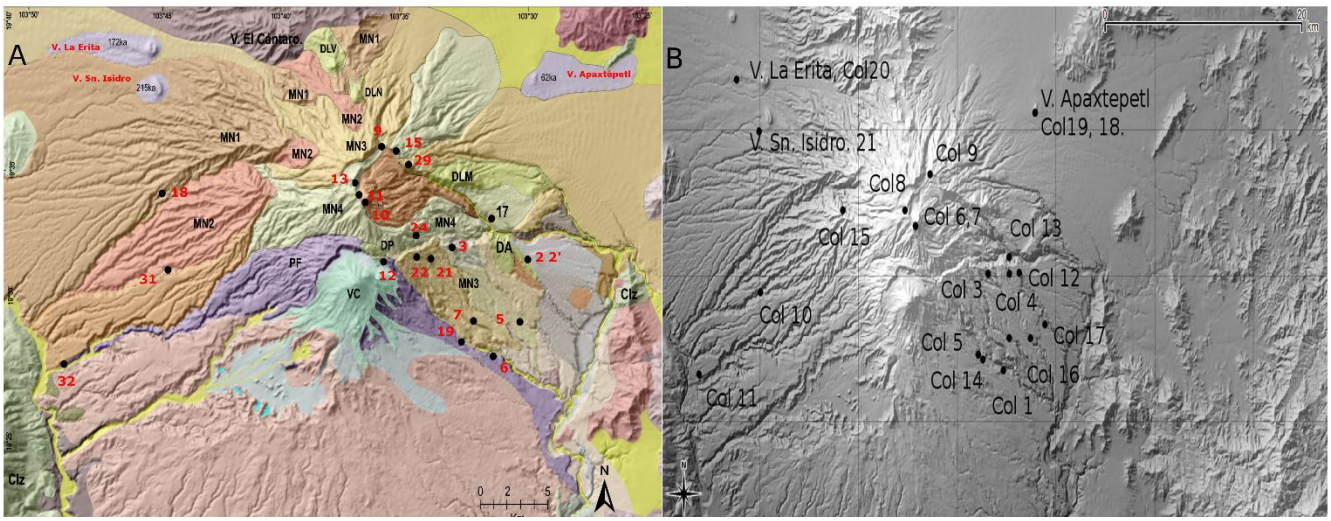


**Figure 5.2**. Geological map of Volcanic Field Colima (VFC) area showing sample site locations. a) All 30 available radiometric dates from the area Córtes et al., 2015. b) Location of 21 paleomagnetic sites for this study.

## 5.4 Identification of magnetic carriers

In order to identify the magnetic carriers responsible for the remanent magnetization and to obtain information about their paleomagnetic stability, several rock-magnetic experiments were carried out. These experiments included:

1. The acquisition of continuous thermomagnetic curves (susceptibility in low field as a function of temperature) to determine the Curie temperatures of the main magnetic minerals with the use of the differential method of Tauxe (1998). Continuous (*K*-T) measurements in air were performed with a MS2 Bartinton susceptibility bridge equipped with a temperature range of 30°C-650°

2. Magnetic hysteresis experiments. The hysteresis loops and associated isothermal remanet magnetization (IRM) acquisition curves were measured using a variable field translation

balance. Measurements were carried out on whole-rock powdered specimens, and in each case, first IRM acquisition and backfield curves were recorded first.

Typical results of rockmagnetic experiments are reported in the Figure 5.3. (Sites Col 2, 3, and 7). In most of the cases the thermomagnetic curves reveal, with a Curie temperature Tc of 560°C, the presence of Ti-poor titanomagnetite as the unique carrier of remanence and indicate moderate degree of alteration due to heating. In some specimens, Ti-rich titanomagnetite seems to co-exist with the almost pure magnetite phase (sample 94C064 corresponding to site Col 7).

Corresponding hysteresis curves are symmetric yielding quite similar parameters, near to the origin, without evidence of wasp-waisted behaviour (Tauxe et al., 1996), which probably reflect very restricted ranges of the opaque mineral coercivities. When judging the ratios obtained from the hysteresis curves, it seems that the samples have a pseudo simple domain PSD in the Day plot provided by Dunlop (2002) (Figure 5.3d)

Isothermal remanence acquisition curves are sensitive to the magnetic mineralogy, concentration and grain size properties. Almost all samples are saturated at about at about 300 mT applied magnetic field, which indicate the presence of a ferromagnetic phase with moderate coercivity as may be expected from magnetite and titanomagnetite grains (Tauxe, 2010).

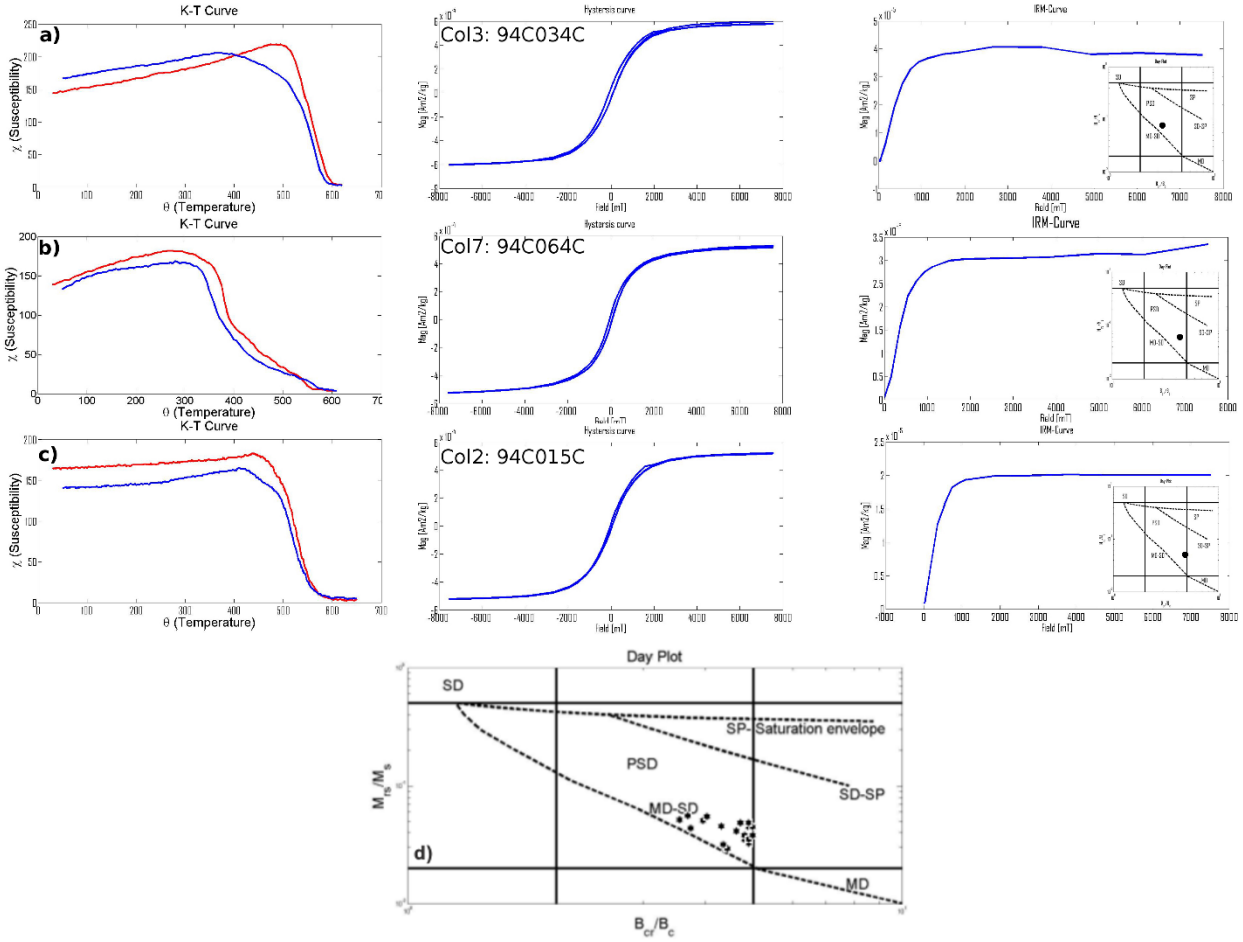


**Figure 5.3.** A summary of rock-magnetic experiments for the most representative samples: Susceptibility vs. Temperature curves, the red curve represent the heating curve and the blue is the cooling curve. Hysteresis curves for an induced magnetic field. Isothermal remanence acquisition curves obtained with a variable field translation balance with the Day Plot (see also Dunlop, 2002a) to estimate the domain state (Single-Domain, SD; pseudo-single-domain, PSD; multidomain, MD; superparamagnetic, SP; MD-SD and SD-SP, mixture) of magnetic carriers of hysteresis parameters $M_{rs}/M_s$ versus $B_{cr}/B_c$. a)Sample 94C034A from Col 3, b)Sample 94C064C from Col 7, c)Sample 94C015C from Col 2 and d) Relation of the ratios of hysteresis parameters for the remained samples.

## 5.5 Remanence properties

Remanent magnetization was measured using a JR-6 spinner magnetometer. At the initial stage, three specimens (belonging to different cores) per site were selected for detailed thermal and Alternating Field (AF) treatments in order to choose the most suitable demagnetization method. An ASC TD-48 furnace was used during the thermal treatment, while a Molspin AF-demagnetizer allowed sample demagnetization to 5mT up to 95 mT. The components of the remanence for each specimen and the site-mean paleomagnetic directions were determined by the method of the principal component analysis (Kirschvink, 1980) and Fisher statistics (Fisher, 1953).

In most cases, a stable single component was detected (Figure 5.4b, 5.4d and 5.4e; sites Col1 sample 94C001A, site Col4 sample 94C035A and site Col8 sample 94C062A), accompanied by a negligible viscous overprint. In a few cases, however, the presence of secondary components (Figure 5.4a, 5.4c and 5.4f, that correspond to Col3 sample 94C026A, Col2 sample 94C011B and Col10 sample 94C098A, respectively) are observed probably due to viscous magnetic overprint and easily removed. Around 50 samples were thermally demagnetized. However, AF demagnetization was found to be a more efficient cleaning method as may be evidenced for samples 94C011A and 94C011B (Figure 5.4).

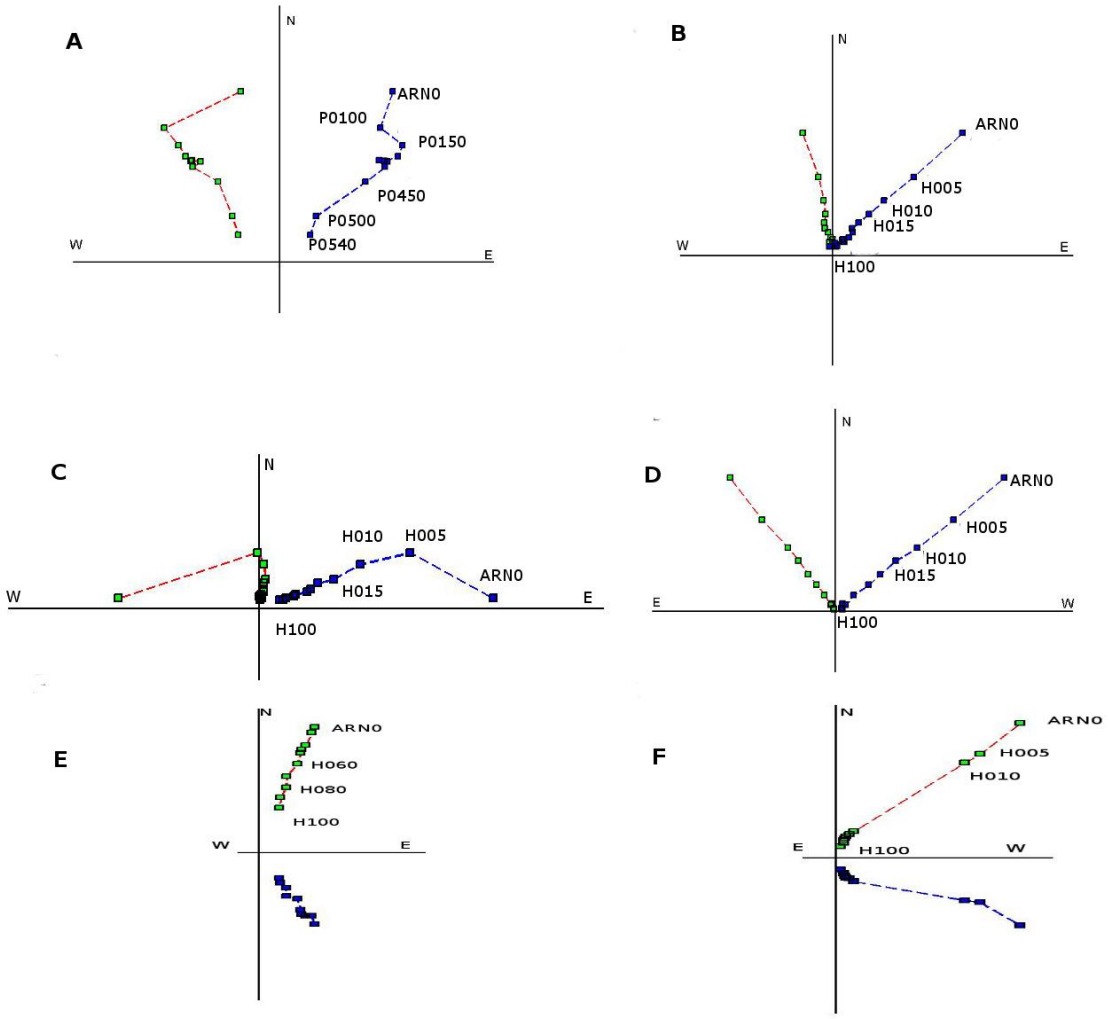


**Figure 5.4.** Examples of orthogonal vector plots, 4a) Thermal demagnetization since ARN0 with steps of 50°C until 540° (label with an initial "P" example P0540) for the sample 94C026A corresponding to the site Col3. Alternating field demagnetization since ARN0 with steps of demagnetization 5mT until 100mT (label with an initial "H" example H100). 4b) Sample 94C001A for the site Col1, 4c) Sample 94C011B for site Col2, 4d) Sample 94C035A site Col4, and including two orthogonal vector plots of events belonging to transitional geomagnetic regime, 4e ) Sample 94C062A site Col8 and 4f) Sample 94C098A site Col10.

It should be also noted that alternative field treatment has a little limitation because in a few samples (example, specimen 94C058A, site Col 6) no complete demagnetization is obtained applying maximum available peak field of 95 mT. However, the determination of characteristic remanence components may be achieved unambiguously for these samples using the principal component analysis (Kirschvink, 1980). Site-mean paleodirections were determined for all sites (Table 5.1). These directions are quite precisely determined since in all cases the values of $\alpha_{95}$ are less than 10° which is common for volcanic outcrops.

| Site | Coordinates | | Age ± error | n/N | Directions | | k | $\alpha_{95}$ | VGP's | | Pol. |
|---|---|---|---|---|---|---|---|---|---|---|---|
| | °N | °W | (ka) | | In(°) | Dc(°) | | | $\lambda_p$, | $\phi_p$ | |
| Col6 (M10) | 19.56 | 103.61 | 28 ± 8 | 10/10 | 36.2 | 10.8 | 25.9 | 9.7 | 79.8 | 341.5 | N |
| Col8 (M13) | 19.57 | 103.62 | 30 ± 12 | 4/9 | 8.8 | 313.7 | 95.6 | 7.2 | 42.49 | 154.1 | T |
| Col7 (M11) | 19.56 | 103.61 | 34 ± 7 | 10/10 | 41 | 11.4 | 39.5 | 7.8 | 78.7 | 324 | N |
| Col13 (M6) | 19.47 | 103.52 | 44 ± 15 | 8/10 | 43.9 | 344.2 | 656 | 2.8 | 74.2 | 192.5 | N |
| Col14 (M18) | 19.47 | 103.52 | 44 ± 15 | 9/10 | 39.4 | 351.4 | 166 | 3.6 | 81.5 | 187.5 | N |
| Col2 (M2') | 19.53 | 103.52 | 49 ± 22 | 6/9 | 21.3 | 28.8 | 35.5 | 9.6 | 60.9 | 359.2 | N |
| Col3 (M6) | 19.53 | 103.51 | 49 ± 22 | 7/9 | 14.8 | 25.6 | 38.6 | 8.5 | 66.4 | 8.7 | N |
| Col5 (M15) | 19.54 | 103.52 | 61 ± 8 | 8/9 | 27.4 | 352.6 | 74.7 | 5.8 | 81.3 | 132.2 | N |
| Col18 (V.Ap.) | 19.62 | 103.49 | 62 ± 14 | 10/10 | 50.6 | 347.3 | 77 | 5.4 | 73.6 | 215 | N |
| Col19 (V.Ap.) | 19.62 | 103.49 | 62 ± 14 | 9/9 | 52.6 | 346.3 | 224 | 3.4 | 71.7 | 217.2 | N |
| Col11 (M32) | 19.47 | 103.82 | 69 ± 5 | 7/9 | 33.2 | 2.5 | 36.1 | 10 | 84.6 | 154.1 | N |
| Col17 (M4) | 19.48 | 103.49 | 81 ± 8 | 9/10 | 41.4 | 352.3 | 46 | 7.7 | 81.6 | 198.9 | N |

| | | | | | | | | | | | |
|---|---|---|---|---|---|---|---|---|---|---|---|
| Col12 (M7) | 19.49 | 103.52 | 83 ± 5 | 9/9 | 40.9 | 9.6 | 66.7 | 6.4 | 80.2 | 321.1 | N |
| Col1 (M3) | 19.53 | 103.54 | 91 ± 7 | 9/9 | 41.9 | 359.1 | 39.9 | 7.4 | 85.3 | 246.5 | N |
| Col4 (M19) | 19.48 | 103.55 | 97 ± 13 | 5/9 | 35.2 | 349.4 | 48.1 | 9 | 85.4 | 114.2 | N |
| Col9 (M9) | 19.59 | 103.59 | 104 ± 9 | 8/9 | 43.2 | 354.3 | 66 | 7.4 | 82.34 | 213.9 | N |
| Col20 (V.E) | 19.62 | 103.76 | 172 ± 21 | 10/10 | 38.8 | 353.8 | 184 | 3.6 | 83.7 | 188.8 | N |
| Col16 (M4) | 19.49 | 103.50 | 184 ± 10 | 9/9 | 38.1 | 14.3 | 39 | 8.2 | 76.5 | 335.9 | N |
| Col21 (Sn.I.) | 19.64 | 103.75 | 215 ± 18 | 9/10 | 35.8 | 354.5 | 68 | 6.7 | 84.8 | 169.2 | N |
| Col10 (M31) | 19.52 | 103.76 | 300 ± 95 | 8/9 | -42.9 | 333.9 | 32 | 8.6 | -38.7 | 289.5 | T |
| Col15 (M18) | 19.57 | 103.68 | 372 ± 8 | 7/9 | 35.2 | 358.9 | 67.3 | 7.4 | 88.9 | 158.9 | N |
| **Mean (direction)** | | | | 19/21 | 36.2 | 10.8 | 39.1 | 5.5 | 87.6 | 270.1 | N |
| | | | | | | | **K** | $A_{95}$ | | | |
| **Scatter VGPs** | | | | | | | 35.9 | 5.3 | | | |

**Table 5.1.** Results of flow mean paleodirections for CVC lavas. Site: Name of the sample sites as described in Cortés *et al.* (2015); Coord: Geographical coordinates of the sampled sites; Age: Ar-Ar ages of the flows in kyr; n/N number of specimens used from the total of the specimens sampled; Directions: Flow-Mean inclination (In) and declinations (Dc); k and $\alpha_{95}$: precision of parameters of Fisher statistics; VGPs: Virtual Geomagnetic Pole positions; Pol: Magnetic Polarity, N Normal and T Transitional; K is the dispersion of the VGP, and $A_{95}$ is the quality factor of the VGP.

## 5.6 Main Results and Discussion

Nineteen lava flows yielded a normal polarity magnetization, while two sites gave clearly defined transitional paleodirections (Table 5.1). Both transitional lavas were radiometrically dated. The

paleodirections from site Col8 (Table 5.1), was dated as 30±12 kyr, correspond to the transitional geomagnetic regime. Tentatively, it may correspond to the Mono Lake (Benson *et al.* 2003, Negrini *et al.*, 1984) or Laschamp (Denham and Cox, 1960, Liddicoat and Coe, 1979) excursion, according to the available Ar-Ar radiometric ages. The Laschamp excursion was the first reported geomagnetic excursion, and is certainly the best known event in the Brunhes Chron (Chaîne des Puys, Massif Central, France; Bonhommet and Babkine, 1967). The mean paleodirection of Col8 is based on only four out of nine samples demagnetized. However, the directions are grouped yielding VGP latitude of about 42°, strongly deviated from the GAD (Geomagnetic Axial Dipole) directions. These transitional directions can be correlated with the Mono Lake or the Laschamp events, which are dated at 28 kyr and 40–45 kyr, respectively. The Mono Lake event may be considered, the best candidate because it is usually found in North America (Negrini *et al.*, 2014; Benson *et al.*, 2003). Site Col10 shows as well defined transitional magnetic polarity and may be related to the Calabrian Ridge I and Portuguese Margin events, both found in marine sediments: in the Ionian sea (Langereis *et al.*, 1997) for the Calabrian Ridge I and in the north-east Atlantic Ocean for the Portuguese Margin (Thouveny *et al.*, 2004; Carcaillet *et al.*, 2004). Site Col10, dated as 300 ± 90 kyr, yields a VGP latitude of -38° pointing to the intermediate geomagnetic regime; this can be correlated to Portuguese margin, located in the North Atlantic Ocean with has an age about 290 kyr documented by Thouveny *et al.* (2004), Carcaillet *et al.* (2004) using marine sediments and correlated to The Calabrian Ridge I (Langereis *et al.*, 1997), an excursion event located in the temporal window around 315-325 kyr.

Traditionally, sites with low VGP latitudes (Figure 5.5) are removed from Time Average Field (TAF) and paleosecular variation (PSV) studies for recent times (<5 Myr) (Johnson *et al.*, 2008). Generally speaking, the scatter of the VGP obtained should characterize the paleosecular variation (PSV) of the geomagnetic field for the given latitude and age (Cox, 1969), but at the same time the dispersion may be

biased by the transitional data which represents an excursions of the geomagnetic field. Thus, these data must be rejected from the population before to attempt characterize the PSV. Transitional data commonly are not taken into account by the use of a conventional cut-off angle of 45° and 60° (Watkins, 1973) in order to separate the paleosecular variation and transitional regimen ( Johnson *et al.*, 2008).

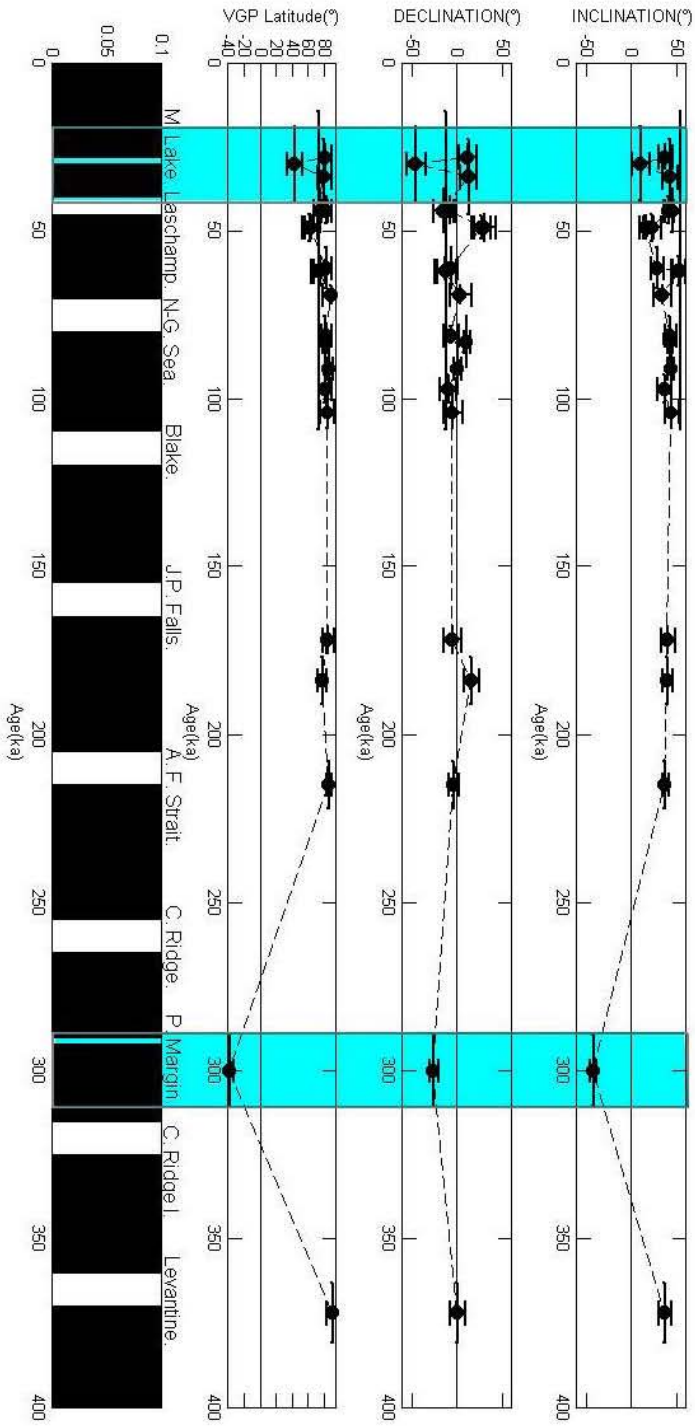
INCLINATION(°)
DECLINATION(°)
VGP Latitude(°)
Age(ka)
M.Lake
Laschamp
N-G. Sea
Blake
J.P. Falls
A. F. Strait
C. Ridge
P. Margin
C. Ridge I.
Levantine

**Figure 5.5**. Mean directions, inclinations, declinations and paleolatitudes of the 21 volcanic flows from the Volcanic Field of Colima, against age underlying the duration transitional events in these periods of time.

The mean paleomagnetic direction obtained in this study, rejecting two transitional sites, is: Dm = 1.2°, Im = 38.2°, $N$ = 19, $\alpha_{95}$ = 5.5°, and $k$ = 39.1 (Figure 5.6a). The corresponding paleomagnetic pole (Figure 5.6b) position is $\lambda_p$ = 270.1°, $\varphi_p$ = 87.6° ($A_{95}$ = 5.3°, $K$ = 35.9). The obtained direction is very close to the expected direction $D_{BC}$ = 3.8°, $I_{BC}$ = 38.1°, and $D_T$ = 1.6°, $I_T$ = 35.1° obtained for the last 5 Myr (Pliocene) and 10 Myr (part of the Miocene), as derived from the available reference poles for the North American craton (Besse and Courtillot, 2002 and Torsvik *et al.*, 2012, respectively), and no present a rotation or flattening

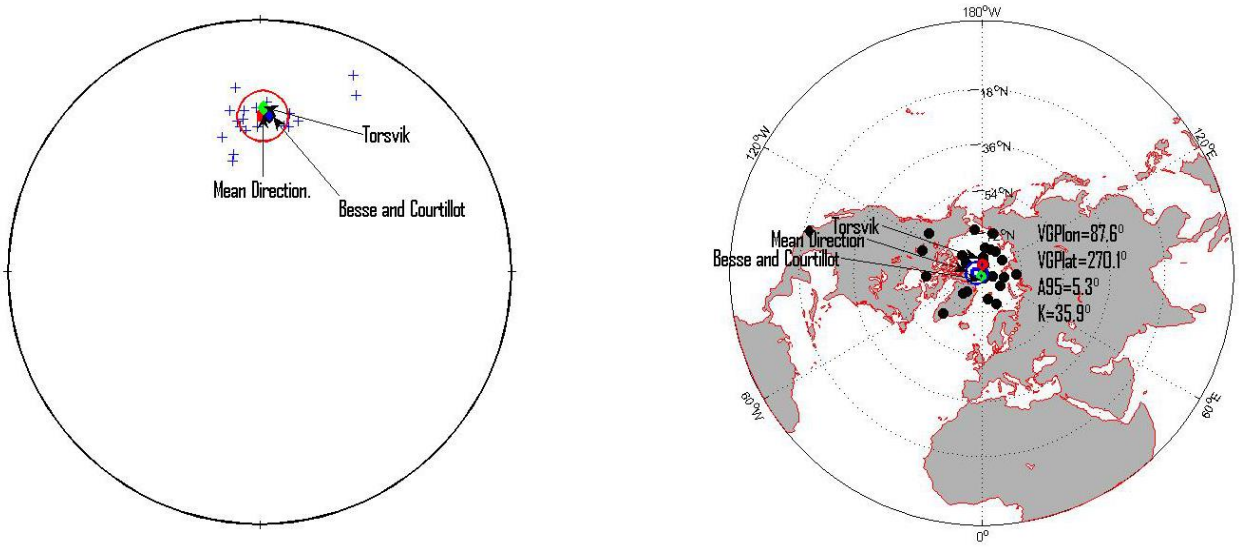


**Figure 5.6.** a) Equal area projection of the mean paleomagnetic directions obtained in this study, b) projection of the VGPs together with reference paleomagnetic poles recalculated from the stable North America (Besse and Courtillot, 2002; Torsvik *et al.*, 2012).

An important issue discussed during the last decade in paleomagnetism, is the relationship between the latitude and the VGPs scatter; this implies that at higher latitudes the scatter increases (McElhinny and Mc Fadden 1997; Johnson *et al.*, 2008; Linder and Gilder 2012). The point of the latitude dependence of VGPs scatter (Cox and Doell, 1960) depends critically on latitudinal set of data about 20° of latitude as argued by Johnson *et al.* (2008). The angular dispersion

$$S_F^2 = S_T^2 - \frac{S_W^2}{\acute{n}}, \quad (1)$$

is the formula used to estimate the paleosecular variation,

$$S_T = \left(\frac{1}{N-1}\right)\sum_i^n (\delta_i^2)^{1/2} \quad (2)$$

(Cox, 1969) is the total angular dispersion; $N$ is the number of the sites used, $\delta_i$ is the angular distance of the $i^{th}$ virtual geomagnetic pole (VGP) from the axial dipole, $S_W$ within-site dispersion, $\bar{n}$ the average number of samples per site. The dispersion obtained in this study is $S_F$ = 13.0°, the lower confidence limit $S_L$ = 12.7°, and the upper confidence limit $S_U$ = 15.2° using the calculation method of Cox (1969). The values agree relatively well (within the uncertainty) with the model G of McElhinny and McFadden, 1997 for the last 5 Myr (Figure 5.7). However, our data agree almost completely with the TK03 curve proposed by Tauxe and Kent (2013) but different to the model G of Johnson *et al.* (2008), mainly due the different selection criteria using a cut-off value dependence on dispersion parameter $k$. Moreover, in the compilation of Johnson *et al.* (2008), a single reference from Mexico is used (Mejia *et al.*, 2005) with only 16 mean directions reported mainly from the Matuyama chron. The dispersion parameters obtained in present investigation is compatible to the sites of similar latitude, such as Réunion and the South Pacific but a little bit higher than Hawaii for Bruhnes (0–0.78 Ma, Lawrence *et al.*, 2006). In Mexico, Mejia *et al.* (2005) studied the secular variation for the Holocene reporting a mean direction of Dm=358.8°, Im=31.6°, $\alpha_{95}$ = 2.0° and k=29° and a scatter of 12.7 ° and with lower and upper 95%

confidence limits of 11.9° and 14.1°. Conte-Fasano *et al.* (2006) conducted similar analysis of the Michoacán Guanajuato Volcanic Field reporting almost similar paleodirections: Dm=357.9°, Im=28.4, $\alpha_{95} = 7.3°$ , *k*=21 while the VGP scatter estimated as 15.4° with lower and upper 95% confidence limits of 19.6° and 12.7°. These values are slightly higher than those obtained in present study and even to the values reported in the model G of Johnson *et al.* (2008). The value of the dispersion of VGP's obtained in this study are still consistent with the values expected from the models G and Tk03, 13.6° and 12.9°, respectively, however it's low compared with the model G of Johnson *et al.* (2008) with a value of 14.5.

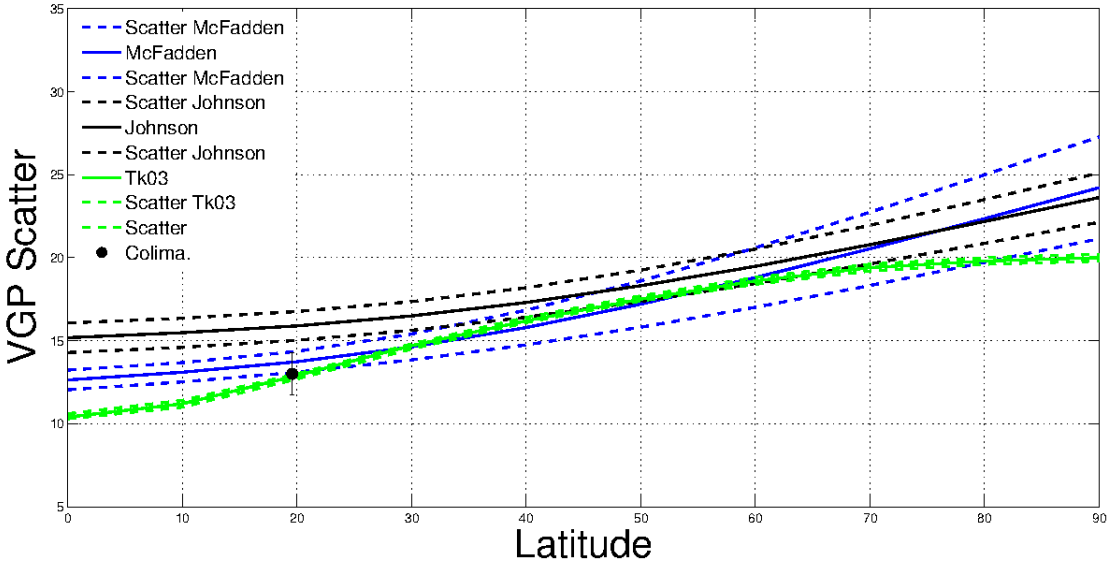


**Figure 5.7**. Scatter of the VGP as function of the latitude for the last 5 Myr, compared with the model G of McElhinny and McFadden *et al.* (1997) (blue line), Johnson *et al.*, 2008 (black line) and the Tk03 model propose by Tauxe and Kent (2013) (green line).

## 5.7 Concluding Remarks

The flow-mean directions obtained in this study may be considered to be of primary origin (characteristic remanence). A full battery of rock-magnetic experiments show that the magnetization is carried in most cases by Ti-poor titanomagnetite, probably resulting oxy-exsolution of original titanomagnetite during the initial flow cooling. In addition, relatively high unblocking temperature spectra and moderate to high coercivities point to pseudo-single domain magnetic structure grains as responsible for remanence.

The paleodirections are rather precisely determined for all 21 analyzed sites, yielding relatively low within site dispersion. All sites point to normal polarity magnetizations as should be expected for the cooling units erupted during the Bruhnes chron. Two sites however yielded clearly defined intermediary paleodirections that may be correlated to Mono Lake or Calabrian Ridge I short geomagnetic excursions respectively.

The mean paleomagnetic direction obtained in this study, rejecting two transitional sites, is: Dm = 1.2°, Im = 38.2° (N = 19, $\alpha_{95}\alpha_{95} = 5.5°$, k = 39.1°). The corresponding paleomagnetic pole (Figure 5.7) position is $\lambda_p = 270.1°$, $\varphi_p = 87.6°$ ($A_{95} = 5.3°$, K = 35.9°). These directions are practically undistinguishable (Figure 5.6a and Figure 5.6b) from both the spin axis and the expected Plio-Quaternary paleodirections, as derived from reference poles for the North American craton (Besse and Courtillot, 2002; Torsvik *et al.*, 2012). This may indicate that no major regional tectonic rotation occurred in the area since about Pleistocene.

The dispersion parameters obtained in present investigation is compatible to the sites of similar latitude like Réunion and the South Pacific but a little bit higher than Hawaii for the last 1 Myr and agree well to the secular variation model of Tauxe and Kent (2013).

**Acknowledgements**

This paper is part of the first author's doctoral thesis. This research was funded by the CONACYT, Universidad Nacional Autónoma de México and program UNAM DGAPA-PAPIIT-IA104215. We are grateful to the Editor Dr. Thierry Calmus and reviewers Dr. Vicente Carlos Ruiz Martínez and one anonymous reviewer for all the corrections and suggestion that improved this manuscript.

**References**

Benson, L., J.Liddicoat, J.Smoot, A. SarnaWojcicki, R. Negrini, and S. Lund., 2003, Age of Mono Lake Excursion and associated tephra, Journal Quaternary Science Reviews, 22, 2-4, 135–140.

Besse, J., Courtillot, V., 2002, Apparent and true polar wander and the geometry of the magnetic field in the last 200 million years, Journal of Geophysical Research, v. 107, no. B11, 2300. http://dx.doi.org/10.1029/2000JB000050.

Bonhommet N., and Babkine J., 1967, Sur la présence d'aimantations inverses dans la Chaîne des Puys. Comptes Rendus Hebdomadaires des Séances de l'Academie des Sciences 264, B, 92-94.

Carcaillet, J., Bourlès, D.L., Thouveny, N., and Arnold,M., 2004. A high resolution authigenic 10Be/9Be record of geomagnetic moment variations over the last 300 ka from sedimentary cores of the Portuguese margin, Journal of Earth and Planetary Science Letters, v. 219, p. 397–412.

Conte-Fasano G., Urrutia-Fucugauchi J., Goguitchaichivili A., Morales-Contreras J., 2006, Low-latitude paleosecular variation and the time-averaged field during the late Plioceno and Quaternary-Paleomagnetic study of the Michoacan-Guanajuato volcanic field, Central Mexico: Earth, Planets and Space, 58, 1359-1371.

Cortes, A., Garduño, V.H., Macías, J.L., Navarro-Ochoa, C., Komorowski, J.C., Saucedo, R., and Gaviles, J. C., 2010. Geologic mapping of Colima volcanic complex (México) and implications for hazard assessment. Journal of The Geological Society of American Special, v. 464, p. 1-16.

Cortes, A., Garduño, V.H., Navarro –Ochoa, C., Komorowski, J.C., Saucedo, R., Macias, J.L., and Gaviles, J.C., 2005, Carta geológica del Complejo Volcánico de Colima: México, D.F., Universidad Nacional Autónoma de México, Instituto de Geología, Cartas Geológicas y Mineras 10 sacale1:100, 000, 1 sheet, 37 text.

Cortes, A., 2015. Historia eruptiva del volcán Nevado de Colima y su evolución dentro del Complejo Volcánico de Colima (CVC). PhD Tesis, National University of Mexico, UNAM, 113 pp.

Cox, A., 1969. Confidence limits for the precision parameter k. Geophysical Journal of the Royal Astronomical Society, v. 18, p.545-549.

Cox, A., Doell, R.R., 1960, Review of Paleomagnetism: Geological Society of America, 71(35), 645-768.

Denham C.R. and Cox A., 1971, Evidence that the Laschamp polarity event did not occur 13,300–34,000 years ago. Earth and Planetary Science Letters, v. 13, p. 181–190

Dunlop D.J., 2002, Theory and application of the Day plot ($M_{rs}/M_s$ *versus* $H_{cr}/H_c$); 1. Theoretical curves and tests using titanomagnetite data: Journal of Geophysical Research, 107(B3), doi: 1029/2001JB000486.

Fisher R.A., 1953, Dispersion on a sphere: Proceedings of the Royal Society of London A, 217, 295-305.

Goguitchaichvili, A., Martin-Del Pozzo, A.L., Rocha-Fernandez J.L., Urrutia-Fucugauchi, J. Soler-Arechalde A.M., 2009, Paleomagnetic evidence from volcanic units of Valsequillo basin for the Lashamo geomagnetic excursión: implications for early human occupation in Central, Mexico: Earth, Planets and Space, 61, 205-2012.

Glatzmaier, G. A. & Roberts, P. H., 1997. Simulating the geodynamo. Contemp. Phys, v. 38, p. 269–288.

James F.A, 1986, Geology of the Northern Colima and Zacoalco Grabens, southwest Mexico–Late Cenozoic rifting in the Mexican Volcanic Belt: Geological Society of America Bulletin, 97, 473-485.

Johnson, C.L., Constable , G., Tauxe, L., Barendregt, R., Coe, R S., Layer, P., Mejia, V., Opdyke, D., Singer, B. S., Staudiel, H., Stone, D.B., 2008, Recent investigations of the 0-5 Ma geomagnetic field recorded in lava flows: Geochemistry, Geophysics, Geosystems, 9(4), 1525-2027, Q04032, doi:10.1029/2007GC001696.

Kirschvink, J.L, 1980. The least-square line and plane and analysis of paleomagnetic data. Geophys. J.R. Astron. Soc, v. 62, no. 3, p. 699-718.

Komorowski, J.C., Navarro, C., Cortés, A., Saucedo, R., Gavilanes, J.C., 1997, The Colima Complex: Quaternary multiple debris avalanche deposits, historical pyroclastic sequences (pre-1913, 1991 and 1994), *in* IAVCEI, Plenary Assembly, Fieldtrip guidebook: Guadalajara, Jalisco: Puerto Vallarta, México, Gobierno del Estado de Jalisco, Secretaría General, Unidad Editorial, 1-38.

Laj, C., Channel, J.E.T., 2007, Geomagnetic excursions, *in* Kono M., (ed.) Treatise on Geophysics, v. 5, Geomagnetism: Amsterdam, Elsevier, 373-416.

Langereis CG, Dekkers MJ, de Lange GJ, Paterne M, and Van Santvoort PJM , 1997 Magnetostratigraphy and astronomical calibration of the last 1.1 Myr from an eastern Mediterranean piston core and dating of short events in the Brunhes. Geophysical Jorunal International, v. 129, no. 1, p. 75-94.

Lawrence, K.P., Constable, C.G., Johnson, C.L., 2006, Paleosecular variation and the average geomagnetic field at ±20° latitude: Geochemistry, Geophysics, Geosystems, 7(7), 1525-2027.

Liddicoat J.C. and Coe RS., 1979, Mono lake geomagnetic excursion. Journal of Geophysical Research, v. 84, p. 261–271.

Linder, J.M., and S.A. Gilder, 2012, Latitude dependency of the geomagnetic secular variation S parameter: A mathematical artifact, *Geophysical Research Letters*, *39*, L02308, doi:10.1029/2011GL050330.

Luhr, J.F., Carmichael, I.S.E., 1990, Geology of Volcan de Colima. Bol. Inst.Geol:, UNAM, no. 107, p. 101.

Luhr, J.F., Prestegaard, K. L., 1988, Caldera formation at Volcán de Colima, Mexico, by a large Holocene volcanic debris avalanche: Journal of Volcanology and Geothermal Research, 35, 335-348

Mejia, V., Böhnel, H., Opdyke, N.D., Ortega-Rivera, M.A., Lee J.K.W., Aranda-Gomez J.J., 2005, Paleosecular variation and time-averaged field recorded in Late Pliocene-Holocene lava flows from Mexico: Geochemistry, Geophysics, Geosystems, 6(7), Q07H19, doi: 10.1029/2004GC000871.

Merrill, R.T., McFadden, P.L., 2003, The geomagnetic axial dipole field assumption: Physics of the Earth Planetary Interiors. 139, 171-185.

Negrini, R.M., Davis, J.O., Verosub, K.L., 1984. Mono Lake geomagnetic excursion found at Summer Lake, Oregon. Geology, v.12, p. 464–643.

Negrini R.M., McCuan D.T., Horton R.A., Lopez J.D., Cassata W.S., Channell J. E.T., Verosub K.L., Knott J.R., Coe R.S., Liddicoat J.C., Lund S.P., Benson L.V., Sarna-Wojciki A.M., 2014, Nongeocentric axial dipole field behaviour during the Mono Lake excursion: Journal of Geophysical Research: Solid Earth, 119, doi:10.1002/2013JB010846.

Prévot, M. et al., 1985, How the geomagnetic field vector reverses polarity. Journal Nature,

316, 6025, 230–234.

Robin, J., Mossand, P., Camus, G., Cantagrel, J.M., Gourgand, A., and Vincent, P. M., 1987, Eruptive history of the Colima volcanic complex (México): Journal of Volcanology and Geothermal Research, 31, 99-113.

Tauxe, L., 2010, Essentials of Paleomagnetism: University of California Press, 512 pp.

Tauxe, L., Kent, D.V., 2013, A Simplified Statistical Model for the Geomagnetic Field and Detection of Shallow Bias in Paleomagnetic Inclinations: Was the ancient Magnetic Field Dipolar?, *in* Channell, J.E.T., Kent, D.V., Lowrie, W., Meert, J.G. (eds.), Timescales of the Paleomagnetic Field: American Geophysical Union, Geophysical Monograph Series, 145, 101-113.

Tauxe, L., Mullender, T.A.T., Pick, T., 1996, Potbellies, wasp-waists, and superparamagnetism in magnetic hysteresis: Journal of Geophysical Research, 101(B1), 571-583.

Thouveny N, Carcaillet J, Moreno E, Leduc G, and Negrini D. 2004, Geomagnetic moment variation and paleomagnetic excursions since 400kyr BP: A stacked record from sedimentary sequences of the Portugese margin. Earth and Planetary Science Letters, 219, 377–396.

Torsvik, T.H., van der Voo, R., Preeden, U., Mac Niocail, C., Steinberger, B Hinsbergen, B., Doubrovine, P. V., van Hinsbergen, D.J.J., Domier, M., Gaina, C., Tohver, E., Meert, J.G., McCausland, P.J.A., Cocks, L.R.M., 2012, Phanerozoic polar wander, paleography and dynamics, Journal Earth-Science Reviews, 114, 325-368, http://dx.doi.org/10.1016/j.earscirev.2012.06.007.

Watkins, N.D., 1973, Brunhes epoch geomagnetic secular variation on Reunion Island: Journal of Geophysical Research, 78(32), 7763-7768

# 6. A rock-magnetic and paleomagnetic survey on dated lava flows erupted during the Bruhnes and Matuyama Chrons: The Mascota Volcanic Field Revisited (Western Mexico)

## 6.1 Abstract

A rock magnetic and paleomagnetic investigation was performed on some selected, radiometrically dated lava flows from the Mascota Volcanic Field (MVF), western Trans-Mexican Volcanic Belt. A full battery of rock-magnetic experiments and standard paleomagnetic analysis were carried out on 19 sites spanning the time interval from 2268 to 72 kyr. The paleomagnetic directions are anchored to absolute radiometric ages while no such information was available in previous studies. This makes possible to correctly evaluate the fluctuation of Earth's Magnetic Field from Pliocene to Pleistocene and reveal the firm evidence of possible Levantine excursion.

Both Ti-poor and Ti-rich titanomagnetites seem to carry the remanent magnetization with Curie temperatures ranging from 350° C to 537° C. Thirteen flows correspond to the Brunhes chron, one of them exhibits transitional directions, while the remaining six sites belong to the Matuyama chron. New and existing dataset for MVF were used to estimate the paleosecular variation parameters. The selected data include 35 Plio-Quaternary lava flows. After excluding the poor quality data ($N < 4$, $\alpha_{95} > 10°$) as well as the transitional directions, the mean paleodirection is $D_m = 356.1°, I_m = 39.9°$ ($k = 20.0, \alpha_{95} = 6.4°$) which agree well with the Geocentric Axial Dipole (GAD) and the expected paleodirections for the Plio-Pleistocene, as derived from the reference poles for the stable North America. The corresponding mean paleomagnetic pole is defined as longitude $\varphi_p = 226.7°$, latitude $\lambda_p = 86.0°$ ($K = 27.6, A_{95} = 5.3°$). The virtual geomagnetic pole (VGP) scatter for the MVF ($S_B = 15.2°$) is consistent with the value expected from model G at latitude of 20°. The combined paleomagnetic data, supported by positive reversal test, indicate no paleomagnetically detectable vertical-axis rotations in the

study area. The evidence of one transitional directions was detected, which may correspond to the Levantine excursion (360-370 kyr) or unnamed event between 400-420 kyr.

**Keywords.**

Mascota Volcanic Field, Paleosecular Variation, Plio-Quaternary, Geocentric Axial Dipole, Western Mexico.

## 6.2 Introduction

Main paleomagnetic applications are based on the geocentric axial dipole (GAD) hypothesis that provides a coordinate reference frame over long-time scales. Paleomagnetic studies for the past 5 Myr essentially support the GAD, showing that more than 90% of paleofield power corresponds to the geocentric axial dipole. Present and paleofield studies also indicate the presence of higher order structures (Merril and McElhinny, 1985; Johnson and Constable, 1995, 1998). Many studies confirm that the GAD is a first order approximation but some anomalous spatial-temporal paleosecular variation (PSV) patterns were also documented (Wilson, 1972; Wilson and McElhinny, 1974; Schneider and Kent, 1990). Zonal and latitudinal dependent paleosecular variation (PSV) models have been developed during the last decades which permit to constraint PSV characteristics and persistent non dipole anomalies. Some studies also underlined the occurrence of regional PSV anomalies such as the Pacific dipole window and other minor PSV patterns characterized by low secular variation rates (McElhinny et al., 1996). PSV analyses at low latitudes, e.g., at ± 20° N (the case of Central Mexico and Hawaii) have reported contrasting results. Lawrence and Constable (2006) have concluded that low PSV and smaller persistent GAD anomalies has characterized the low latitude zone during the Brunhes chron.

Volcanic rocks are reliable paleomagnetic recorders of the Earth's magnetic field because of high stability of the thermoremanent magnetization (*e.g.*, Prévot *et al.*, 1985). In ideal case, the PSV and GAD studies should rely on paleomagnetic data from radiometrically dated volcanic rocks. Volcanic data

represent sporadic measurements, and thus time varying studies are limited by the number of paleomagnetic directions. Central México is characterized by stratovolcanoes and volcanic monogenetic fields that form the Trans-Mexican Volcanic Belt (TMVB). TMVB is an arc built on the continental margin related to plate subduction at the Middle America trench and presents large arc parallel variation in volcanic style (Ferrari, 2000.).

The present study is aimed to increase high quality paleomagnetic data from the Jalisco Block adding nineteen radiometrically dated sites (Ownby et al., 2008). These new results permit to increase the robustness of existing (Maillol and Bandy, 1993; Maillot et al., 1997) data from the region during the Pliocene trough Pleistocene. The combined paleomagnetic database better knowledge of both the tectonic evolution of Western TMVB and fine characteristics of the Earth's Magnetic Field through the paleosecular analysis.

### 6.3 Geological Setting and Sampling

The Mascota volcanic field (MVF) is located within the JB (western Mexico), between the TMVB and Sierra Cacoma. It lies south-west of the 250 km long Tepic-Zocoalo rift and north-west of the 65 km long Colima, two of the main known rift systems. MVF occupies the west part of the TMBV containing the volcanism mainly associated to the subduction process (Bandy et al., 2001).

The MVF presents one of the four volcanic fields (together with Los Volcanes, Ayutla, and Talpa) in the JB characterized by high potassium contents, slag cones, lava flows including absarokites, andesites, basaltic andesite minettes, basic hornblende lamprophyres and minettes in close spatial proximity to cones and flows of basaltic andesite and andesite (Ownby et al., 2008) and it is part of the alkaline volcanic fields within N-S to NE-SW (Wallace and Carmichael; 1989; Lange and Carmichael, 1990; Righter and Carmichael, 1992). MVF itself contains some deposits of Plio-Quaternary mafic rocks. The volcanism in the MVF is confined to the Talpa and Mascota grabens, with a few cones to the north that lie in an adjacent linear valley (Carmichael et al., 1996). The volcanism of Mascota appears to be the youngest of the four potassic volcanic fields in the JB (Lange and Carmichael 1991, Carmichael et al., 1996), with reported ages of $< 1\ Myr$.

Volcanic rocks are distributed on an extensive area about 2000 $km^2$, which contains approximately 87 cones. Ownby et al., (2008) reported 35 $^{40}Ar/^{39}Ar$ dates revealing the eruptive history of the MVF. The oldest lavas are located in the southern sector, with dates between 2.4 Myr to 0.5 Myr. The younger lavas are mainly in the northern sector with dates predominantly $< 0.5$ Myr. In this study, 19 independent lava flows were sampled (Figure 6.1) The sample collection campaign was largely conditioned by detailed geochronology work of Ownby et al., (2008) since we tried to sample apparently fresh lava flows with available radiometric dates in unaltered and easy to Access outcrops. Sixteen flows were directly dated by Ownby et al., (2008) and range between 2268 kyr and 72 kyr. They are composed mainly by minette (MAS_01, MAS_09), absorkite (MAS_05, MAS_06, MAS_12 and MAS_19), basic hornblende lamprophyre (MAS_04, MAS_11, and MAS_14), basaltic andesite (MAS_03, Mas_13, MAS_15, MAS_16, MAS_17 and MAS_18) and andesite (MAS_10). Remaining three flows sampled are not dated by means of Ar-Ar systematics and may be described as follow: Mas_02 is a basic hornblende lamprophyre reported in the geological map of Ownby et al., (2008) to the south of MAS-419 and MAS-52, this flow was sampled due to the proximity with MAS_13 and MAS_14 and has not been reported previously ; other flow sampled without age information is MAS_07 composed by minette and located close to MAS_06 and finally the site MAS_08 which is a lava flow composed of basaltic hornblende lamprophyre. Most of the studied flows are located in the MVF southern sector, near the Talpa Allende, with few flows located in the northern sector, near the San Sebastian area (Figure 6.1), Seven out of 19 flows reported here were sampled in previous paleomagnetic studies by Maillol and Bandy (1993) and Maillol et al., 1997 (Fig. 1, MAS_09, MAS_11, MAS_14, MAS_16, MAS_15, MAS_17 and MAS_18). Eight to nine standard paleomagnetic cores were obtained from each independent cooling units and oriented using both magnetic and sun compasses.

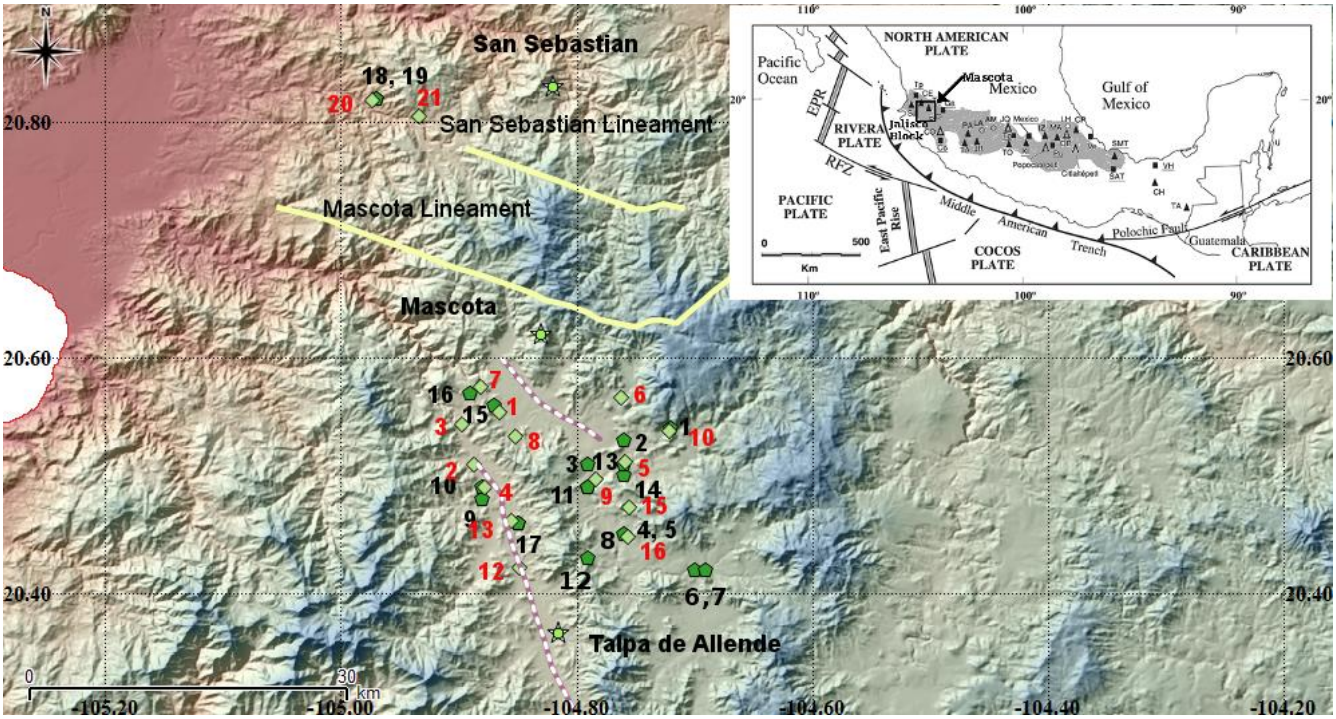


**Figure 6.1** Location of sampled lava flows from MVF, Talpa and San Sebastian, the black number are the sampled flows for the present study and the red number represent the flows sampled by Maillol and Bandy 1993 and Maillol et al., 1997.

### 6.4 Magnetic Measurements

In order to identify the magnetic carriers responsible for the remanent magnetization and to obtain information about their paleomagnetic stability several rock-magnetic experiments were carried out. These experiments included:

- Acquisition of thermomagnetic curves in low field as a function of temperature helps to observe the proportional changes during the heating and cooling cycles and determine the Curie temperatures of the main magnetic minerals by means of the differential method described in Tauxe (2002). These changes may involve the formation of new magnetic substances and different Curie points or changes in the phase. Continuous measurements in air were performed with a Curie Balance from room temperature about 22°C through 600°C.
- Magnetic hysteresis experiments were carried out to reveal the magnetic mineralogy. The hysteresis loops and associated Isothermal Remanent Magnetization (IRM) acquisition curves

were measured using a Variable Field Translation Balance (VFTB). Measurements were carried out on whole-rock powdered specimens, and in each case, IRM acquisition and backfield curves were recorded first.

- Thermal and alternating field demagnetization techniques were applied to retrieve the Characteristic Remanent Magnetization (ChRM). All remanences were measured in the "Laboratorio Interinstitucional de Magnetismo Natural" (LIMNA), with JR-6A (AGICO LtD) spinner magnetometer.

The thermomagnetic curves provided information about samples magnetic mineralogy through the Curie temperatures calculated using the differential method of Tauxe (2002). This analysis revealed Curie temperatures between 350°C to 537°C indicating the presence of Ti-rich and Ti-poor titanomagnetites with moderate degrees of alteration due to heating (see representative examples in Figure 6.2a and Figure 6.2b ). Some specimens, reveal coexistence Ti-rich titanomagnetites with almost pure magnetite (Figure 6.2a). Only three flows, that were composed by basaltic hornblende lamprophyre and minette, show evidence of hematite (Mas_2, Mas_7 and Mas_8) yielding Curie temperatures close to 650°C (Figure 6.2c), that were composed by basaltic hornblende lamprophyre and minette.

The hysteresis experiments provided simple curves pointing to the assemblages of pseudo-single domain (PSD) ferromagnetic grains which are efficient in acquiring remanet magnetization and resistant to demagnetization exhibiting significant coercivity. Near to the origin, no evidence of wasp-waisted or potbellied behaviour is observed which suggest a very restricted ranges of coercivities for the ferromagnetic (s.I.) fractions (Dunlop, 2002; Figure 6.2), and discarded the presence of two or more distinct coercivity population (Roberts et al., 1995; Tauxe et al., 1996). The isothermal remanence (IRM) acquisition curves are also sensitive to the magnetic mineralogy in terms of concentration and grain size properties. The analysis of coercivity spectra shows the correspondence of the magnetic saturation with the sample magnetic mineralogy. Most samples show saturation at about 300 mT applied magnetic field, which indicates presence of ferrimagnetic phases with moderate coercivity as may be expected from magnetite and titanomagnetite grains (Tauxe, 2002).

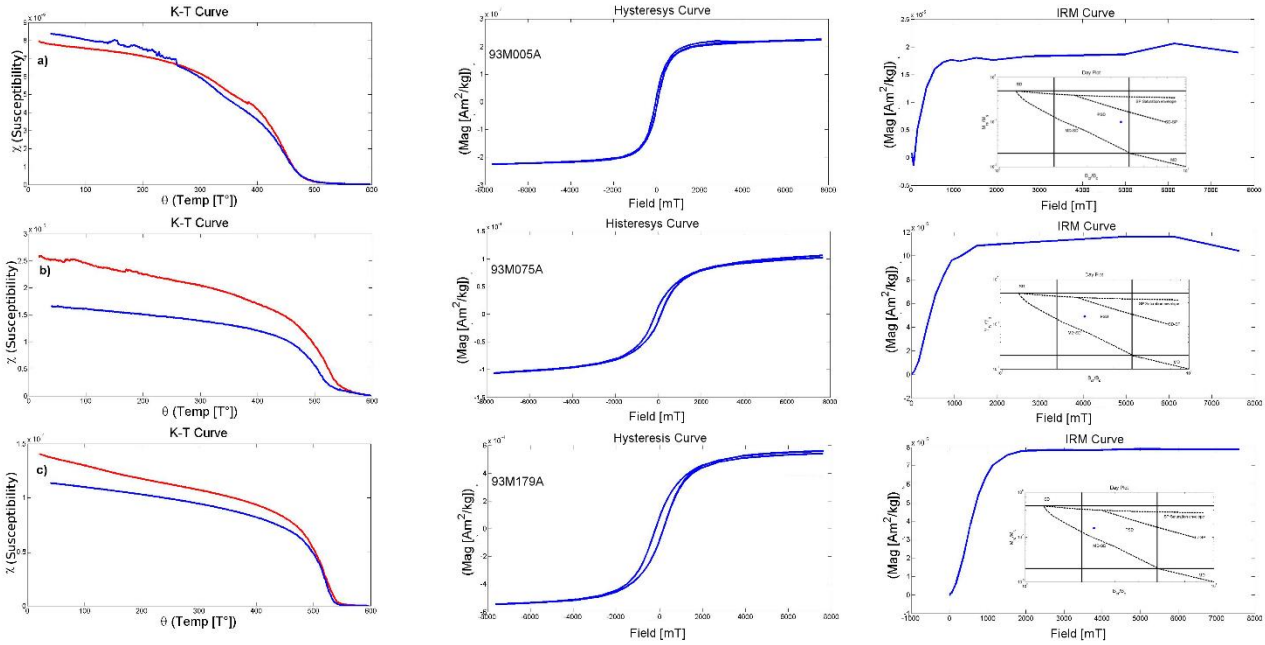


**Figure 6.2.** A summary of rock-magnetic experiments for the most representative samples:

a)Sample 93M005A from MAS_01, b)Sample 93M075A from MAS_09, c)Sample 93M179 from MAS_19; that provided Susceptibility vs. Temperature curves, where the red curve represent the heating curve and the blue the cooling curve. Hysteresis experiments and associated isothermal remanence acquisition curves obtained with a variable field translation balance (also Dunlop, 2002) to estimate the magnetic domain state trough the ratios $M_{rs}/M_s$ versus $B_{cr}/B_c$.

The initial stage of the measurement of the natural remanent magnetization (NRM) was achieved for **five** different specimens (pilot samples) from each of the 19 flows and were subjected to detailed thermal (two specimens) and alternating field demagnetization (AF, three specimens) in order to choose the most suitable demagnetization method for this study. An ASC TD-48 furnace was used during the thermal treatment from 50°C up to 560°C, while a Molspin AF-demagnetizer allowed demagnetizations starting from 5 mT up to 95 mT. The analysis of these pilot tests showed that AF demagnetization was more efficient (Figure 6.3a, 6.3b, 6.3c and 6.3d) observed in 57 pilot samples. However, about 40 samples were thermally demagnetized with excellent results (Figure 6.3d, and 6.3f). All remaining samples were demagnetized using alternating fields yielding Median Destructive Fields (MDF) ranging from 25mT to 40mT as should be expected from the pseudo-single domain ferromagnetic grains.

The remanence component directions and angular dispersion parameters for each one of the specimens

and the paleomagnetic site-mean directions were determined by the method of the principal component analysis (Kirschvink, 1980) and Fisher statistics (Fisher, 1953). Although all these 8 samples per sites were demagnetized using either alternating field or thermal treatments, in average 5 to 6 samples were used for site-mean paleodirections determination. Remaining samples were rejected from the analysis because their maximum angular deviation (MAD) exceeded 2°. In some cases, we observe a well-defined ChRM direction, accompanied by secondary components easily removed (Figure 6.3b, 6.3e and 6.3f), and in a few samples we detected a simple component accompanied by a negligible viscous overprint (Figure 6.3a, 6.3c and 6.3d). The mean paleodirections determined for all sites in this study are quite precisely determined since for most cases the values of $\alpha_{95}$ are less than 10°. They were combined with previous paleodirections reported form studies of the same area (Table 1; Maillol et al., 1997.) in order to increase the robustness of paleomagnetic analysis.

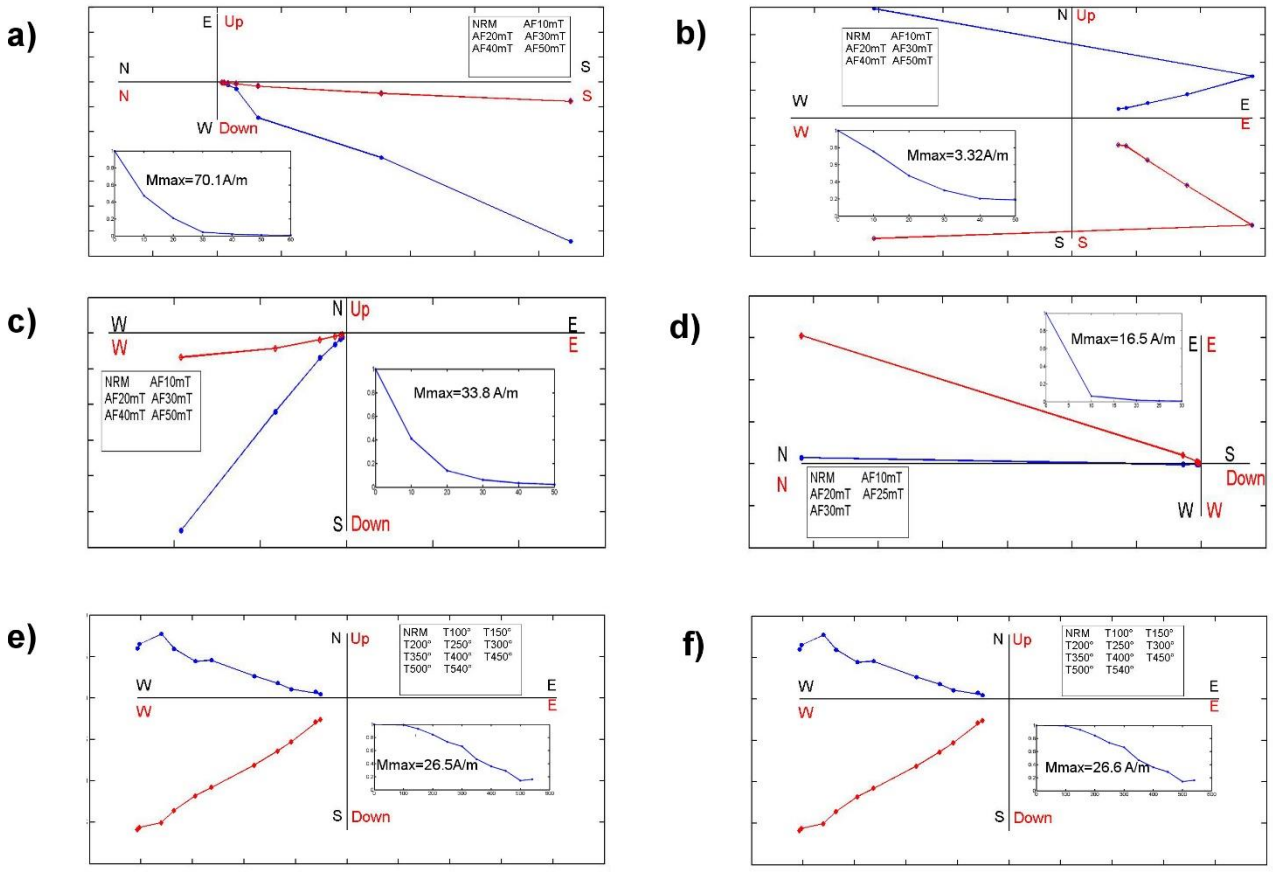


**Figure 6.3.** Representative examples of orthogonal vector plots illustrating either alternative field or thermal treatments for representative samples: a) 93M020A of the flow MAS_03, b) 93M032A of the

flow MAS_04, c)93M053A of the flow, MAS_06, d) 93M107A of the flow MAS_13, e)93M120A of the flow MAS_14 and f) 93M136A of the flow MAS_15.

### 6.5 Main Results and Discussion

The 19 paleodirections obtained (16 of them directly dated by means of $^{40}Ar/^{39}Ar$ systematics), were distributed in ten paleodirections for the Brunhes chron and six paleodirections to the Matuyama chron (Fig. 4) while three undated flows (MAS_02, MAS_07 and MAS_08) belong to Brunhes chron judged from their magnetic polarity (Table 1). The evidence of transitional directions was detected for the flow MAS_15 (Table 6.1) which may correspond to the Levantine excursion ($360 - 370$ kyr) an unnamed event between $400 - 420$ kyr (Laj and Channell, 2007). Both apparent transitional events are poorly defined (Ryan, 1972; Singer et al., 2002), although, the Levantain event was already reported by Rodríguez et al. (2006) in lava flows associated to the TVF. It is interesting to note that same flow, previously studied by Maillol and Bandy (1993) (Site Mas-1), also yielded the anomalous paleodirections (Table 6.1, and Fig. 4b). Both determinations are well constrained based on 5 samples for the present study while Maillot et al., (1993) reported analysis carried out on 8 paleomagnetic cores.

The identification of low technical quality data and transitional events are required to correctly characterize the PSV (Johnson et al., 2008), for this reason the paleomagnetic data with $N \leq 4$, $\alpha_{95} \geq 10°$, and $VGPLat < 60°$ were omitted for further analysis to result in a mean paleodirection from eleven paleodirections $D_m = 359.2°, I_m = 39.6°, k = 17.96, \alpha_{95} = 9.8°$.

A previous study performed by Maillol et al. (1997) reported data from 16 lava flows, meet to the basic selection criteria (Table 6.1, Figure 6.4) yielding a mean direction $D_m = 354.5°$, $I_m = 36.3°$, $k = 22.04, \alpha_{95} = 7.9°$ for $N = 14$, a combined paleomagnetic direction based on 22 independent flows yield a mean of $D_m = 356.8°, I_m = 39.9°, k = 22$, and $\alpha_{95} = 6.4°$.

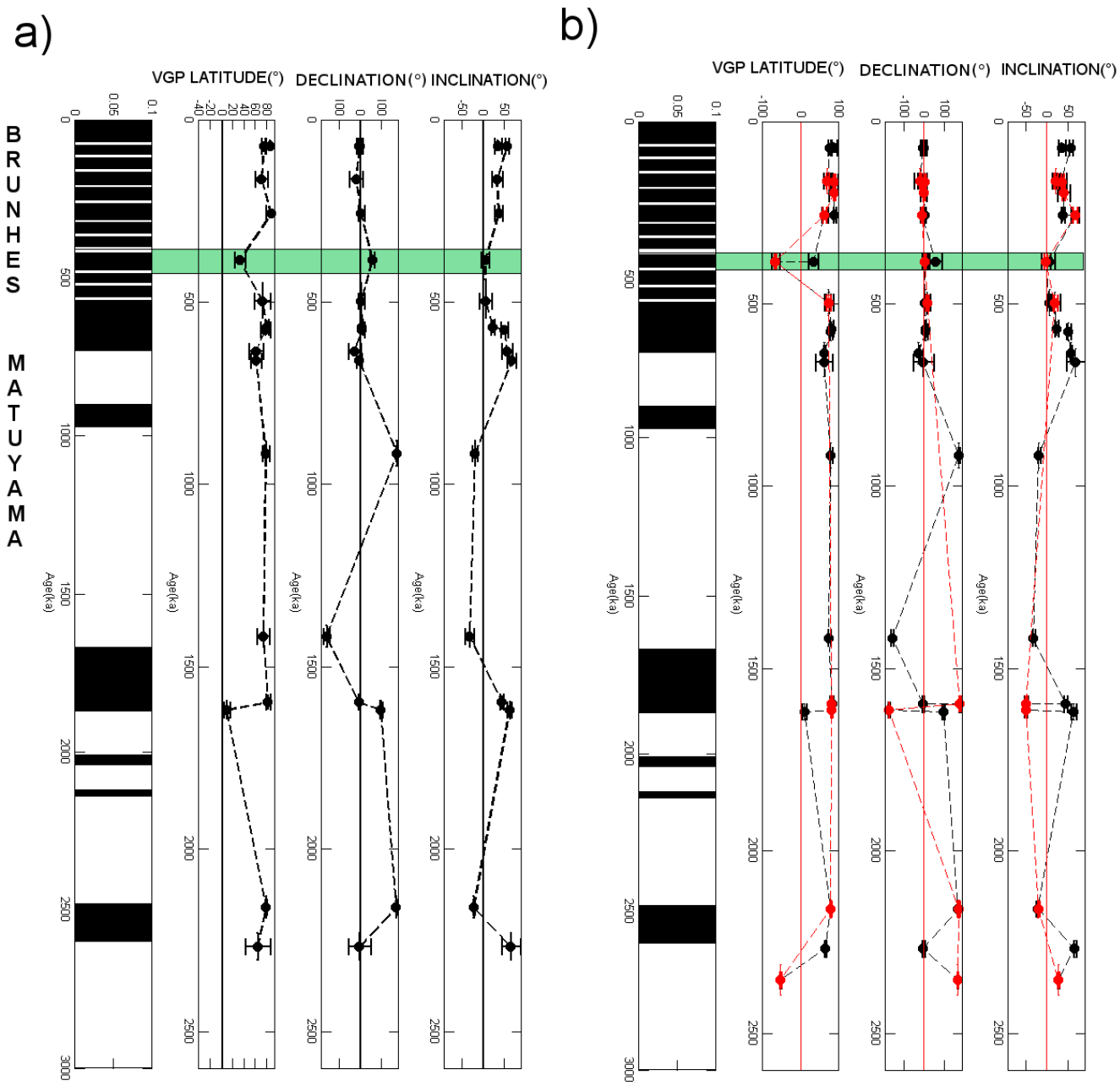


**Figure 6.4. a)** Mean paleomagnetic inclination, declination and VGP latitude against the age for the flows of MVF, Talpa and San Sebastian, black dots for the paleomagnetic data of this study and **b)** red dots for Maillol and Bandy 1993 and Maillol et al., (1997) (see text for more details).

| Site | Lat(°) | Long(°) | Dec(°) | Inc(°) | k | $\alpha_{95}$(°) | N | Age(kyr) | $\sigma_{Age}$ (kyr) | VGPLon(°) | VGPLat(°) | Ref |
|---|---|---|---|---|---|---|---|---|---|---|---|---|
| MAS_01 | 20.54 | 104.72 | 355.20 | 54.70 | 76.20 | 8.70 | 6.00 | 73.00 | 14.00 | 269.69 | 74.72 | T.S. |
| MAS-5 | 20.51 | 104.76 | 340.70 | 20.10 | 122.50 | 4.70 | 9.00 | 163.00 | 13.00 | 169.02 | 68.84 | M |
| MAS_14 | 20.51 | 104.76 | 339.46 | 32.42 | 46.71 | 10.24 | 4.00 | 163.00 | 13.00 | 189.76 | 70.39 | T.S. |
| MAS-7 | 20.58 | 104.88 | 3.30 | 35.30 | 181.20 | 5.70 | 5.00 | 166.00 | 22.00 | 33.52 | 86.72 | M |
| MAS-6 | 20.50 | 104.76 | 356.80 | 38.20 | 422.40 | 2.70 | 8.00 | 196.00 | 11.00 | 213.45 | 86.86 | M |
| MAS_16 | 20.57 | 104.89 | 356.36 | 33.90 | 44.80 | 11.20 | 5.00 | 248.00 | 39.00 | 165.28 | 86.03 | T.S. |
| MAS-20 | 20.82 | 104.97 | 2.60 | 34.60 | 198.00 | 3.40 | 10.00 | 257.00 | 24.00 | 50.70 | 86.97 | M |
| MAS_18 | 20.82 | 104.97 | 2.71 | 36.40 | 90.61 | 5.19 | 8.00 | 257.00 | 24.00 | 27.46 | 87.40 | T.S. |
| MAS-1 | 20.55 | 104.87 | 1.90 | -3.60 | 221.20 | 3.70 | 8.00 | 385.00 | 35.00 | 279.88 | -67.57 | M |
| MAS_15 | 20.56 | 104.87 | 56.50 | 4.90 | 326.30 | 6.50 | 5.00 | 385.00 | 35.00 | 25.31 | 32.10 | T.S. |
| MAS-13 | 20.46 | 104.86 | 14.00 | 18.80 | 878.30 | 1.70 | 9.00 | 497.00 | 19.00 | 51.46 | 72.72 | M |
| MAS_17 | 20.46 | 104.85 | 2.80 | 5.60 | 348.20 | 4.20 | 5.00 | 497.00 | 19.00 | 95.70 | 72.14 | T.S. |
| MAS_19 | 20.82 | 104.97 | 4.68 | 22.39 | 618.16 | 1.99 | 8.00 | 568.00 | 30.00 | 82.44 | 77.96 | T.S. |
| MAS_06 | 20.42 | 104.70 | 7.90 | 50.00 | 68.20 | 9.50 | 5.00 | 576.00 | 8.00 | 317.55 | 77.43 | T.S. |
| MAS_04 | 20.49 | 104.79 | 331.78 | 55.58 | 142.30 | 4.18 | 8.00 | 635.00 | 11.00 | 233.21 | 60.82 | T.S. |
| MAS_05 | 20.49 | 104.79 | 354.80 | 66.70 | 31.50 | 11.90 | 5.00 | 661.00 | 8.00 | 277.80 | 60.93 | T.S. |
| MAS-3 | 20.54 | 104.90 | 341.30 | 19.80 | 331.30 | 2.70 | 10.00 | <780 | NA | 167.83 | 69.25 | M |
| MAS-8 | 20.53 | 104.35 | 359.50 | 47.40 | 397.00 | 2.60 | 9.00 | <780 | NA | 281.20 | 81.99 | M |
| MAS-9 | 20.50 | 104.79 | 344.60 | 55.00 | 54.00 | 7.10 | 9.00 | <780 | NA | 246.07 | 69.79 | M |
| MAS-10 | 20.54 | 104.72 | 345.70 | 18.80 | 42.40 | 8.00 | 9.00 | <780 | NA | 158.55 | 72.44 | M |
| MAS-15 | 20.47 | 104.76 | 347.90 | 65.00 | 529.10 | 2.40 | 8.00 | <780 | NA | 267.20 | 61.71 | M |
| MAS-21 | 20.81 | 104.93 | 352.80 | 31.50 | 39.30 | 7.80 | 10.00 | <780 | NA | 167.17 | 82.22 | M |
| MAS_02 | 20.53 | 104.76 | 300.00 | -52.10 | 70.74 | 11.00 | 4.00 | <780 | NA | 123.40 | 11.18 | T.S. |
| MAS_07 | 20.42 | 104.70 | 14.80 | 51.70 | 52.30 | 9.60 | 6.00 | <780 | NA | 329.64 | 72.21 | T.S. |
| MAS_08 | 20.50 | 104.76 | 338.20 | 52.30 | 62.20 | 9.70 | 5.00 | 780.00 | NA | 231.85 | 66.99 | T.S. |
| MAS_10 | 20.49 | 104.88 | 174.80 | -19.10 | 29.30 | 14.30 | 5.00 | 915.00 | 48.00 | 130.81 | 78.21 | T.S. |
| MAS_12 | 20.43 | 104.79 | 196.90 | -32.30 | 65.20 | 8.60 | 4.00 | 1416.00 | 8.00 | 22.20 | 73.77 | T.S. |
| MAS-12 | 20.42 | 104.85 | 179.80 | -49.00 | 442.50 | 2.30 | 10.00 | 1597.00 | 16.00 | 283.80 | 80.51 | M |
| MAS_11 | 20.46 | 104.85 | 352.69 | 42.96 | 415.80 | 3.60 | 6.00 | 1597.00 | 16.00 | 229.98 | 81.89 | T.S. |
| MAS-2 | 20.51 | 104.89 | 180.90 | -50.00 | 280.00 | 3.10 | 9.00 | 1613.00 | 6.00 | 289.21 | 79.69 | M |
| MAS_03 | 20.51 | 104.79 | 97.05 | 61.69 | 13.24 | 22.24 | 3.00 | 1618.00 | 37.00 | 332.20 | 8.87 | T.S. |
| MAS-4 | 20.49 | 104.88 | 173.30 | -20.50 | 248.90 | 3.20 | 9.00 | 2159.00 | 6.00 | 138.95 | 78.19 | M |
| MAS_09 | 20.48 | 104.88 | 172.06 | -22.82 | 31.39 | 9.44 | 7.00 | 2159.00 | 6.00 | 147.63 | 78.51 | T.S. |
| MAS_13 | 20.45 | 104.76 | 355.10 | 64.60 | 48.77 | 12.30 | 4.00 | 2354.00 | 42.00 | 277.14 | 63.67 | T.S. |
| MAS16 | 20.45 | 104.76 | 168.00 | 26.40 | 635.90 | 2.20 | 8.00 | 2354.00 | 42.00 | 304.66 | -53.65 | M |

**Table 6.1.** Results of flow mean paleodirections for MVF lavas. Site: Name of the sample sites as described in Ownby *et al.* (2008); Lat, Long: Geographical coordinates of the sampled sites; Flow-Mean inclination (Inc) and declinations (Dec); k and $\alpha_{95}$:precision of parameters of Fisher statistics; N: Number of specimens used for mean calculation; Age: Ar-Ar ages of the flows in ka; $\sigma_{Age}$ Dispersion of the age provided by the radiometric dating (Ar-Ar) in kyr; VGPs: Virtual Geomagnetic Pole positions for latitude and longitude; A95 and K: precision parameters of the VGPs; Ref: Reference of the samples, that indicate M: for the previous paleomagnetic results obtained by Maillol and Bandy 1993 and Maillol et al., 1997, and TS: Represent the paleomagnetic results for the present study.

The selected paleodirections span two polarity chrons (Table 6.2):

1. The Brunhes chron (approx. 780 kyr to present) is represented by 17 flows yielding $D_{Bm} = 354.7°, I_{Bm} = 40.1°, k = 19.8$, and $\alpha_{95} = 7.6°$.
2. The Matuyama chron is represented by (between 780 kyr to 2.48 Myr) five flows with a mean paleodirection $D_{Mm} = 0.8°$,.$I_{Mm} = 39.4°, k = 30.3$, and $\alpha_{95} = 11.4°$.

| Group | Cutoffang | Dec(°) | Inc(°) | k | $\alpha_{95}$(°) | N | A95(°) | K | VGPLong(°) | VGPLat(°) | Sp(°) |
|---|---|---|---|---|---|---|---|---|---|---|---|
| T. S. | 60 | 359.22 | 39.61 | 17.96 | 9.95 | 11 | 8.73 | 23.37 | 264.37 | 86.47 | 16.82 |
| Maillol | 60 | 354.52 | 36.33 | 22.04 | 7.96 | 14 | 6.76 | 30.62 | 207.38 | 84.86 | 13.97 |
| All | 60 | 356.08 | 39.99 | 22.02 | 6.36 | 22 | 5.71 | 27.23 | 239.05 | 84.78 | 16.49 |
| All. B. | 60 | 354.66 | 40.12 | 19.78 | 7.63 | 17 | 6.87 | 24.4 | 232.85 | 83.58 | 17.75 |
| All. M. | 60 | 360.78 | 39.35 | 30.27 | 11.37 | 5 | 9.68 | 41.82 | 299.59 | 87.35 | 12.89 |

| | | | | | | | | | | | |
|---|---|---|---|---|---|---|---|---|---|---|---|
| All<br>Rad | 60 | 359.23 | 38.01 | 25.21 | 7.45 | 14 | 6.65 | 31.62 | 256.17 | 87.91 | 14.65 |

**Table 6.2.** Paleomagnetic analysis for the paleomagnetic data of this study with the previous work by Maillol et al (1997) and composite (22 flows) dataset, to compared the best distribution based on the cutoff angle (Cutoff ang) to obtained mean directions (Dec, Inc), their respective parameters of quality (k, $\alpha_{95}$), the number of data used ($N$), and their respective pole parameters of quality (A95, K), the VGP (VGPLong, VGPLat), and the angular standard deviation (Sp).

Based on this analysis, we conclude that the most representative direction for the MVF is the mean paleodirection that involve the 22 lava flows (Table 6.2, Figure 6.5).

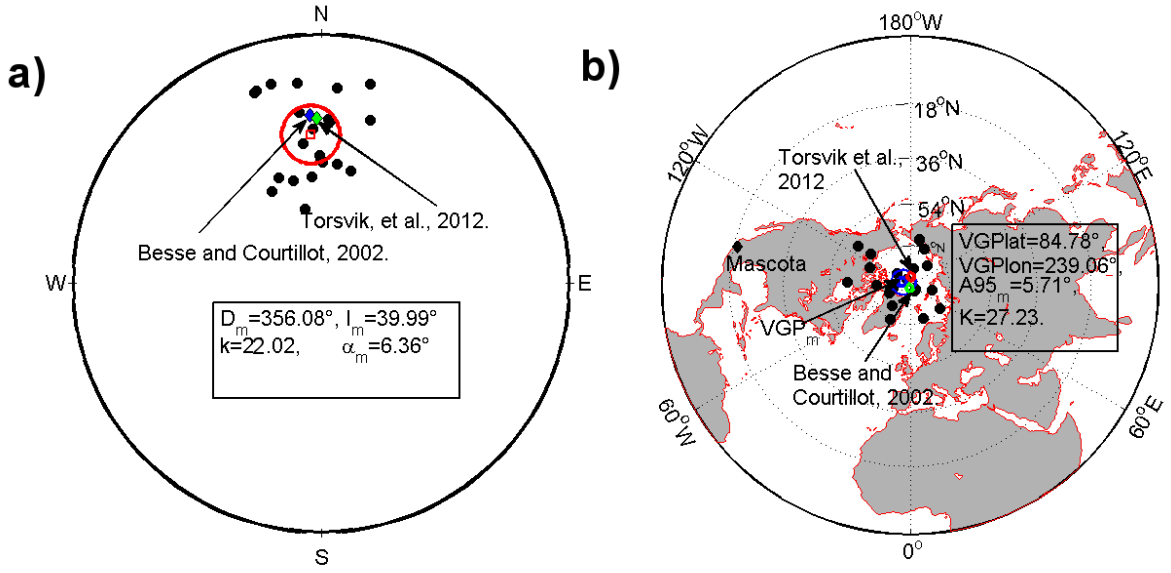


**Figure 6.5.** a) Equal area projection of the mean paleomagnetic directions obtained in this study, b) projection of the VGPs together with reference paleomagnetic poles calculated from the stable North America (Besse and Courtillot, 2002; Torsvik *et al.*, 2012).

These directions are practically undistinguishable from the expected directions retrieved from both Besse and Courtillot (2002) and Torsvik et al., (2012) reference poles (Figure 6.5) with difference observed in the flattening parameter $F_{BC} = -5.09 \pm 5.97$ and rotation parameter $R_{BC} = -0.31 \pm 7.0$ and $F_T = -3.00 \pm 5.91$ and $R_T = -2.01 \pm 7.0$ respectively. The mean paleodirection was compared with the Geomagnetic Axial Dipole (GAD) direction for the geographic coordinate of Mascota at $20°32'N, 104°49'W$ and indicate a slight difference $\Delta D = 3.92°$ and $\Delta I = 3.19°$ (Figure 6.6). Moreover, same paleodirections were compared with the study of Lawrence et al. (2006), which performed an analysis from several areas showing that the VGP dispersion parameters for about 20°N latitudes are consistent with the present study. This comparation test also indicates that the mean inclination difference are also smaller during the Matuyama than Brunhes (Table 6.2) in agreement with the results presented by Lawrence et al. (2006), from México.

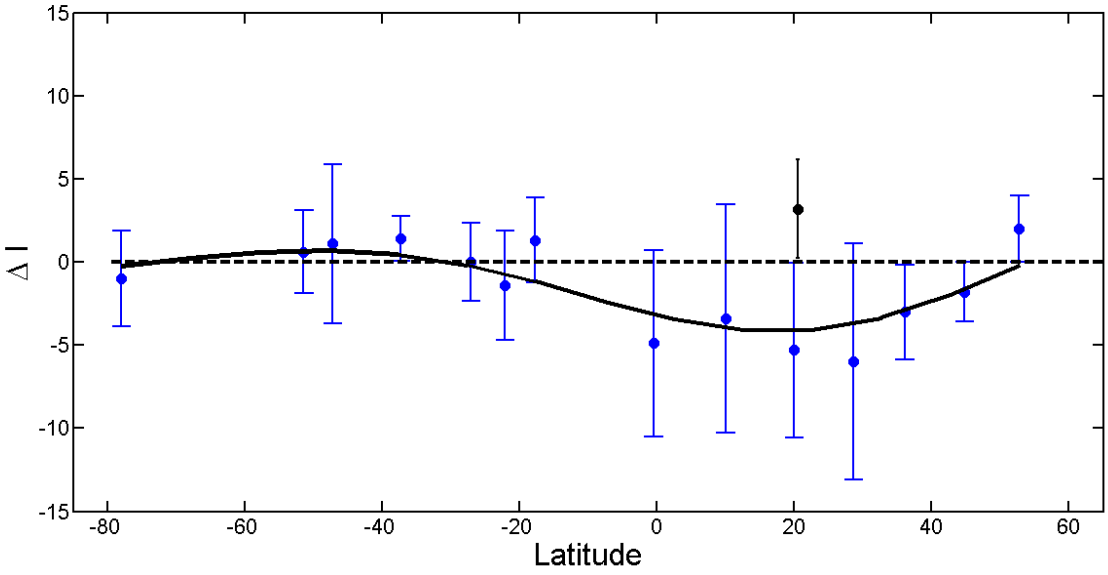


**Figure 6.6.** Inclination anomaly versus latitude for normal and reverse data compiled by Johnson el al., 2008 (data in blue color), with a 95% confidence intervals (error bars), and best-fit two.parameter zonal field model (solid line). The Inclination anomaly for the Mascota Volcanic Field with respect a mean geographic average latitude is labeled by black color.

A reversal test applied to the site mean paleodirections is positive yielding type C (Figure 6.7, Table 6.3) as derived from calculations reported in (McFadden and McElhinny, 1990).

| Site | Critical angle | Observed angle | Rc | k1 | k2 | Classification |
|---|---|---|---|---|---|---|
| Maillol | 21.88° | 5.47° | 13.25 | 20.35 | 22.71 | INDETERMINATE |
| T.S | 22.03° | 19.83° | 15.1 | 17.95 | 34.15 | INDETERMINATE |
| All | 17.75° | 6.61° | 20.91 | 20.98 | 24.47 | C |

**Table 6.3.** Classification of the Reversal Test (McFadden and McElhinny 1990) for flow of MVF, Talpa and San Sebastian, using all selected paleodirections to obtained the Critical angle: useful to determine the classification between both distribution; Observed Angle is the angle between both distribution; Rc: Critic value associated to the critical angle; k1 and k2: Values associated with the distribution precisions; Classification: Is the classification obtained by the Reversal Test.

The angular standard deviation (often called angular dispersion) of the virtual geomagnetic poles (VGPs) yields a value of $S_B = 16.49°$ with the lower confidence limit $S_{BL} = 15.13°$ and the upper confidence limit $S_{BU} = 18.10°$ (Cox, 1969). The value of the angular dispersion matches with the Model G of Johnson et al. (2008) and which gives a value of about 16° for the latitudes around 20°. This however is true for Bruhnes chron while little bit higher dispersion is expected for the Matuyama chron. It should be noted that the model of Johnson et al. (2008) was developed using a criteria for data selection very similar to present study. Some differences observed between the Model G of McFadden et al. (1997) and TK03 of Tauxe and Kent, (2004) is probably due to the fact that the Model G used lest strict selection criteria while TK03 is based made on different materials than volcanic flows.

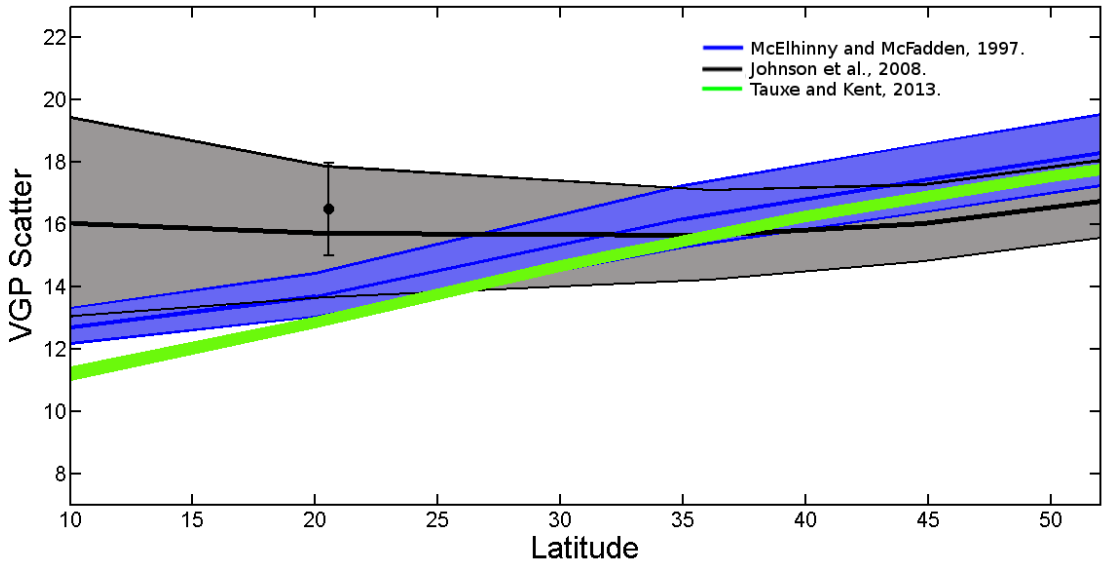


**Figure 6.7.** Scatter of the VGP as function of the latitude for the last 5 Myr, compared with the Model G of McElhinny and McFadden (1997) (blue line), Johnson *et al*., 2008 (black line) and the Tk03 Model propose by Tauxe and Kent (2004) (green line).

The dispersion parameters obtained in present investigation is compatible to other studies carried out along the central and western Mexico (Mejia et al., 2005, Conte-Fasano et al., 2006, Ruiz-Martinez et al., 2010). The same is true to sites belonging to similar latitudes, as Réunion, the South Pacific and Hawaii (Lawrence et al., 2006). The possible occurrence of Levantine geomagnetic event in MVF lavas is supported by two independent nearby lava flows belonging to Tequila Volcanic Field dated as 362±13 and 354±5 kyr respectively yielding transitional paleodirections (Rodríguez et al., 2006). Levantine excursion at about 360 kyr is classified in Singer et al., 2002 geomagnetic instability time scale as a poorly defined excursion (Ryan, 1972). Some evidence of this short event was also reported by Torii et al. (1974) from the Osaka area (370-380 kyr) and Negrini et al., (1988) from the Summer Lake (360-370 kyr).

### 6.6 Conclusions

- A detailed rock-magnetic experiments which included continuous thermomagnetic curves, isothermal remanent magnetization and hysteresis measurements indicates that ferrimagnetic phases with low to moderate coercivities corresponding to both Ti-poor (almost magnetite phase)

and Ti-rich titanomagnetites are responsible of magnetization in majority of cases.

- The present study increased the number of high standard paleomagnetic data from the Jalisco Block adding nineteen radiometrically dated sites which allowed to increase the robustness of existing data from the western part of the Trans-Mexican Volcanic Belt during Plio-Pleistocene.

- Thirteen flows correspond to the Brunhes chron, one of them exhibits transitional directions, while the remaining six sites belong to the Matuyama chron. The combined paleomagnetic dataset, supported by positive reversal test, indicate no paleomagnetically detectable vertical-axis rotations in the study area.
- The evidence of one transitional directions was detected, which may correspond to the Levantine excursion (360-370 kyr) or unnamed event between 400-420 kyr.

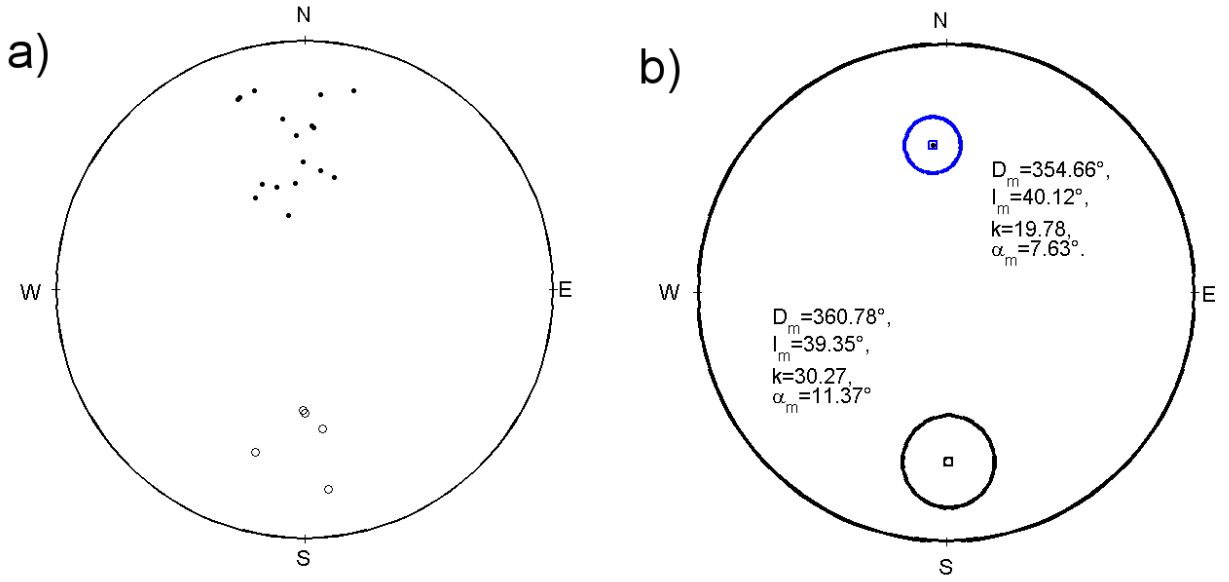


- **Figure 6.8.** Results of the F-Test as reported by McFadden and McElhinny 1990 for the MVF lava flows.

**References**


Bandy W. L., Urrutia-Fucugauchi J., McDowell F. M., and Morton-Bermea O., 2001. K-Ar ages of four mafic lavas from the Central Jalisco Volcanic Lineament: Supporting evidence for NW migration of volcanism within the Jalisco block, western Mexico. *Geof. Int.*, **1**, 259-269, 4.

Besse, J., and Courtillot, V., 2002. Apparent and true polar wander and the geometry of the geomagnetic field in the last 200 Myr. *J. Geophys. Res.*, **107**, EPM 6-1-EPM 6-31, B11, 10.1029/2000JB000050.

Carmichael I. S. E., Lange R. A., and Luhr J. F., 1996. Quaternary minettes and associated volcanic rocks of Mascota, western Mexico: a consequence of plate extension above a subduction modified mantle wedge. *Contrib Mineral Petrol.*, 124, 302-333.

Conte-Fasano G., Urrutia-Fucugauchi J., Goguitchaichivili A., Morales-Contreras J., 2006, Low-latitude paleosecular variation and the time-averaged field during the late Pliocene and Quaternary-Paleomagnetic study of the Michoacán-Guanajuato volcanic field, Central Mexico: *Earth, Planets Space*, **58**, 1359-1371, 10.1186/BF03352632.

Dunlop D.J., 2002a, Theory and application of the Day plot ($M_{rs}/M_s$ versus $H_{cr}/H_c$) 1. Theoretical curves and tests using titanomagnetite data. *J. Geophys Res.*, **107**, EPM 4-1-EPM 4-22, 10.1029/2001JB000486.

Ferrari L., 2000, (Avances en el conocimiento de la Faja Volcánica Transmexicana durante la última época), Advances in the understanding of the Trasnmexican Volcanic Belt during the last period. *Bol. Soc. Geo. Mex.*, **V**, 84-92.

Fisher R.A., 1953, Dispersion on a Sphere. *Proceedings of the Royal Society of London A: Mathematical, Physical and Engineering Sciences*, **217**, 295-305, 10.1098/rspa.1953.0064.

Johnson, C. L and Constable C. G., 1995, The Time-average field record by lava flows over the past 5 Myr, *Geophys. J. Int*., **122**, 489-519.

Johnson, C. L and Constable C. G., 1998, Persistently Anomalous Pacific Geomagnetic Fields, *Geophys. Res. Lett.*, **25**, 1011-1014.

Johnson, C.L., Constable C.G., Tauxe L., Barendregt R., Brown L.L. Coe R. S., Layer P., Mejia V., Opdyke N.D., Singer B.S., Staudigel H,. and Stone D. B., 2008, Recent investigations of the 0-5 Ma geomagnetic field recorded by lava flows. *Geochemistry, Geophysics, Geosystems*, **9**, 1525-2027, 10.1029/2007gc001696.

Kirschvink, J.L., 1980, The least-square line and plane and analysis of paleomagnetic data. *Geophys. J. Int.*, 62, 699-718, 10.1111/j.1365-246X.1980.tb02601.x

Laj, C., Channel, J.E.T., 2007, Geomagnetic Excursions, *1st Edn, 5, Elsevier Science, Treatise on Geophysics*.

Lange, R. A., and Carmichael I. S. E., 1990, Hydrous basaltic Andesites Associated with Minette and Related Lavas in Western Mexico. *J. Petrology*, 31, 1225-1259, 10.1093/petrology/31.6.1225.

Lange R. A., and Carmichael, I.S.E., 1991, A potassic volcanic front in western Mexico: The lamprophyric and related lavas of San Sebastian, *Geol. Soc. Amer.*, 103, 928-940.

Lawrence K. P. and Constable C. G., 2006. Paleosecular variation and the average geomagnetic field at ±20°latitude, *Geochem Geophys Geosyst*, 7, 10.1029/2005GC001181.

Luhr,. J. F., Nelson A. S., Allan F. J., and Carmichael I. S. E., 1985, Active rifting in southwestern Mexico: Manifestations of an incipient eastward spreading-ridge jump. *Geology*,13, 54-57, 10.1130/0091-7613(1985)13<54:ARISMM>2.0.CO;2.

Maillol. J. M. and Bandy, W. L., 1993, Paleomagnetism of the Talpa de Allende and Mascota grabens western Mexico: A preliminary Report., *Geo. Int.*, 33, 153-160.

Maillol. J. M., Bandy, W. L. and Ortega Ramírez, J., 1997, Paleomagnetism of Plio-Quaternary basalts in the Jalisco block, western Mexico, *Geo. Int.*, 36.

McElhinny, M.W., McFadden, P.L., and Merrill R. T. 1996, The Time-average paleomagnetic field 0-5 Ma, *J. Geophys. Res.*, 101, 25007-25027, 10.1029/96JB01911.

McElhinny, M.W., McFadden, P.L., 1997, Paleosecular variation over the past 5 Myr based on a new generalized database. *Geophys. J. Int.*, 131(2), 240-252, 10.1111/j.1365-246.X.1997.tb01219.x.

McFadden P. L, and McElhinny M. W. 1990, Classification of the reversal test in paleomagnetism, *Geophys. J. Int*, 103, 725-729, 10.1111/j.1365-246X.1990.tb05683.x

Mejia, V., Böhnel, H., Opdyke, N.D., Ortega-Rivera, M.A., Lee J.K.W., Aranda-Gomez J.J., 2005, Paleosecular variation and time–averaged field recorded in Late Pliocene–Holocene lava flows from Mexico, *Geochemistry, Geophysics, Geosystems*, 6, 10.1029/2004GC000871.

Merril R.T., and McElhinny M.W. 1985, The Earth's Magnetic Field. Its History, Origin and Planetary Perspective. 122(3), *London: Academic Press,* 10.1017/S0016756800031630.

Negrini, R. M., Verosub K. and Davis O., 1988, The middle to late Pleistocene geomagnetic field recorded in fine-grained sediments from Summer lake, Oregon and Double Hot Springs, Nevada, USA, *Earth Planet. Sci. Lett.*, 87, 19-38, 10.1016/0012-821X(88)90073-8.

Ownby S. E., Lange R. A. and Hall C. M., 2008, The eruptive history of the Mascota volcanic field, western Mexico: Age and volume constraints on the origin of andesite among a diverse suite of lamprophyric and calc-alkaline lavas, *J. Volcanol. Geotherm Res.* 117, 1077-1091.

Prévot, M., Mankinen E. A., Gromme S. C., and Coe R. S., 1985, How the geomagnetic field vector reverses polarity, *Nature*, 316, 230–234, 10.1038/316230a0.

Rigthter, K., and Carmichael I. S. E., 1992, Hawaiites and related lavas in the Atenguillo graben, western Mexican Volcanic Belt. *Geol. Soc. Am. Bull.*, 104, 1592-1607, 10.1130/0016-7606(1992)104<15:HARLIT>2.3.CO;2

Rodríguez C. M., Goguitchaichvili A, Calvo-Rather M., Morales C. J., Alva-Valdivia. L. A., Rosa. E. Jose., Urrutia F. J., and Delgado G. H., 2006, Paleomagnetism of the Pleistocene Tequila Volvanic Field(Western Mexico), *Earth Planet Space*, 58, 1349-1358, 10.1186/BF03352631.

Roberts A. P., Cui Y., and Verosub K. L., 1995. Wasp-waisted hysteresis loops: mineral magnetic characteristics and discrimination of components in mixed magnetic systems. *J. Geophys. Res.* 1000, 17909-17924, 10.1029/95JB00672.

Ruiz-Martinez V. C., Urrutia-Fucugauchi J. and Osete M. L., 2010, Paleomagnetism of the Western and Central sectors of the Trans-Mexican volcanic belt-implications for the tectonic rotations and paleosecular variation in the paste 11 Ma., *Geophys. J. Int*, 180, 577-595, 10.1111/j.1365-246X.2009.04447.x.

Ryan, W. B., 1972 Stratigraphy of late Quaternary sediments in the eastern Mediterranean. In The Mediteranean Sea: *a natural sedimentation laboratory*, D. J. Stanley, Dowden, Hutchinson & Ross, Stroudsburg.

Schneider, D. A., and Kent D. V. 1990, The time-average paleomagnetic field, *Rev. Geophys.*, 28, 71-96, 10.1029/RG28i001p00071.

Singer, B. S., Relle M. K., Hoffman K. A., Battle A., Laj C., Guillou H., and Carracedo J., 2002, Ar/Ar ages from transitionally magnetized lavas on La Palma, Canary Islands, and the geomagnetic instability timescale, *J. Geophys. Res*., 107, EPM 7-1-EPM 7-20, 10.1029/2001JB001613.

Tauxe L., Mullender, T. A. T., and Pick, T., 1996. Potbellies, wasp-waists, and superparamagnetism in magnetic hysteresis, *J. Geophys. Res*. 101, 571-583, 10.1029/95JB03041.

Tauxe, L., 2002. *Paleomagnetic Principles and Practice*. 1Frst Edn, *18*, Kluwer Academic Publisher Dordrecht

Tauxe L., and Kent D.V., 2004, *A Simplified Statistical Model for the Geomagnetic Field and Detection of Shallow Bias in Paleomagnetic Inclinations: was the Ancient Magnetic Field Dipolar?*, Timescales of the Paleomagnetic Field, American Geophysical Union, D.C., 10.1029/145GM08

Torii M., Yoshikawa S., and Itihara M., 1974. Paleomagnetism in the water-laid volcanic ash layer in the Osaka Group, Sennan and Senpoku hills, southwest Japan, *Rock Magn. Paleogeophys.*, 2, 34-37.

Torsvik, T.H., Van der Voo, R., Preeden, U., Mac Niocail, C., Steinberger, B Hinsbergen, B., Doubrovine, P.V., van Hinsbergen, D.J.J., Domier, M., Gaina, C., Tohver, E., Meert, J.G., McCausland, P.J.A., Cocks, L.R.M., 2012, Phanerozoic polar wander, palaeogeography and dynamics: *Earth-Science Reviews*, 114, 325-368, 10.1016/j.earscirev.2012.06.007.

Wallace, P., and Carmichael I. S. E., 1989. Minette lavas and associated leucitites from the western front of the Mexican Volcanic belt: Petrology, chemistry, and origin. *Contrib. Mineral Petrol.*, 103, 470-492, 10.1007/BF01041754.

Wilson R.L., 1972, Palaeomagnetic differences between normal and reverse field sources, and the problem of far-side and right-handed pole positions, *Geophys. J. R. Astron. Soc*., 28, 295-304.

Wilson, R. L. and McElhinny M. W., 1974, Investigation of the large scale palaeomagnetic field over the past 25 million years: eastward shift of the Icelandic spreading ridge, *Geophys. J. R. Astron. Soc*. 39, 570-586.

# 7. Paleomagnetism and Aeromagnetic Survey from Tancitaro Volcano (Central Mexico) - PaleoSecular Variation at Low Latitudes During the Past 1 Ma

## 7.1 Abstract

The Tancitaro volcano (TV) is part of the Michoacan-Guanajuato monogenetic volcanic field (MGVF) in the central-western sector of the Trana-Mexican Volcanic Belt (TMVB). Results of a paleomagnetic study of radiometrically dated lava flows from the Tancitaro volcano are used to investigate the paleosecular variation (PSV) and time averaged field (TAF) at low latitudes. Ar-Ar dates range from ~70 to 960 kyr spanning the Brunhes and Matuyama polarity chrons. All samples yielded well defined normal polarity magnetization. Two flows are correlated to the Jaramillo polarity event, which provide a useful marker for the volcanic activity in the MGVF. For the PSV and TAF analysis, paleodirections are combined with previously reported high standard results. The aeromagnetic survey around the Tancitaro volcano is characterized by a trend of regional anomalies over the volcanic structures. The residual field shows several positive and negative anomalies. The Tancitaro volcano is marked by a broad positive anomaly suggesting the presence of a large underground source. Spectral analysis of this anomaly field gives an average estimate to the top of the source bodies between 2-3km.

**Key words:** Paleosecular variation, Geomagnetic Axial Dipole, Jaramillo excursions, Tancitaro volcano, Aeromagnetics.

## 7.2 Introduction

Study of radiometrically dated lava flows permits understanding the behavior of the Earth magnetic field (EMF) during the geological periods. The paleomagnetic records provide valuable information about the

directions and intensity stored in each independent cooling unit. Sediments may provide quite continuous records of magnetic field variation, while lavas, due to the sporadic character of volcanic eruptions, yield rather discontinuous records of geomagnetic field fluctuations. On the other hand, the results obtained from lavas are generally more reliable because of nature and physical principles of the TRM (thermoremanent magnetization) acquisition (Prévot et al., 1985). Many high resolution volcanic records have documented polarity transitions and intervals of constant polarity termed chrons and relatively short duration of $10^3 - 10^4$ year's events or excursions inside (e.g., Merrill and McFadden 2003). The transitional episodes are generally defined in terms of a deviations in intervals less than $10^3$ years of the Virtual Geomagnetic Pole (VGP) position from the Geomagnetic Axial Dipole (GAD).

Whole TMVB represent and excellent target for high standard paleomagnetic study since it offer more than 3000 Plio-Quaternary lava flows (mainly monogenetic volcanoes) being many of them radiometrically dated using either K-Ar or Ar-Ar systematics. The present investigation is aimed to contribute to the Time Averaged Field (TAF) study for the past 1 $My$ and improve knowledge on the paleosecular variation (PSV) at low latitudes (20°) extending the previous work of Maciel et al. (2009) from Tancitaro volcano and the surrounding Michoacan-Guanajuato Volcanic Field (VFMG).

Johnson et al.'s (2008) analysis of a new generation paleomagnetic data provides new insights about the latitudinal dependence of VGP (Virtual Geomagnetic Pole) scatter showing that this relationship is much less comparing to previous studies (i.e. Mankinen and Cox, 1988, see also Tauxe et al. 2004). It appears that the latitude dependence of VGP angular dispersion depends critically on a dataset from the moderate latitudes about 20° north including numerous data from Hawaii and Central Mexico. In other hand, modeling of the aeromagnetic anomalies in the area permits to investigate the subsurface structure, and

stratigraphy, in particular about distribution of magnetic sources related to magmatic bodies and volcanic structures.

### 7.3 Geological setting and sampling details

Tancitaro volcano (TV) is an andesitic-dacitic stratovolcano located in the Michoacán-Guanajuato volcanic Field (MGVF). The MGVF has an extension of 40,000 km² and is part of the central portion of the TMVB. The MGVF has geographic boundaries $18°45'N$ and $20°15'N$ in latitude and 100°25'W and 102°45'W longitude; contains over 2000 small-sized monogenetic volcanoes including basaltic monogenetic cinder cones (Hasenaka and Carmichael, 1985; Connor, 1987, 1990), maars, tuff rings, lava domes and lava flows with hidden vents. Volcanic products are predominant calc-alkaline, but some alkaline and transitional rocks are present. Silica content varies $47\%$ to $70\%$ for olivine basalt and basalt-andesite rocks (Hasenaka, 1994; Hasenaka et al., 1994).

The TV is a highest stratovolcano in the MGVF with a height of $3840$ mts (Ownby et al., 2007), and has a large amount of dated flows. The activity start $\geq 793 \pm 22$ kyr, and its last eruption was around $237 \pm 4$ kyr, most of these events were dated by the radiometrical method $Ar^{40}/Ar^{39}$ for Ownby et al., 2007 and 2010. The present study sampled 8 lava flows to complement previous work made by Maciel et al. (2009). These lava flows (Figure 7.1) have been reported by Ownby et al. (2010) who present 39 new Ar-Ar dates that complement 26 flows with radiometric age also reported by Ownby et al., (2007).

The volcanic flows for this study correspond to flows with radiometric age, easy access, and sampled roadside of almost continuous structures of lava flows that not being rotated or unaltered outcrops and not sings of being near of a geological fault which was corroborate with the geological map of the National Geological Service. The eight samples were obtained with a gasoline powered portable drill, oriented with a magnetic compasses to obtained several samples along each flow $N \geq 8$.

The eight flows sampled cover an age range of ~70 kyr to 957 kyr, and complements previous work by Maciel et al., 2009, that included 11 flows with an age range of 82 kyr to 612 kyr, since the TV is an important source of unrecorded flows that could provide important paleomagnetic information with aged of a good accuracy.

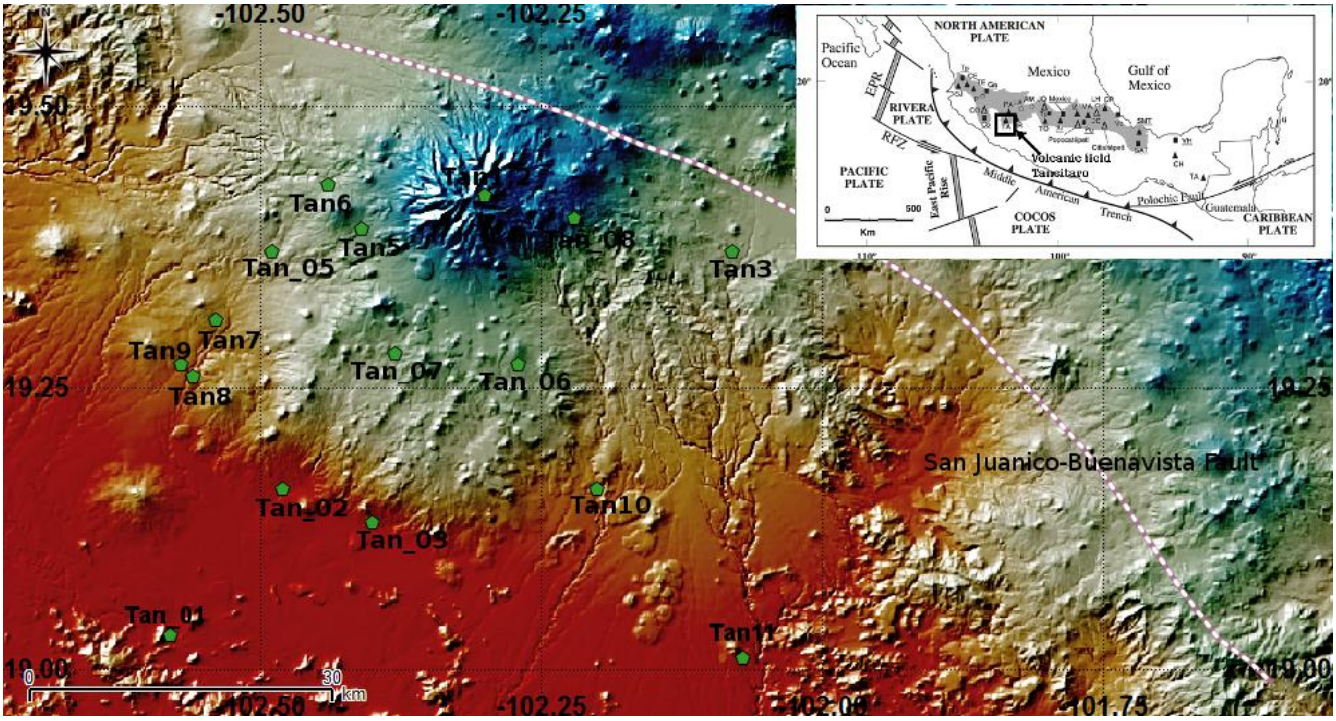


**Figure 7.1**. Location of the Tancitaro Volcano in the western sector of the TMVB showing the setting of sites reported in this study (Tan_01-08) and the previously sampled flows by Maciel et al., 2010 (Tan1-11).

### 7.4 Magnetic Measurements and Data Analysis

#### 7.4.1 Remanence measurements

All specimens were demagnetized by peak alternating fields which proved to be highly efficient to isolate the characteristic, primary remanence. A Molspin AF-demagnetizer with available alternating fields from 5 $mT$ to 95 $mT$ was used while magnetization was measured with spinner magnetometer JR6A (AGICO)

spinner magnetometer with nominal sensitivity$\sim 10^{-9} Am^2$. The determination of the main magnetization components for each specimen was achieved with the method of principal component analysis (Kirschvink, 1980) and the directions were averaged by unit based on Fisher statistics (Fisher, 1953).

In most of the cases we observed a stable, univectorial characteristic remanent magnetization (ChRM) (Figure 7.2 a) for Tan1 and Figure 7.2 d) for Tan7) occasionally accompanied by a negligible viscous overprint (Figure 7.2 b) for Tan 2 and Tan5) easily removed after the first step of demagnetization Figure 2. Most of the specimens were completely demagnetized until $100\, mT$. The site mean directions are quite precisely determined since all $\alpha_{95}$ are found less than 10°. For one out eight studied lava flows (Tan4) not paleodirection are determined due the erratic and unstable behavior during the magnetic cleanings of specimens.

The other seven volcanic flows gave stable paledirections, and were divided in two groups, the first group are all the directions that belong to the chron of Brunhes (5 of the 7 paleodirections) and the second group are the paleodirections that belong to the chrons of Matuyama. The directions that belong to the chron of Matuyama has the peculiarity of corresponded to the same event of transition due the normal polarity

and the radiometric age assigned at these flows by Ownby et al., (2010). The transitional event has known as Jaramillo, and was first recognized by (Doell and Dalrymple 1966).

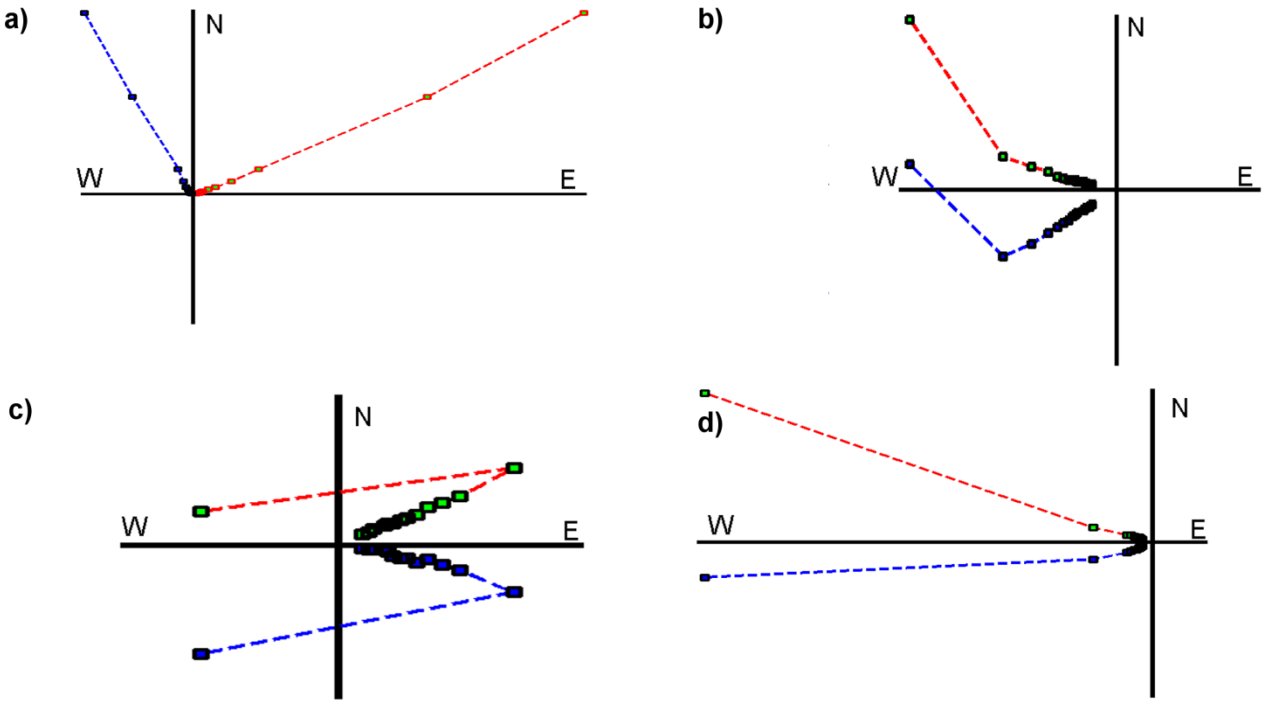


**Figure 7.2**. Representative examples of demagnetization experiments using peak alternative fields up to 95 mT, with the orthogonal vector plots, (Zijderveld diagrams) a) For the sample 94T004A and the site Tan1 b) Sample 94T015A and site Tan_02, c) Sample 94T047A corresponding to Tan_05 and d)Sample 94T060A for the site Tan_07.

### 7.4.2 Rock magnetism

The acquisition of thermomagnetic curves for representative samples are reported on Figure 7.3. Curie temperatures were estimated using the differential method of Tauxe (1998) for the analysis of the Magnetic vs Temperature curves. These analysis evidenced the low temperature phase in the heating

process (red line Figure 7.3) Tc 492°C for sample 94T002A corresponding to site Tan_01 (Figure 7.3a) with two phases in the heating process (red line) that may indicates the presence Titanomagnetite with medium Ti content. Using the method of Moskowitz (1981), it results that the highest Curie temperatures are 591°C for 94T016A corresponding to site Tan_02 (Figure 7.3b), and 511°C for 94T028A corresponding to Tan_03 (Figure 7.3c). In some cases the heating and cooling curves are not perfectly reversible (Tan_01). This may be due to the high to moderate mineralogical alteration at high temperatures occurred during the laboratory heating's.

The hysteresis loops were analyzed using a RockMagAnalyzer1.0 software (Leonhard, 2006). Near to the origin, there is no evidence of wasp-waisted behavior (Tauxe et al., 1998), which reflect restricted coercivity ranges. When judging the ratios obtained from the hysteresis curves, samples fall in the pseudo-single domain PSD field (Figure 7.3). Isothermal remanence acquisition curves, are sensitive to the magnetic mineralogy, concentration and grain size properties. Almost all samples are saturated at about 300 mT applied magnetic field, which indicate the presence of ferromagnetic phase with moderate coercivity as may be expected from magnetite and titanomagnetite grains (Tauxe, 1998). The lack of total symmetry on the hysteresis plots is generally attributed to the instrumental errors excepting the study performed by Chandra et al. (2012) where the exchange bias seem to be the principal cause.

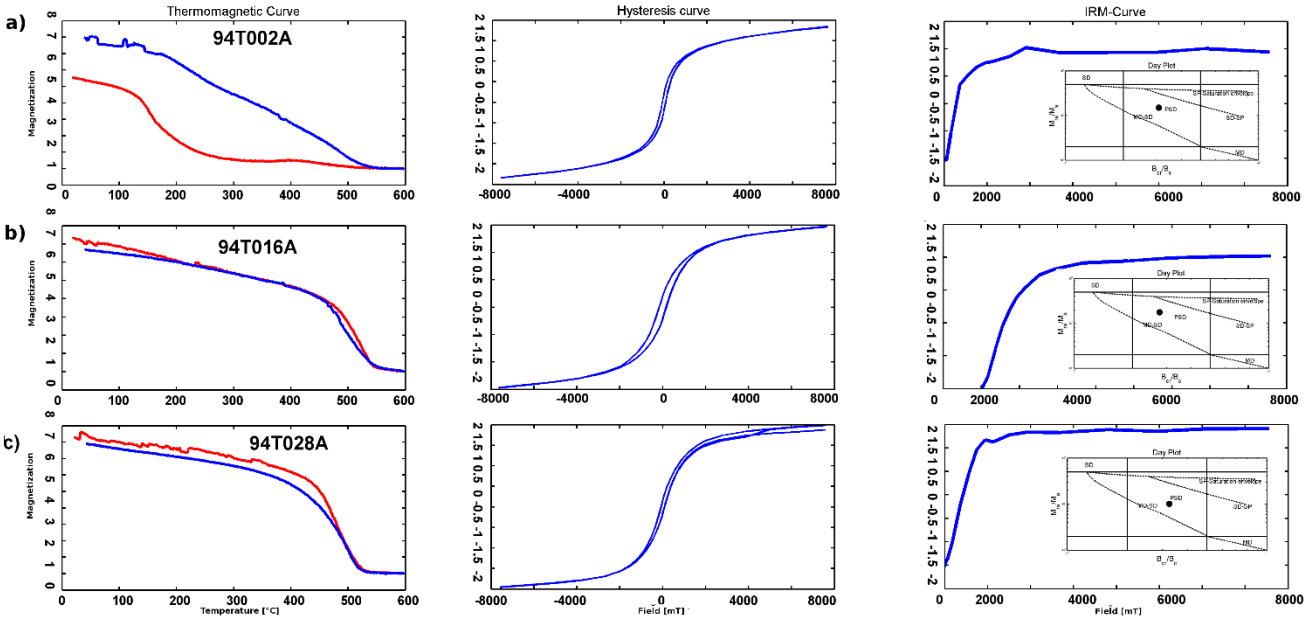


**Figure 7.3**. A summary of rock-magnetic experiments for the most representative samples:

Temperature dependence of magnetization (magnetization $10^{-5}\ Am^2kg^{-1}$), the red curve represent the heating process and the blue the cooling curve. Hysteresis loops for an induced magnetic field in blue (magnetization $10^{-4}\ Am^2kg^{-1}$). Isothermal remanence magnetization acquisition curves (IRM, $10^{-5}Am^2/kg$)obtained with Variable Field Translation Balance with the respective Day Plot (Dunlop, 2002), to estimate the domain state of magnetic carriers and the relation of the ratios of the hysteresis parameters for the remained samples.

## 7.5 Main Results and Discussion

All lava flows associated to the TV yielded a normal polarity magnetization. The paleodirections were divided in two groups, five of them (Tan_01, Tan_02, and Tan_06-08) correspond to Brunhes chron and the other two (Tan_03 and Tan_05) belong to Matuyama Chron.

The mean paleodirection obtained from the seven flows is $Inc = 40.88°$, $Dec = 0.30°$, with an uncertainty $\alpha_{95} = 8.21°$ and $k = 13.89$, which correspond to the pole position of $Plat = 83.06°$, $Plong = 294.86°$, $A95 = 14.49°$. These paleodirections are combined with the paleodirections obtained by Maciel et al., 2009 who reported 11 normal polarity directions within normal Brunhes chron (Table 7.1, Figure 7.4 and 7.5). For the global mean calculation purpose we selected sites with $N \geq 4$ samples per site and $\alpha_{95} \leq 10°$. Moreover, transitional polarity data are rejected as common in studies of paleosecular variation (PSV) and time average field (TAF) for age less than 5 Myr (Johnson et al., 2008, Ruiz-Martinez et al., 2008) to obtained a mean calculation.

| Site | Dec | Inc | k | a95 | N | lat | long | Age(Ka) | VgpLon | VgpLat | Ref: |
|---|---|---|---|---|---|---|---|---|---|---|---|
| TAN_04 | - | - | - | - | - | 19.15 | 102.32 | 51± 82 | | | T.S. |
| TAN_08 | 350.15 | 24.79 | 117.35 | 5.28 | 6.00 | 19.40 | 102.22 | <70 | 159.61 | 78.59 | T.S. |
| Tan10 | 1.20 | 32.80 | 69.00 | 7.30 | 7.00 | 19.16 | 102.20 | 82± 24 | 60.80 | 88.27 | M. P. R. 2009 |
| TAN_02 | 7.51 | 46.00 | 109.17 | 5.06 | 7.00 | 19.16 | 102.48 | 110± 33 | 321.09 | 79.28 | T.S. |
| Tan11 | 349.30 | 43.60 | 198.00 | 4.30 | 7.00 | 19.01 | 102.07 | 163± 37 | 227.09 | 78.19 | M. P. R. 2009 |
| Tan1 | 7.80 | 23.80 | 56.00 | 16.50 | 3.00 | 19.42 | 102.30 | 209± 41 | 54.12 | 79.76 | M. P. R. 2009 |
| Tan2 | 353.50 | 43.50 | 199.00 | 3.90 | 8.00 | 19.42 | 102.30 | 209± 41 | 238.28 | 81.54 | M. P. R. 2009 |
| Tan6 | 17.90 | 58.60 | 41.00 | 9.60 | 7.00 | 19.43 | 102.44 | 256± 18 | 316.43 | 64.83 | M. P. R. 2009 |
| Tan5 | 348.50 | 41.20 | - | - | 2.00 | 19.39 | 102.41 | 269± 22 | - | - | M. P. R. 2009 |
| Tan4 | - | - | - | - | - | - | - | 339± 23 | - | - | M. P. R. 2009 |
| TAN_01 | 354.14 | 31.18 | 92.10 | 5.16 | 8.00 | 19.03 | 102.58 | 347± 50 | 172.01 | 84.01 | T.S. |
| Tan7 | 348.60 | 28.10 | 115.00 | 6.30 | 6.00 | 19.31 | 102.54 | 373± 61 | 172.47 | 78.27 | M. P. R. 2009 |
| TAN_07 | 12.68 | 34.08 | 46.98 | 8.34 | 6.00 | 19.28 | 102.38 | 374± 31 | 13.12 | 78.00 | T.S. |
| Tan3 | 339.90 | 60.90 | 242.00 | 3.60 | 8.00 | 19.37 | 102.08 | 429± 64 | 249.41 | 61.73 | M. P. R. 2009 |
| Tan8 | 2.50 | 27.70 | 359.00 | 2.90 | 8.00 | 19.26 | 102.56 | 612± 41 | 74.47 | 84.86 | M. P. R. 2009 |
| Tan9 | 352.70 | 31.30 | 39.00 | 9.20 | 8.00 | 19.27 | 102.57 | 612± 41 | 174.94 | 82.67 | M. P. R. 2009 |
| TAN_06 | 343.63 | 19.55 | 78.19 | 6.46 | 6.00 | 19.27 | 102.37 | 768± 14 | 164.50 | 71.70 | T.S. |
| TAN_03 | 10.40 | 51.21 | 17.35 | 7.94 | 6.00 | 19.13 | 102.40 | 925± 135 | 311.04 | 76.30 | T.S. |
| TAN_05 | 36.20 | 75.40 | 189.54 | 4.40 | 7.00 | 19.37 | 102.49 | 957± 157 | 303.43 | 40.20 | T.S. |

**Table 7.1**. Summary of all the data used in this article. Site: are the label of the site sampled; Dec and Inc :are the paleodirection treated in this study; k and a95: parameters of quality within the cone of 95%; N: Is the number of samples used to obtain the paleodirection; lat and long: Are the coordinate for each one of the sampled sites. Age: Are the age obtain by the method of Ar-Ar with the respective dispersion; VGP: are the virtual geomagnetic pole for the latitude and longitude; Ref: Differentiate the paleo-direction of this study (T.S) and the paleodirection obtained of the work by Maciel et al., 2010 (M.P.R., 2009).

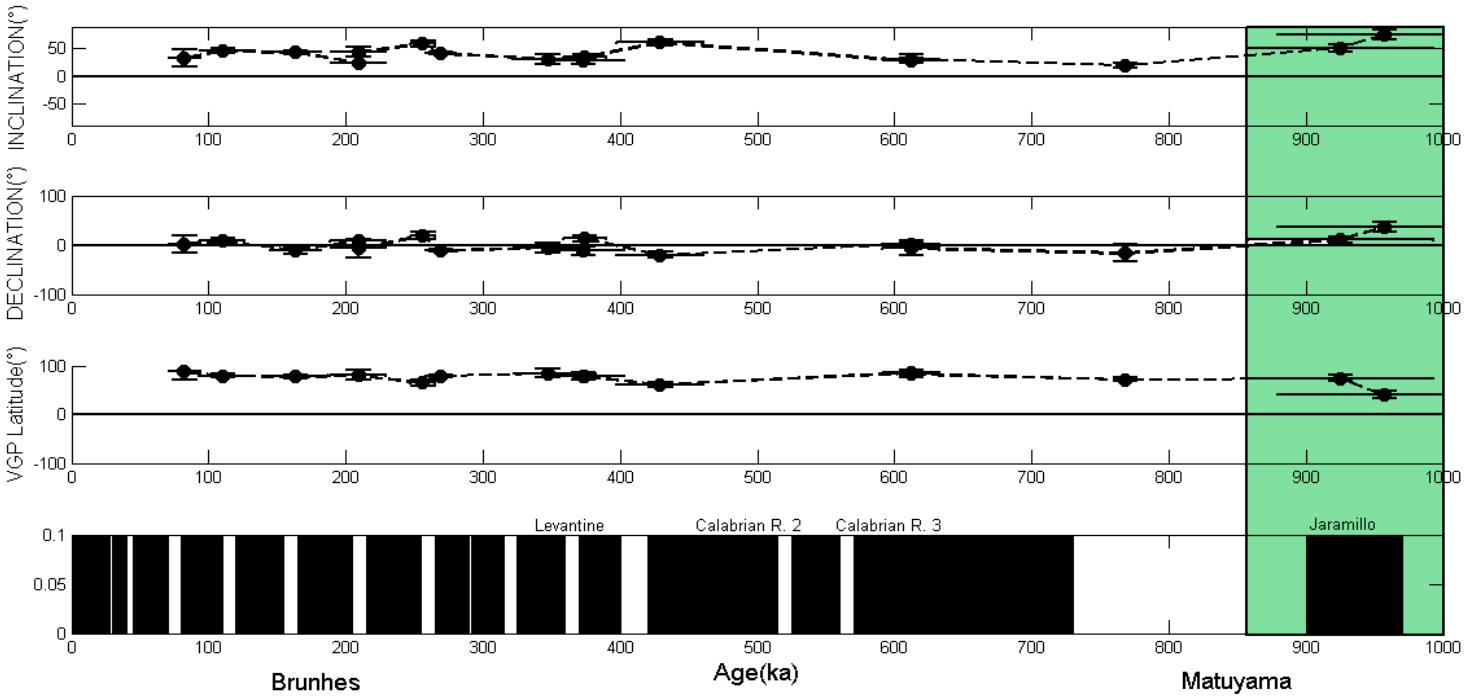
INCLINATION(°)
DECLINATION(°)
VGP Latitude(°)
Levantine
Calabrian R. 2
Calabrian R. 3
Jaramillo
Brunhes
Age(ka)
Matuyama

**Figure 7.4.** The corresponding VGP of the paleodirection with the mean VGP, and compared with the poles of reference for the las 5 Myr.

The mean paleomagnetic direction obtained in these study is $I_m = 37.46°$, $D_m = 358.39°$, $\alpha_{95m} = 6.4°$, $k = 34.15$ and $N = 15$ (Figure 7.5a). The corresponding paleomagnetic pole position is $P_{latm} = 86.57°$, $P_{longm} = 246.34°$, $A_{95m} = 6.21°$ and $K_m = 33.87$ (Figure 7.5b).

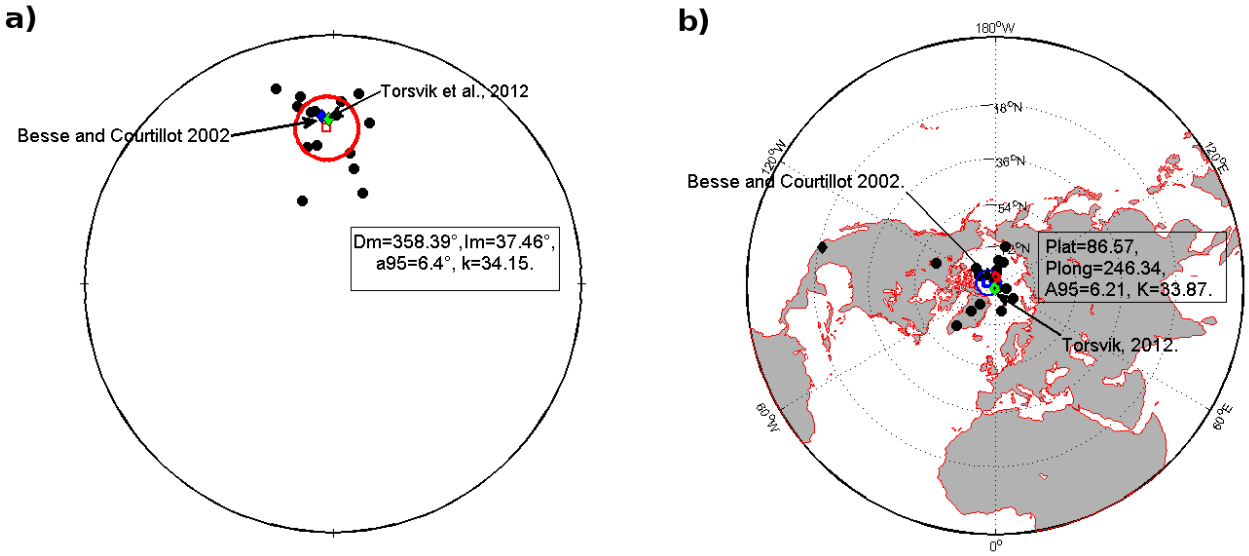


**Figure 7.5**. a) Projection of the paleodirection for the Tancitaro volcano with the respective mean paleodirection compared with the direction of reference for the Craton of North America provided by Besse and Courtillot (2002) and Torsvik et al., 2012. b) The corresponding VGP of the paleodirection with the mean VGP, and compared with the poles of reference for the las 5 Myr.

The mean paleodirection obtained was compared with the expected direction derived from the reference pole positions for North American Craton proposed by Besse and Courtillot (2002) and Torsvik et al., (2012) yielding $D_B = 356.1,\ I_B = 33.1\ °$ and $D_T = 358.5,\ I_T = 34.2,$ respectively. The use of

North American reference poles is a common practice in almost all previous paleomagnetic surveys (García-Ruiz, et al., 2016, 2017; Maciel et al., 2009, 2014; Ruiz-Martínez et al., 2010.) in order to avoid and kind of bias due to the neotectonic activity. For instance, the San Juanico Buenavista Fault located just beneath Tancitaro Volcano may potentially produce some minor tectonic rotations.

The mean direction agree with the expected directions within the uncertainty and this may be corroborated with the angle of deviation $\delta_B = 4.54$ (with respect to Besse and Courtillot, 2002 reference pole) and $\delta_T = 3.34$ (with respect of Torsvik et al., 2012 poles). For each paleomagnetic study, it may result useful to calculate the Flattening and Rotation (Butler, 1991) parameters together with their corresponding statistics. These analysis indicate the absence of any important tectonic movements since the values are relatively low $R_B = 1.66 \pm 7.22,\ F_B = -4.44 \pm 6.33$ (for Besse and Courtillot, 2002) and $R_T = -0.73 \pm 7.22,\ F_T = -3.34 \pm 6.33$ (for Torsvik 2012). These values also agree to the study carried out by Ruiz-Martínez et al., (2010) at different areas within the TMVB, specially for western and central sector, where similar small values are obtained ($|R| < 6°$ and $|F| < 5°$).

Most paleomagnetic studies make the implicit assumption that when averaged over some time interval, the paleomagnetic directions are close to the geocentric axial dipole (GAD) for at least the last 5 Myr, as globally average palepoles should reflect mainly the GAD field (Tauxe and Kent, 2004, Carlut and Courtillot, 1998). Under this assumption, we developed an analysis of TAF and a statistical comparison with the GAD. The mean direction of GAD was calculated for a mean latitude $\lambda_m = 19°16.08'$ obtaining $D_{GAD} = 0°,\ I_{GAD} = 34.96°,$ yielding a difference of $\Delta I = 2.48°$ and $\Delta D = 2.32°$. These values are even lower that found by Maciel et al. (2009) in previous studies and reasonably close to the GAD directions. The inclination anomaly found in this study is also compared with the value reported by Lawrence et al.,

(2006), for similar latitudes $\lambda = \pm 20^\circ$ as Hawaii, Mexico, South Pacific and Reunion. All these regions yielded statistically indistinguishable values (Figure 7.6).

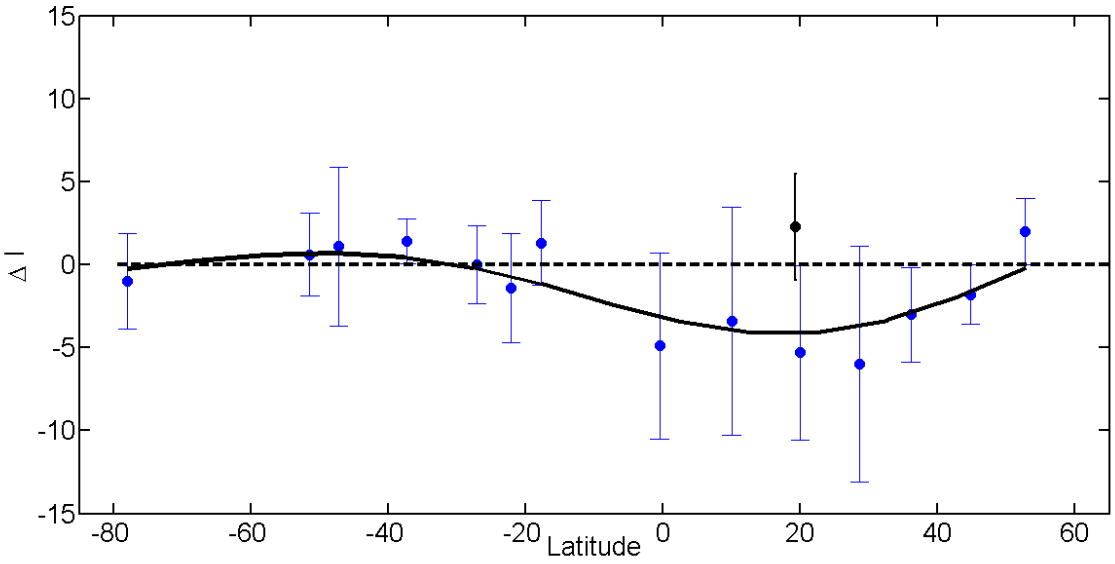


**Figure 7.6**. Curve of the best fit with respect of the anomalies of the inclination for several latitudes, with the average of the inclinations anomalies (blue dots) and the anomaly inclination of Tancitaro (Black dot).

A PSV analysis are very important to estimate the paleofield location for any time known and when a multiples site sampling is collected the influence of the error is reduced. The PSV analysis was developed complementing the directions presented in this study with the directions of Maciel et al., 2010 and the use of_angular standard deviation $s_w = \frac{81^\circ}{\sqrt{k}}$, to obtained$s_w = 14.09$, the standard deviation as $S_p^2 = (1/N-1)\sum_i^n \delta_i$ which result $S_p = 14.33,$ , the root mean square of the angular deviation of VGP about the geographic axis $S_B = \sqrt{(1/N-1)\sum_i^N (\delta_i^2 - s_{wi}/N)}$ result $S_B = 14.23,$ with respective lower confidence limit 13.6 and upper confidence limit 15.61, with the uses of the method of Cox (1970).

These results were compared with the model G proposed by McElhinny and McFadden et al., 1997 generated by global paleomagnetic dataset of lava flows exclusively. This database was reanalyzed by Johnson et al., 2008 using the bootstrap method under the main assumption that the paleomagnetic field closely approximates with the GAD for the last 5 Myr (see also a simplified statistical model Tk03.GAD by Tauxe and Kent (2004). Our results show a good agreement with the model G proposed by McElhinny and McFadden et al., 1997 (Figure 7.7) for a latitude of $\lambda = 20°$, and a dispersion of $S_M = 14$, and it's close to the limits of uncertainty of the dispersion for the model G of Johnson et al., 2008, with a value of $S_J = 14.8$, but when it's compared with theTk03.GAD model some disagreement is observed due this model predict a low value of $S_T = 12.9$ with respect to the latitude of $\lambda = 20°$.

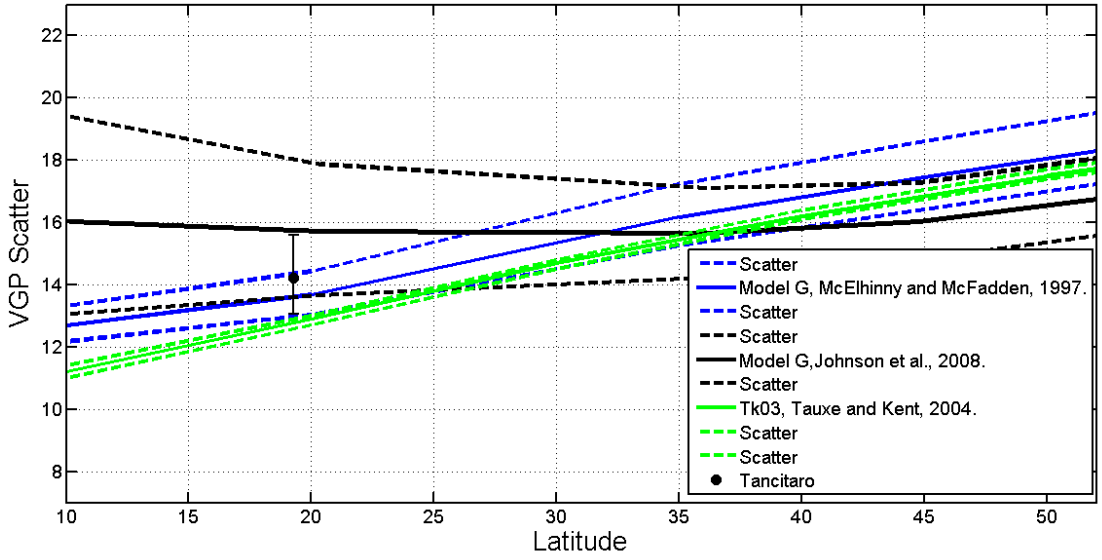


**Figure 7.7**. Scatter of the VGP as function of the latitude for the last 5 Myr, compared with the curves of reference provided by de Model G proposed by McElhinny and McFadden 1997 and Johnson et al., 2008, also with the Tk03.GAD model of Tauxe et Kent 2004.

For the studies developed around of the TMVB, it were obtained dispersion $S = 15.06 \pm 0.6°$ and $S = 14.9^{14.8}_{13.3}$ for studies made by Lawrence et al., (2006) and Ruiz-Martinez (2010) respectively, with dispersion a little bit higher, due the biased to Brunhes chron.

Two paleodirections obtained on sites Tan-3 and Tan-5 yielded normal polarity paleodirections within reverse polarity Matuyama chron. They may be erupted during the worldwide observable Jaramillo event (Doell and Dalrymple, 1966, Mankinen and Dalryple (1979),Laj and Channel (2007).

Aeromagnetic data of Tancitaro volcano area was obtained by the Mexican Geological Survey (SGM) in 1999, using the following equipment: Islander Airplane BN2-A21; Geometrics magnetometer G-822A optically pumped cesium vapor with sensitivity of 0.001 nT; data acquisition system, Picodas P-101 AG; Base station magnetometer, GEM Systems GSM-19 Overhauser, sensitivity 0.01 nT; Radar altimeter, Sperry RT-220 Navigation system, GPS Ashtech CG24GPS + Glonnas, 16m. Flight parameters were: contour flights at a height of 300 m; direction of flight lines North-South; distance between flight lines 1,000 m; distance between control lines (East-West) 10,000 m; electronic navigation (GPS). The data was initially processed by a digital compilation for correcting the movement plane (magnetic compensation), and daytime drift. From total magnetic field data we subtracted the International Geomagnetic Reference Field (IGRF 1995) obtaining the Residual Magnetic Field (RMF, Figure 7.8)

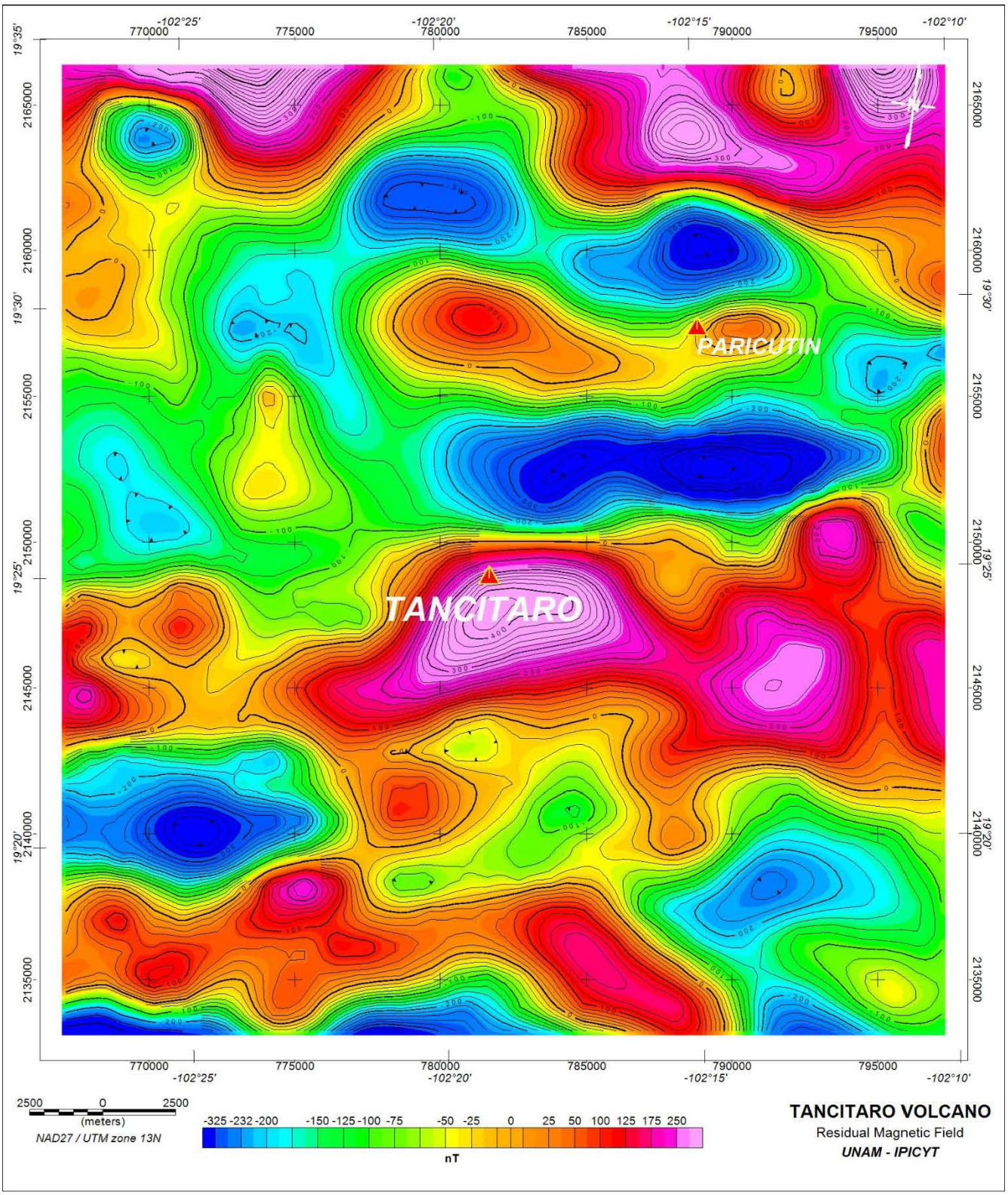
-102°25'
770000
775000
-102°20'
780000
785000
-102°15'
790000
795000
-102°10'
19°35'
19°30'
19°25'
19°20'
2165000
2160000
2155000
2150000
2145000
2140000
2135000
PARICUTIN
TANCITARO
2500 0 2500
(meters)
NAD27 / UTM zone 13N
-325 -232 -200 -150 -125 -100 -75 -50 -25 0 25 50 100 125 175 250
nT
TANCITARO VOLCANO
Residual Magnetic Field
UNAM - IPICYT

**Figure 7.8**. Map showing the calculated Residual Magnetic Field (RMF) of the Tancitaro volcano (TV). The RMF map represents the magnetic field strength with isovalues curves in nT and color range, indicating with red the magnetic highs and with blue the magnetic lows. Note the position of the of the TV respect the magnetic anomaly.

TMF - IGRF (1995) = RMF. The data were leveled using the control lines and microlevelling. All the processes described above were carried out by the SGM.

From the digital aeromagnetic information of the SGM, we plotted the RMF using the means of the Inclination and Declination data, in order to calculate the Reduced to the Magnetic Pole (RMP, Figure 9) (Baranov and Naudy, 1964). Based on the RMP, we calculated map of the Derivative in the Z direction (1 order, Figure 10) (Henderson and Ziets, 1949) and the Upward continuations (Henderson 1970,) among others.

The information processed was configured obtaining the Residual Magnetic Field (RMF, Figure 7.8). The mean values for the Magnitude in the aeromagnetic survey data (06/1999) was 41,725 nT, the Inclination 46°31´ and declination 7°45´, which means that the RMF anomaly was displaced from the source associated with them. It is a common practice in the processing of aeromagnetic data using a mathematical algorithm (Baranov and Naudy, 1964) its application allows us to place the area with respect to the north pole, where the Inclination is 90° and the Declination is 0° and therefore the magnetism sources will be located below the magnetic anomaly.

Contour map of the RMP shows us the existence of zones with different magnetization intensities (different colors in Figure 7.9). This enables us to group them into what is called aeromagnetic domains (AMD, Lopez-Loera, 2002) that can be associated with rocks having similar magnetic susceptibility values. This means that each AMD is associated with a different geological unit. At a regional scale, the

entire study area correlates with one AMD, mainly associated with volcanic rocks. At more local scale we can differentiate three aeromagnetic subdomains (AMSD) described below.

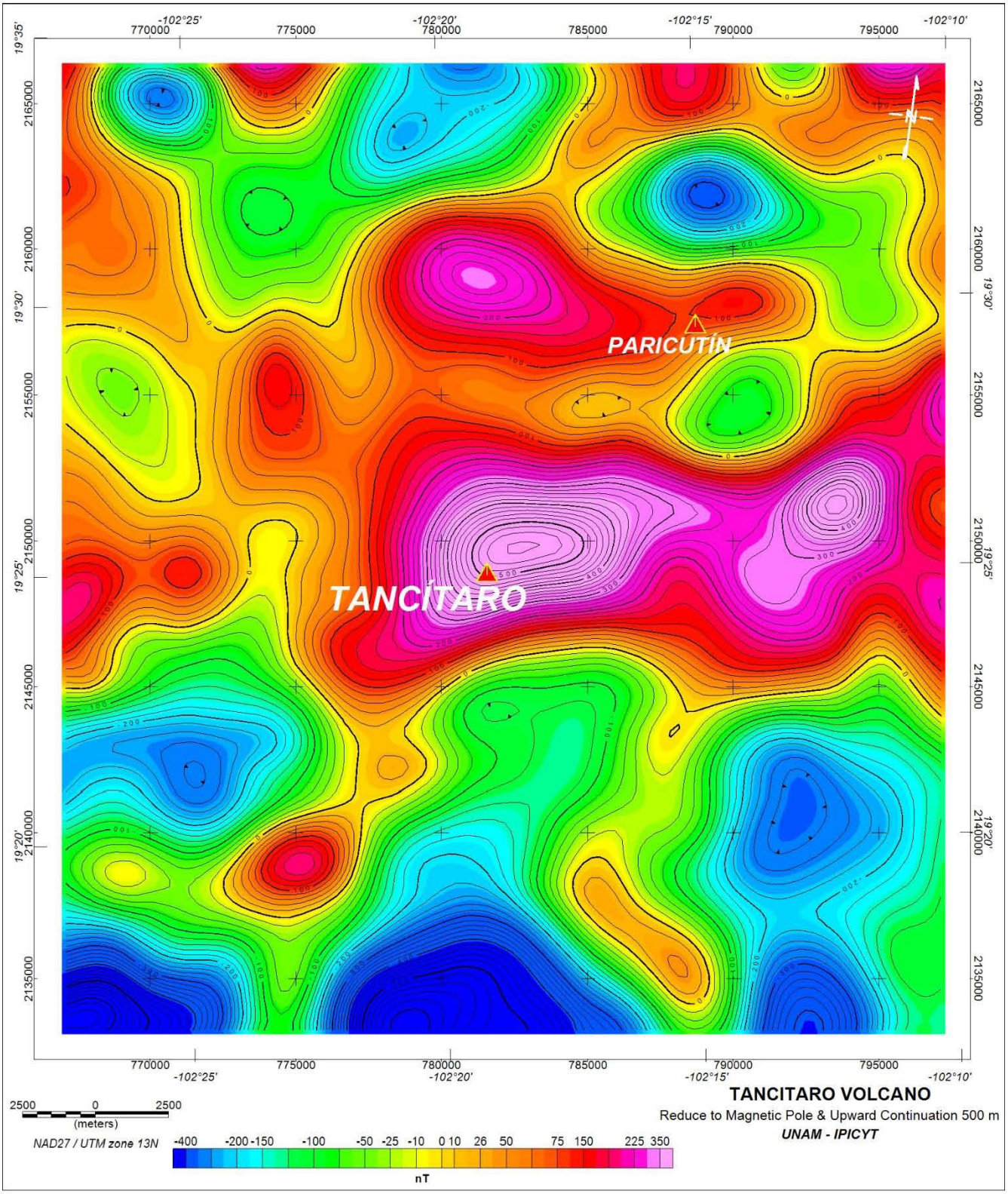
-102°25'
770000
775000
-102°20'
780000
785000
-102°15'
790000
795000
-102°10'
19°35'
19°30'
19°25'
19°20'
2165000
2160000
2155000
2150000
2145000
2140000
2135000
N
PARICUTÍN
TANCÍTARO
2500 0 2500
(meters)
NAD27 / UTM zone 13N
-400 -200 -150 -100 -50 -25 -10 0 10 26 50 75 150 225 350
nT
TANCITARO VOLCANO
Reduce to Magnetic Pole & Upward Continuation 500 m
UNAM - IPICYT

**Figure 7.9**. Map of the Reduced to Magnetic Pole (RMP) and Upward Continuation 500 m. The RMP map represents how we would observe our study area if it was located in the north pole, were Inclination =90º and Declination = 0º. Note the position of the TV respect the magnetic anomaly. In this RMP the anomalies move to the north.

**AMSD I**. It is located in most of the study area, it covers the entire central portion and most of the northern side, is undefined to the E, W and N. It is characterized by the existence of the Tancítaro and Paricutin volcanoes (Figure 7.9a). It has two large aeromagnetic anomalies (8.8 km x 5 km) elongated in the E-W direction. The anomalies show values of intensity of magnetization of 563 nT to -271.9 nT.

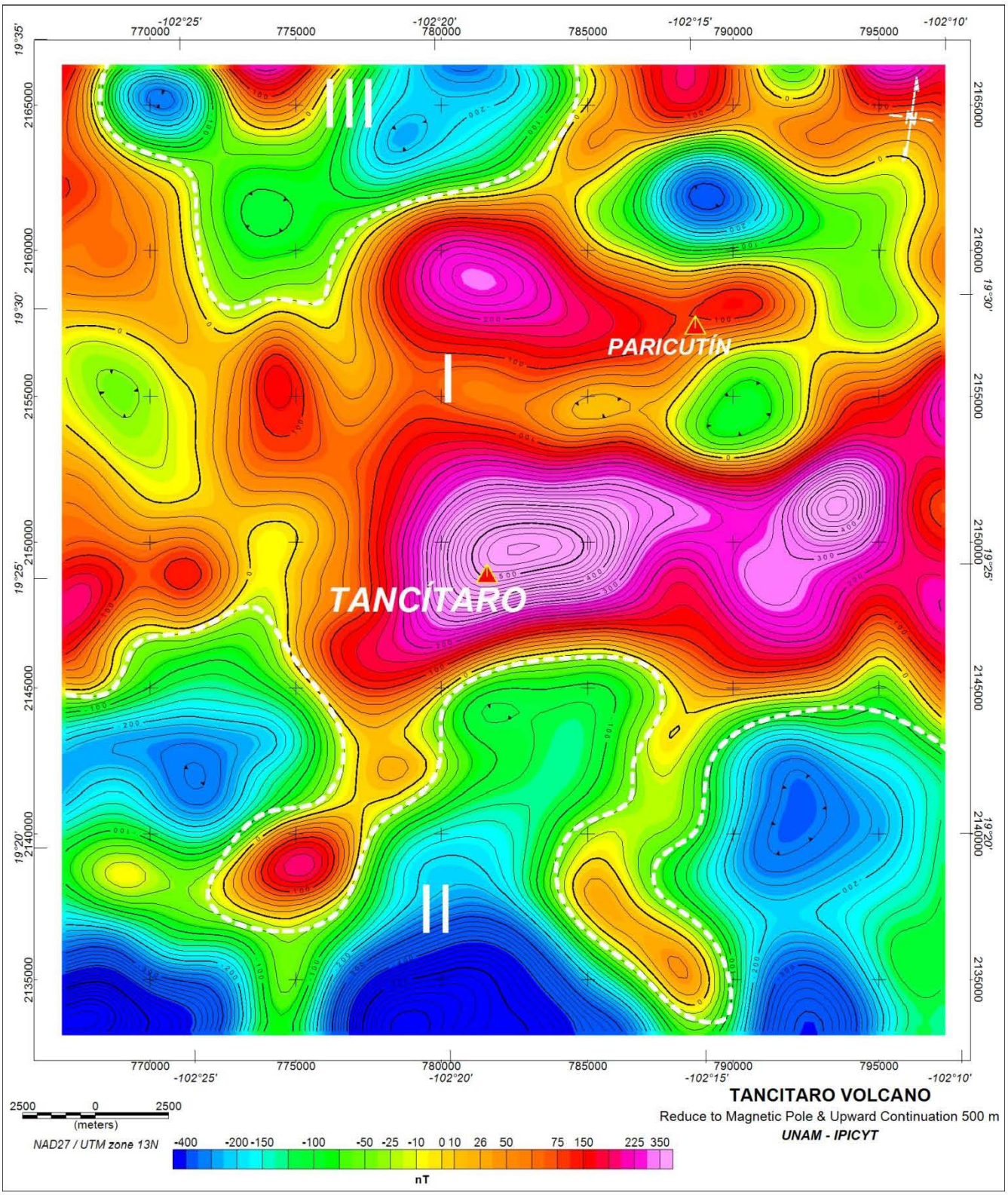
-102°25'
-102°20'
-102°15'
-102°10'
770000
775000
780000
785000
790000
795000
19°35'
19°30'
19°25'
19°20'
2165000
2160000
2155000
2150000
2145000
2140000
2135000
III
I
II
PARICUTÍN
TANCÍTARO
N
2500 0 2500
(meters)
NAD27 / UTM zone 13N
-400 -200 -150 -100 -50 -25 -10 0 10 26 50 75 150 225 350
nT
TANCITARO VOLCANO
Reduce to Magnetic Pole & Upward Continuation 500 m
UNAM - IPICYT

**Figure 7.9a**. Map of the Reduced to Magnetic Pole (RMP) and Upward Continuation 500 m and aeromagnetic subdomains AMSD (I, II and III) of the Tancitaro volcano (TV) and surroundings areas. The AMSD represents a zone with similar magnetic susceptibility.

One of these anomalies is correlated with the Tancítaro volcano, whose crater is located 1.4 km SW of the center of the aeromagnetic anomaly. In the contour map of the Residual Magnetic Field, this geological structure shows normal aeromagnetic anomaly with a 5,450 m of polar distance. According to an analysis of Radial Average Spectrum (Figure 7.10) the host rock of the magma chamber associated with the Tancítaro volcano is located at depths nearly 2 km., and with the method of average width of the anomaly (Figure 7.11) it is estimated that the host rock of the magmatic chamber is between 2.6 km and 3 km. The Tancitaro volcano shows alignments in all direction, which are associated with weakness zones correlated with faults and/or fractures. Topographically this AMSD I, shows altitudes between 2,031 m and 3,792 m, with an average of 2,832 m. Its geological association is with rocks of high magnetic susceptibility as basalts.

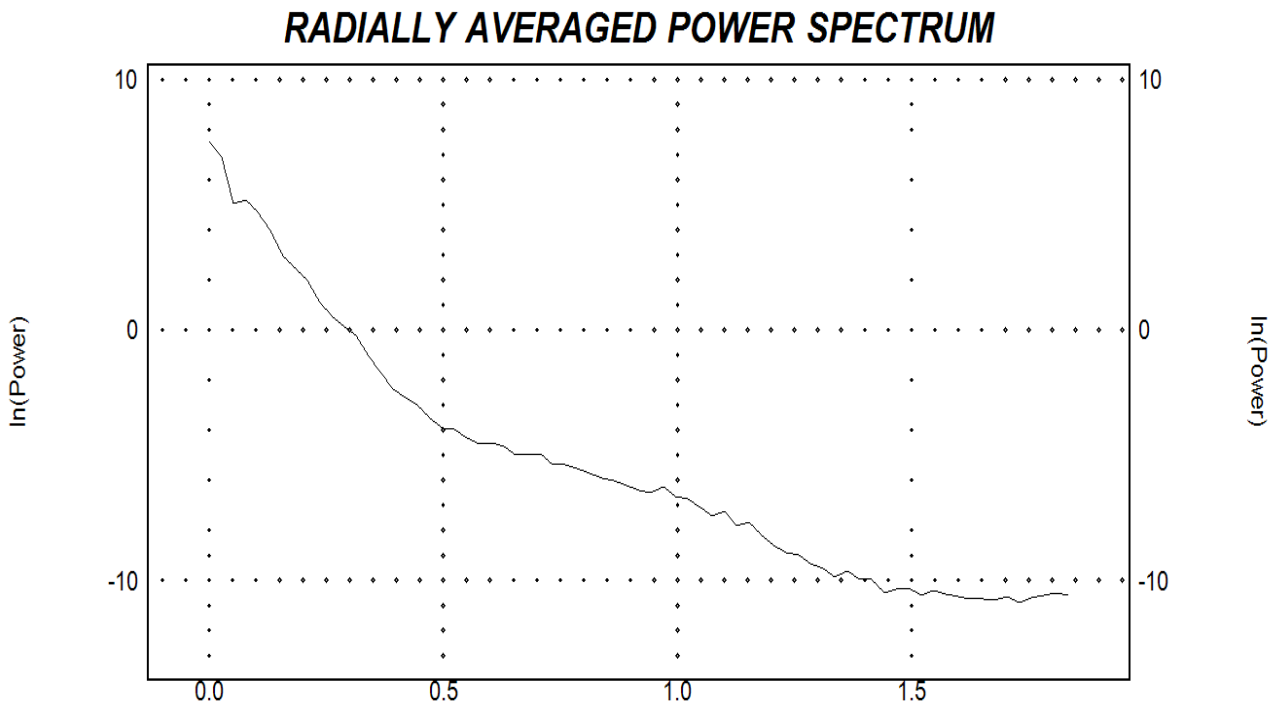


**Figure 7.10**. The profile represents the Radially Averaged Power Spectrum of our study area.

**AMSD II**. It is located across the southern part of the study area and is mainly characterized by a series of aeromagnetic anomalies associated with magnetic lows, showing values of magnetization intensity of -96 nT to -650 nT (Figure 7.11). It has an "E" lying form and is undefined to the S, E and W. Topographically it shows altitudes 1,140 m to 2,141, with an average of 1,785 m. It correlates with geologically rocks with a low magnetic susceptibility, as volcanic breccia and pyroclastic.

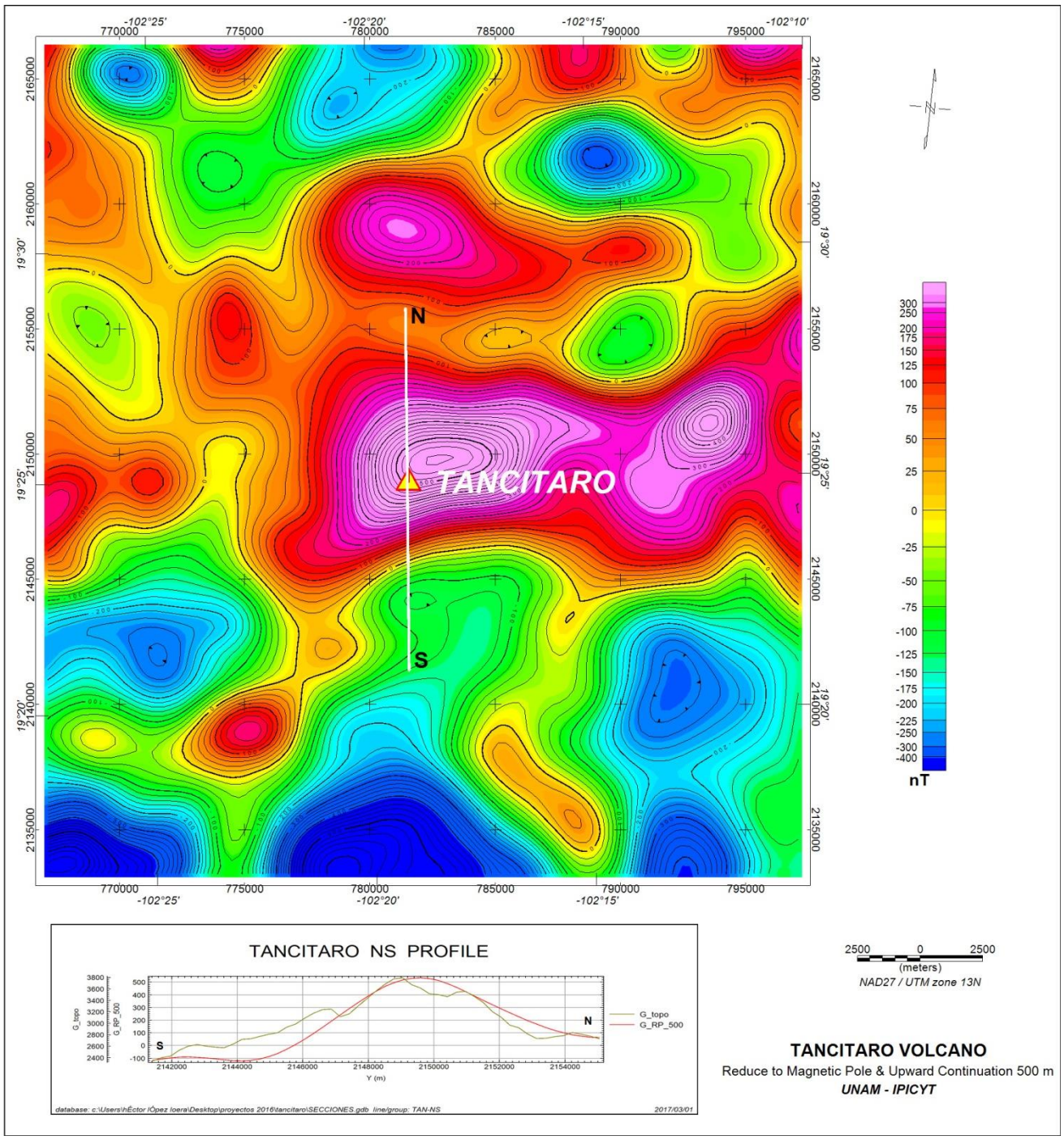


**Figure 7.11**. The profile that is observed with NS direction in the map of the RMP & Upward Cont. 500 m, is the same that is shown in the lower side of the map and that served as base to estimate the depth of the source of magnetic anomaly with the method of average width.

**AMSD III**. This subdomain is located towards the NW portion of the studied area, is undefined to N **(**Figure 7.12**)**. It has a form tending to a half circle where shows in the central portion an anomaly associated with a magnetic high surrounded by magnetic lows. The values of magnetization intensity are between 197 nT to -257 nT. Topographically it has altitudes of 1,475 m to 2,135 m with an average of 1.780 m. Geologically it correlates with rocks with mean magnetic susceptibilities as andesitic rocks.

In summary, the aerial magnetometry on the map of Reduce to Magnetic Pole (RMP) shows the existence of three aeromagnetic subdomains all associated with volcanic rocks. The aeromagnetic anomaly associated with the Tancitaro volcano on the map of RMP is shifted 1.4 km to the NE 50° and has an area of 5 km (N-S) x 8.8 km (E-W) and shows a magnetization intensity of 710 nT. The depth of the magmatic chamber correlated with the Tancitaro volcano is interpreted between 3.2 km and 5 km and the shape is elongated in the E-W direction. It is limited in all directions by alignments correlated with faults and/or fractures.

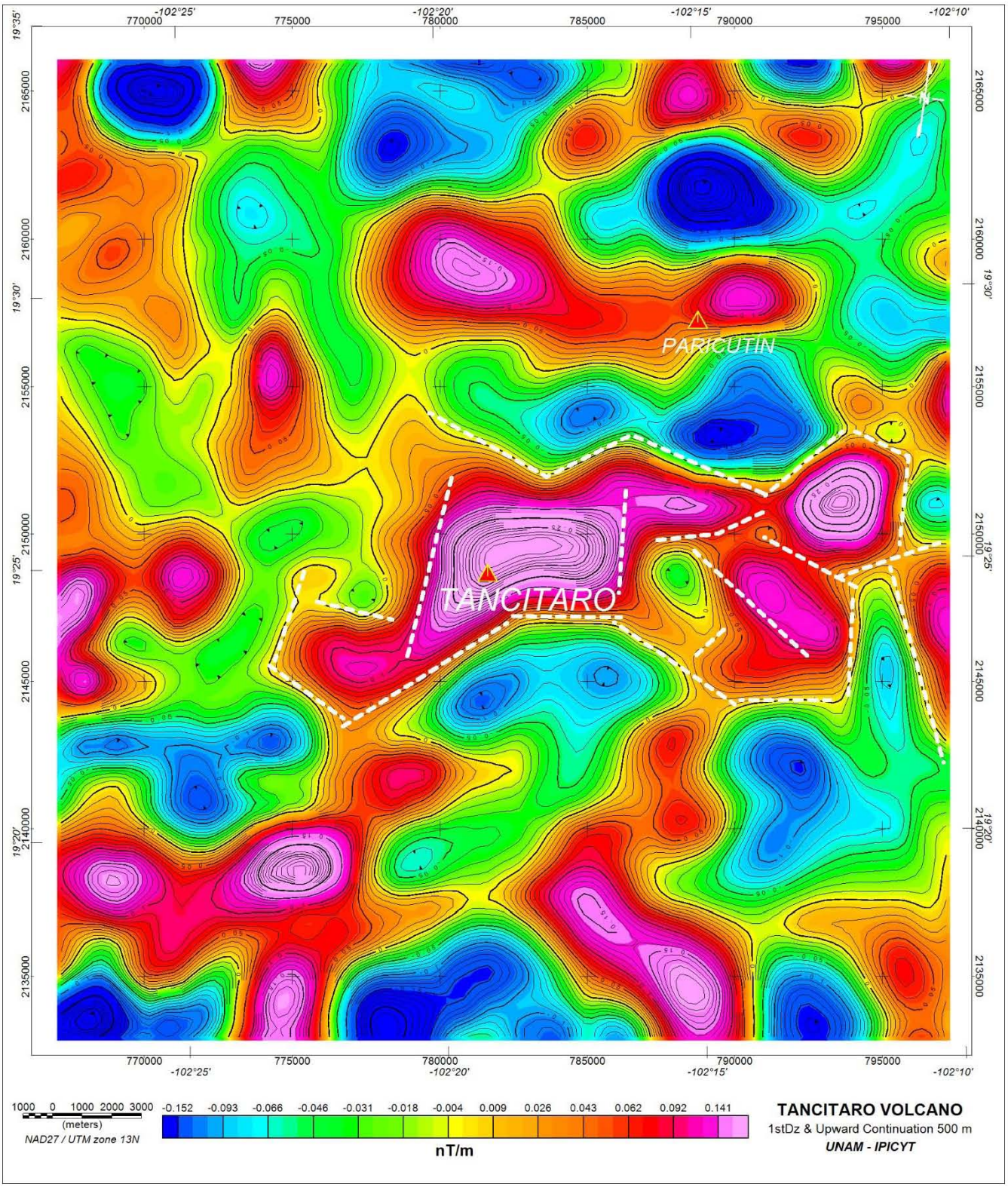


**Figure 7.12.** First derivative in Z direction and upward continuation 500 m map. This map shows the

alignments (white color lines) associated with the anomaly of Tancitaro volcano. This alignments are correlated with faults and/or fractures.

**7.6 Conclusions:**

A detailed rock-magnetic and paleomagnetic study was carried on the lava flows associated to the Tancitato volcano in order to contribute both the new generation Time Averaged Paleomagnetic Field database and estimate the latitudinal dependence of the paleosecular variation trough the virtual geomagnetic pole scatter. The combined dataset incorporating previously reported paleodirections from the same area offer a detailed record of the Earth's Magnetic Field fluctuation for the last 1 My.

Mean paleodirections was found reasonably close to the Geomagnetic Axial Dipole directions and statistically indistinguishable from the expected directions derived from the stable North America which attest that there is no major tectonic deformations occurred during the last 1 My according to the previous studies. All samples yielded well defined normal polarity magnetization. Two flows are correlated to the Jaramillo polarity event, which provide a useful marker for the volcanic activity in the MGVF.

Combined aeromagnetic survey shows the existence of three magnetic subdomains all associated with volcanic rocks. The aeromagnetic anomaly associated with the Tancitaro volcano on the map of RMP is shifted $1.4\ km$ to the Northeast $50\ °$ and has an area of $5\ km$ (North-South) $8.8\ km$ (Est -West) and shows a magnetization intensity of $710\ nT$. The depth of the magmatic chamber correlated with the Tancitaro volcano is interpreted between $3.2km$ and $5km$ and the shape is elongated in the East-West direction. It is limited in all directions by alignments correlated with faults and/or fractures, but this could be inside of the flows or were formed after the events of interest due in the geological maps of the geological national service and in the paleomagnetic results not was observed this relationship that could be reflected with direction that not be near of the direction of reference or the GAD.

**Acknowledgments**

The financial support was given by UNAM-PAPIIT project IN10524 and CONACyT Ciencia Basica (00131191).

**References**


Baranov, V., and Naudy, H., 1964. Numerical calculation of the formula of reduction to the magnetic pole. Geophysics, v. 29, p. 67-79.

Besse, J., Courtillot, V., 2002, Apparent and true polar wander and the geometry of the magnetic field in the last 200 million years, Journal of Geophysical Research, v. 107, no. B11, 2300.

Butler R.F, 1991, Paleomagnetism: Magnetic Domain to Geologic Terranes, Book, Blackwell Science.

Carlut, J., and V. Courtillot, 1998, How complex is the time-averaged geomagnetic field over the past 5 Myr?, Geophys. J. Int., v. 134, p. 527–544,

Connor, C.B., 1987. Structure of the Michoacán–Guanajuato volcanic field, Mexico. J. Volcanol. Geotherm. Res. v. 33, p. 191–200.

Chandra, S., H. Khurshid, M. H. Phan, and H. Srikanth (2012), Asymmetric hysteresis loops and its dependence on magnetic anisotropy in exchange biased Co/CoO core-shell nanoparticles, *Appl. Phys. Lett.*, *101*(23), 8–13, doi:10.1063/1.4769350.

Connor, C.B., 1990. Cinder cone clustering in the TransMexican Volcanic Belt: implications

for structural and petrologic models. J. Geophys. Res. Solid Earth (1978–2012), v. 95 no. (B12), p. 19395–19405.

Cox, A., 1970, Confidence limits for the precision parameter k. Geophysical Journal of the Royal Astronomical Society, v. 18, p. 545-549.

Di Traglia F., Morelli S., Casagli N., Garduño M. V. H., 2014, Semi-automatic delimitation of volcanic edifice boundaries: Validation and application to cinder cones of the Tancitaro-Nueva Italia region (Michoacán-Guanajuato Volcanic Field Mexico)., Geomorphology., n. 219, p. 152-160.

Doell, RR and Dalrymple, GB (1966). Geomagnetic polarity epochs: A new polarity event and the age of the Brunhes-Matuyama boundary. Science, v. 152, p. 1060-1061.

Dunlop David J.., 2002, Theory and application of the Day plot (Mrs/Ms versus Hcr/Hc) 2. Application to data for rocks, sediments, and soils. Journal of Geophysical Research, v. 107, no. B3, p 2057, 10.1029/2001JB000487.

Fisher R.A., 1953, Dispersion on a sphere. Proceedings of the Royal Society of London A, v.217, p. 295-305.

García-Ruiz R., Goguitchaichvili A., Cervantes-Solano M., Cortés-Cortés A., Morales-Contreras J., Maciel-Peña R., Rosas-Elguera J. and Macías-Vázquez J. L., 2016, Secular variation and excursions of the Earth magnetic field during the Plio-Quaternary: New paleomagnetic data from radiometrically dated lava flows of the Colima volcanic complex (western Mexico), Revista Mexicana de Ciencias Geológicas, v. 33, no. 1, p., 72-80.

García-Ruiz R., Goguitchaichvili A., Cervantes-Solano M., Morales J., Maciel-Peña R., Rosas-Elguera J., Cejudo-Ruiz R., and Urrutia-Fucugauchi J., Rock-Magnetic and paleomagnetic survey on dated lava flows erupted during the Brunhes and Matuyama chrons: the Mascota Volcanic Field revisited (Western Mexico), Stud. Geophys. Geod., v. 61, doi: 10.1007/s11200-016-0148-6 (in press).

Hasenaka, T., Carmichael, I.S., 1985. The cinder cones of Michoacán–Guanajuato, central

Mexico: their age, volume and distribution, and magma discharge rate. J. Volcanol. *Geotherm. Res*. v. 25, p. 105–124.

Hasenaka, T., Ban M. and Delgado-Granados H., 1994, Contrasting volcanism in the Michoacán–Guanajuato Volcanic Field, central Mexico: Shield volcanoes vs. cinder cones. *Geophysical International*, v.33, no.1, pp.125– 138.

Hasenaka, T., 1994. Size, distribution, and magma output rate for shield volcanoes of the Michoacán–Guanajuato volcanic field, Central Mexico. Journal of Volcanology and Geothermal Research,v. 63, p.13–31.

Henderson, R. G., 1970. On the Validity of the use of Upward Continuation Integral for Total Magnetic Intensity Data. Geophysics, V. 35, 5, 916-919.

Henderson, R. G. and Zietz, I., 1949. The computation of second vertical derivatives of geomagnetic fields, Geophysics, v. 14, p. 508-516.

IGRF, 1995, International Geomagnetic Reference Field. *IAGA Division V-Mod, Geomagnetic Field Modeling.*

Johnson, CL., Constable G., Tauxe L. et al., 2008, Recent investigations of the 0-5 Ma geomagnetic field recorded in lava flows. Journal of the Earth Scieneces, Geochem. Geophys. Geosyst, v. 9, no. 4, p. 1525-2027, Q04032.

Kirschvink, J.L, 1980, The least-square line and plane and analysis of paleomagnetic data. Geophysical Journal International, v. 62, no. 3, p. 699-718.

Laj C. and Channel J.E.T., 2007, Geomagnetic excursions, Treatise on Geophysics, Geomagnetism, Elsevier, v. 5, p. 373 – 416.

Lawrence K. P. and Constable C. G., 2006. Paleosecular variation and the average geomagnetic field at latitude., Geochemestry Geophysics Geosistems, Journal of the Earth Sciences, v. 7, no. 7.

Leonhardt R., 2006, Analyzing rock magnetic measurements: The RockMagAnalyser 1.0 software, Computer and Geosciences, v. 32, p. 1420-1431.

López-Loera, H., 2002. Estudio de las Anomalias Magnéticas y su relación con las Estructuras Geologicas y Actividad Eruptiva de los Complejos Volcánicos Activos de Colima e Izta-Popocatepetl, México. Tesis Doctoral, Instituto de Geofísica, UNAM. Pp 235.

Maciel, P. R., Goguitchaichvili, A., Garduño Monroy V. H., Ruiz Martínez V. C., Reyes Aguilar B., Morales J., Alva-Valdivia L., Miranda Caballero C., and Urrutia-Fucugauchi J., 2009, Paleomagnetic and rock-magnetic survey of Brunhes lava flows from Tancitaro volcano, México, *Geophysical International*, v. 48, no. 4, pp. 375-384.

Maciel P. R., Goguitchaichvili A., Marie-Noëlle G., Ruiz-Martínez V. C., Calvo R. M., Siebe C., Aguilar R., B., and Morales J., 2014, Paleomagnetic secular variation study of Ar-Ar dated lavas flows from Tacambaro área (Central Mexico): Possible evidence of Intra-Jaramillo geomagnetic excursion in volcanic rocks, Physics of the Earth and Planetary Interiors, v. 299, p. 98-109.

Mankinen EA and Dalrymple GB (1979). Revised Geomagnetic polarity time scale for the interval 0-5 m.y.b.p. Journal of Geophysical Research v. 84, p. 615-626.

McElhinny, M.W., McFadden, P.L., 1997, Paleosecular variation over the past 5 Myr based on a new generalized database. Geophysical Journal International, 203(2), 240-252.

Michalk M. D., Bönhel N. H., Nowaczyk N. R., Aguírre-Diaz G. J., López-Martínez M., Ownby S., and Negendank W. J. F., 2013., Evidence for geomagnetic excursions recorded in Brunhes and Matuyama Chron lavas from the trans-Mexican volcanic Belt, Journal of Geophysical Research: Solid Earth, v. 118, p. 2648-2669, doi: 10.1002/jgrb.50214.

Moskowitz B. M., 1981, Methods for estimating Curie temperatures of titanomaghemites from experimental Js-T data., Earth and Planetary Sciences Letters., v. 53, no. 1, p. 84-88.

Nabighian, M. N., 1972. The analytic signal of two-dimensional magnetic bodies with polygonal cross-section: its properties and use for automated anomaly interpretation, Geophysics, 37(3), 507–517.

Ownby, S. E., H. Delgado-Granados, R. A. Lange and C. M. Hall, 2007. Volcan Tancıtaro, Michoacan, Mexico, 40ar/39ar constraints on its history of sector collapse. J. Volcanology and Geothermal Res., v. 161, no. 1-2, p. 1–14.

Ownby S. E., Lange R. A., Hall C. M., and Delgado-Granados H., 2010, Origin of andesite in the deep crust and eruption rates in the Tancítaro-Nueva Italia Region of the central Mexican arc., Geological Society of America Bulletin, v. 123, no. 1-2, p. 274-294.

Prévot, M., Mankinen E. A., Gromme S. C., Coe R. S., 1985, How the geomagnetic field vector reverses polarity. Journal Nature, v. 316, no. 6025, p. 230–234, doi: 10.1038/316230a0.

Ruiz-Martínez V. C., Urrutia-Fucugauchi J. and Osete M. L., 2010, Paleomagnetism of the Western and Central sectors of the Trans-Mexican volcanic belt-implications for the tectonic rotations and the paleosecular variation in the paste 11 Ma., Geophys. J. Int, v. 180, p. 577-595.

Rodríguez-Ceja M., Goguitchaichvili A., Calvo-Rathert M., Morales-Contreras J., Alva-Valdivia L., Rosas E. J.,Urrutia F. J., and Delgado G. H., 2006, Paleomagnetism of the Pleistocene Tequila Volcanic Field (Western Mexico), Earth Planets Space, v. 58, p. 1349-1358.

Ruiz-Martínez V.C., Urrutia-Fucugauchi J., and Osete M. L., 2010, Palaeomagnetism of the Western and Central sectors of the Trans-Mexican volcanic belt-implications for tectonic rotations and palaeosecular variation in the past 11 Ma, Geophysical Journal International, v. 180, p. 577-595, doi:10.1111/j.1365-246X.2009.04447.x.

Singer, B. S., Hoffman, K.A., Schnepp, E., Guillou, H., 2008, Multiple Brunhes chron excursions in the West Eifel Volcanic field: support for the long-held mantle control on the non-axial dipole field. *Phys. Earth Planet. Inter*. v. 169, pp. 28-40.

Tauxe, L. (1998). Paleomagnetic Principles and Practice. Dordrecht: Kluwer Academic Publishers.

Tauxe L., and Kent D.V., 2004, A Simplified Statistical Model for the Geomagnetic Field and Detection of Shallow Bias in Paleomagnetic Inclinations: Was the ancient Magnetic Field Dipolar?: *Wiley Online Library*, pp. 101-113.

Torsvik, T.H., van der Voo, R., Preeden, U., Mac Niocail, C., Steinberger, B Hinsbergen, B., Doubrovine, P. V., van Hinsbergen, D.J.J., Domier, M., Gaina, C., Tohver, E., Meert, J.G., McCausland, P.J.A., Cocks, L.R.M., 2012, Phanerozoic polar wander, palaeography and dynamics, *Journal Earth-Science Reviews,* v. 114, pp. 325-368.

Urrutia-Fucugauchi J., and Florez-Ruiz J.H., 1996, Bouguer gravity anomalies and regional crustal structure in central Mexico, International Geology, v. 38, p. 176-194.

Watkins, N. D., 1973, Brunhes epoch geomagnetic secular variation on Réunion Island. J. Geophys. Res, v. 78, p. 7763-7768.

## 8. Conclusiones Generales.

1. A partir del trabajo realizado en Mérida para la zona de Ichkaantijo se concluye que las arqueointensidades obtenidas de los 26 especímenes correspondientes a siete de los ocho fragmentos utilizados, se colocan dentro de la categoría A, 12 están en la categoría B y 10 corresponden al tipo C. Luego de utilizar la herramienta de datación de Pavón-Carrasco, *et al.* (2014) se observa que la curva representativa para la región de Mérida no proporciona una edad confiable debido a que las intensidades reportadas tienen una magnitud menor a la esperada.

Se realizó un curva preliminar haciendo uso de intensidades relacionadas a la cultura Maya, haciendo uso de la base de datos GEOMAGIA50.v3 (Brown *et al.,* 2015). Luego de comparar esta curva con otras curvas de referencia construidas por medio de modelos globales, se concluye que estas no reflejan con detalle el comportamiento de las intensidades de Mesoamérica, y plantea la necesidad de generar una curva regional para Mesoamérica más robusta.

Siguiendo el trabajo previo realizado por Petronille *et al.,* (2012), quien reporta un interesante análisis entre el cambio climático y los cambios sociales de la culturas Mesoamericanas, en específico para la cultura Maya mediante la curva correspondiente a el "Lago de Punta Laguna"; se realizó también un análisis y comparación con los cambios climáticos, en donde se observa que la baja intensidad geomagnética absoluta prevaleció en el área Maya entre los 400 D.C. Y 750 D.C., acompañado de condiciones climáticas secas justo antes del colapso Maya.

2. Se cumplió el objetivo desarrollar la primer curva de variación paleosecular, de carácter regional para Mesoamérica basada en datos confiables de intensidades absolutas para los últimos 3 milenios. Basados en el análisis del error de relocalización, fue posible el incorporar intensidades de él sur de Estados

Unidos de Norte América. Esta curva tiene diferencias significativas con los modelos globales SHA.DIF.14k y CALS3k.10, debido a la selección de datos que permite elegir las intensidades absolutas utilizadas con criterios estrictos de calidad y alta confiabilidad. El análisis de dicha curva y la curva de la variación paleoclimática de Punta Laguna, muestra una posible correlación entre dos eventos identificados como *Jerks* y que representan una discontinuidad cultural en la cultura Maya.

Al comparar la curva con las curvas de referencia correspondientes a Europa se aprecia una deriva hacia el este, especialmente con la curva del Este de Europa.

3. Las paleodirecciones obtenidas del CVC se consideran de origen primario y con una magnetización debida a la presencia de la titanomagnetita como mineral predominante con bajo contenido de titanio, de dominio magnético pseudo sencillo. De los 21 flujos de lava estudiados se observa en su mayoría una polaridad normal correspondiente al cron de Brunhes, dos sitios sin embargo mostraron una clara evidencia de pertenecer a eventos de excursión como Mono Lake o Calabrian Ridge I. La dirección media está prácticamente asociada con la dirección correspondiente al Plio-Cuaternario obtenida a partir de los polos de referencias del cratón de Norteamérica.

4. Se realizó un análisis detallado de magnetismo de rocas, para los flujos muestreados del complejo volcánico de Mascota, indicando fases ferrimagneticas con coercitividades de bajas a moderadas y la presencia de titanomagnetita con bajo y alto contenido de titanio y a las cuales se les considera como las responsables de la magnetización de las rocas. Las direcciones obtenidas incrementan el número de paleodirecciones con alta calidad del BJ (Bloque Jalisco), con 19 paleodirecciones la mayoría de ellas con una edad asociada por métodos radiométricos. Estas paleodirecciones están distribuidas entre el cron de Brunhes con 13 paleodirecciones y el cron de Matuyama con 6, al combinarlas, el test de la inversión

es positivo lo que indica que no hay una rotación correspondiente al eje vertical. Se detectó una dirección transicional que corresponde a la excursión de Levantine (360-370kyr).

5. Se realizó un estudio detallado de magnetismo de rocas y de paleomagnetismo en las lavas asociadas al complejo volcánico de Tancitaro, con la idea de contribuir en la base de datos paleomagnética y estimar la dependencia latitudinal de la variación paleosecular a través de la dispersión de los polos virtuales geomagnéticos de referencia. Se incorporan datos correspondientes al CVT de trabajos previos para realizar un análisis más robusto. Los datos comprenden al último millón de años. La paleodirección media se encontró razonablemente cercana a la dirección del dipolo axial geomagnético. La diferencia entre las direcciones esperadas con respecto al polo de referencia para el cratón de Norte América y el polo encontrado estadísticamente es indistinguible, lo cual indica que no hay movimiento tectónico mayor. Dos flujos están relacionados con el evento Jaramillo, este registro proporciona una marca útil de la actividad volcánica del complejo volcánico de Michoacán-Guanajuato.

Se cumple con el objetivo inicial de obtener la primer curva de variación paleosecular para los últimos 3 milenios a partir de nuevas contribuciones y de revisar las arqueointensidades reportadas en trabajos previos mediante el análisis de Bootstrap y el uso de P-Splines generando así la curva paleodireccional para México comprendida para los crones de Brunhes-Matuyama.

## 9. Bibliografía.

Alva-Valdivia, L. M., 2005 Comprehensive paleomagnetic study of a succession of Holoceno olivine basalt flow: Xitle Volcano , Mexico, revisted, Earth. Planet. Sp., v. 57, p. 839-853, doi:10.1186/BF03351862

Bönhel H., and Negendak, 1981, Preliminary results of paleomagnetic measurements of tertiary-quaternary igneous roks from the eastern part of the transmexican volcanic belt. Geofísica Internacional, v. 20, no. 3.

Blatter D., Carmichael I., Deino A., and Renne, P., 2001, Neogene volcanism at the front of the central Mexican volcanic belt: Basaltic andesites to dacites, with contemporaneous shoshonites and high.TiO2 lava: Geological Society of America Bulletin, v. 113, p., 1324-1342.

Bönhel H., y Molina-Garza R., 2002, Secular variation in Mexico during the Last 40 000 years, Physic of the Earth and Planetary Interiors, v. 133, p. 99-109.

Brown M. C., Donadini F., Nilsson A., Panovska S., Frank U., Korhonen., Schuberth M., Korte M., y Constable G., C., 2015, GEOMAGIA50.v3: 2. A new paleomagnetic database for lake and marine sediments, Earth Planet and Space.

Bucha, V., Taylor, R., E., Berger, R., y Haury, W., E., 1970, Geomagnetic Intensity: Changes during the past 3000 years in the western hemisphere, Science, v. 168, p. 111-114.

Cai S., 2016, Archaeointensity results spanning the past 6 kiloyears from eastern China and implications for extreme behaviour of the geomagnetic field, PNAS, v. 114, p. 39-44.

Carlson J. B., 1975, Loadstone compass Chinese or Olmec primacy?, Science, v. 189, p. 735-760.

Coe, M., D., 1967a, Olmec civilization, Veracruz, Mexico: Dating of San Lorenzo Phase, Science, v. 155, p. 1399-1401.

Coe R. S. 1967b, The determination of paleointensities of the Earth magnetic field with special emphasis on mechanisms which could cause nonideal behavior in Thellier method, J. Geomag. Geoelectr., v. 19, p. 157-179.

Conte-Fassano G., Urrutia-Fucugauchi J., Goguitchaichvili A., y Morales-Contreras J. J., 2006, Low-Latitude paleosecular variation and the time average field during the late Pliocene and Quaternary-Paleomagnetic study of the Michoacán-Guanajuato volcanic field. Central Mexico, Earth Planets Space, v. 56, p. 1359-1371.

Cortés Á., 2015, Historia eruptiva del volcán Nevado de Colima y su evolución dentro del Complejo Volcánico de Colima (CVC): México, Universidad Nacional Autonoma de México, Ph. D. Tesis, p. 86.

Deman A., 1978, Caracteristicas del eje neovolcanico TransMexicano y sus Problemas de Interpretación, Univ. Nal. Autón. México, Inst. Geología, Revista, v. 2, no. 2, p., 172-187.

Fanajat, G., Camps, P, Alva-Valdivia L., M., Sougrati M., T., Cuevas-Garcia M., and Perrin M., 2007, First archaeointensity determinations on Maya incense burners from Palenque temples, Mexico: new data to constrain Mesomerica secular variation curve, Earth Planet Sciences Letters, v., 254, p. 146-157, doi: 10.1016/j.epsl.2006.11.026

García-Ruiz R., Goguitchaichvili A., Cervantes-Solano M., Cortés-Cortés A., Morales-Contreras J., Maciel-Peña R., Rosas-Elguera J., y Macías-Vazquez J.L., 2016, Secular variation and excursions of the

Earth magnetic field during the Plio-Quaternary: New paleomagnetic data from radiometrically dated lava flows of the Colima volcanic complex (western Mexico), Revista Mexicana de Ciencias Geológicas, v. 33, p. 77-80.

García-Ruiz R., Goguitchaichvili A., Cervantes-Solano M., Morales-Contrearas J. J. Maciel-Peña R., Rosas-Elguera J., Cejudo-Ruiz R., y Urrutia-Fucugauchi J., 2017a, Rock-magnetic and paleomagnetic survey on dated lava flows erupted during the Brunhes and Matuyama chrons: The Mascota Volcanic Field revisited (Western Mexico), Studia Geophysica et Geodaetica, v. 61, p. 249- 263.

García-Ruiz R., Goguitchaichvili A., Loera H. L., Cervantes-Solano M., Urrutia-Fucugauchi J., Morales-Contrearas J., Maciel-Peña R., y Rosas-Elguera J., 2017b, Paleomagnetism and Aeromagnetism Survey from Tancitaro Volcano(Central Mexico)-PaleoSecular Variation at Low Latitudes During the Past 1 Ma, Geofisica Internacionals (En Prensa.)

Genevey A., Gallet Y., Jesset S., Thébault E., Bouillon J., Lefevre A., y Le Goff M., 2016, New archeointensity data from French Early Medieval pottery production ($6^{th}$ -$10^{th}$ century AD). Tracing 1500 years of geomagnetic field intensity variations in Western Europe, Physics of the Earth and Planetary Interiors, v. 257, p. 205-219.

Glatzmaler G. A., Coe R. S., Hongre L., y Roberts Paul, 1999, The role of the Earth's mantle in controlling the frequency of geomagnetic reversals, *Nature*, v. 401, p. 885-890, doi: 10.1038/44776.

Gómez-Paccard M., Osete M. L., Chauvin A., Pavón-Carrasco F. J., Pérez-Asensio M., Jiménez P., y Lanos P., 2016, New constraints on the most significant paleointensity change in Western Europe over the last two millennia. A non-dipolar origin?, Earth Planet. Sci. Lett., v. 454, p., 55-64.

Góngora S. y Ángel G., 2015, Joo Ajauel. El reino de Joo, Ichkaantijoo. Uniprint-Compañia tipográfica Yucateca. S.A., de C. V.,

Herrero-Bervera E., Urrutia-Fucugauchi J., Martín del Pozzo A., Bönhel H., y Guerrero, 1986, Normal amplitude Brunhes paleosecular variation at low-latitudes: A paleomagnetic record from the Trans-Mexican Volcanic Belt. Geophysical Research Letters, v. 13, p. 1442-1445.

Herrero E., y Surendra P., 1978, Paleomagnetic Study of Sierra de Chichinautzin, Mexico, Geofísica Internacional, v. 17, no 2.

Hernández-Ávila E. R., 2010, Control Cronométrico basado en arqueomagnetismo de Teopancazco, Estado de México, Tesis Licenciatura Física, Fac., Ciencias, UNAM, México, p. 104.

Hervé G., Chauvin A., y Lanos P., 2013, Geomagnetic field variations in Western Europe from 1500 B.C., to 2000 A.D. Part II: New intensity secular variation curve , Phys. Earth Planet Int, v. 218, p. 51-65.

Hueda Y., 2000, Fechamiento arqueomagnéticos de estucos de los sitios de Teopancazco, Teotihucan y Templo Mayor, Tenochtitlán. Tesis Licenciatura Arqueología, ENAH, México, p. 128.

Hueda Y., Soler A., M., 2001, Fechameinto arqueomagnético de estucos en sitios de Teopancazco Teotihuacan, Templo Mayor, Tenochtitlán, Informe presentado al Consejo de Arqueología.

Hueda Y., Soler-Arechalde A., M., Urrutia-Fucugauchi J., Barba L., Manzanilla L., Rebolledo M., Goguitchaishvili A., 2004, Archeomagnetic Studies in central Méxcio-dating of Mesoamerican limeplasters. Physics of the Earth and Planetary Interiors, v.,147, p. 269-283.

Korte M., and Constable C., 2011, Improving geomagnetic field reconstruction for 0-3 ka, Physics of the Earth and Planetary Interiors, v. 188, no. 3-4, p. 247-259.

Kosterov, A. y Prévot, M., 1998, Possibe mechanism causing failure of Thellier palaeointensity experiments in some basalts, Geophys. J. Int., v. 134, p. 554-572.

Laj, C., y Channell, J., E., T., 2007, Geomagnetic excursion, Elsevier B., V.

Lowrie W., 2007, Fundaments of Geophysics, *Cambridge University Press*, 2nd Edition.

Stern P. D., 2001, El Magnetismo después de Gilbert, NASA Privacy, Security, Notices, Capitulo 7.

López-Tellez, J. M., Aguilar-Reyes B., Morales J., Goguitchaichvili A., Calvo-Rathert M., Urrutia-Fucugauchi J., 2008, Magnetic characteristics and archeointensity determination on Mesomaerican Pre-Columbian Pottery from Quiahuiztlan, Veracruz, México. GeofísicaInternacional, v. 47, no. 4, p. 329-340.

Maciel, R., P., Goguitchaichvili A., Garduño Monroy V. H., Ruiz-Martinez V. C., Reyes Aguilar B., Morales J., Alva-Valdivia L., Miranda Caballero C., y Urrutia-Fucugauchi J., 2009, Paleomagnetic and rock-magnetic survey of Brunhes lava flows from Tancitaro volcano, México, Geophysical Intenational, v. 48, no. 4, p. 375-384.

Maillol J. M., and Bandy W. L., 1993, Paleomagnetism of Talpa de Allende and Mascota grabens western Mexico: A preliminary Report. Geofis. Int., v. 33, p. 153-160.

Maillol J. M., Bandy W. L., y Ortega Ramírez J., 1997, Paleomagnetism of Plio-Quaternary basalts in the Jalisco block, western Mexico, Geofis. Int., v. 36.

Malstrom, V., 1976, Knowledge of magnetism in pre-Columbian Mesoamérica, Nature, v. 259, p. 390-391.

Mejia V., Bönhel H., Opdyke N.D:, Ortega-Rivera M.A., Lee J.K.W., y Aranda-Gomez J. J., 2005, Paleosecular variation and time-averaged field recorded in late Pliocene-Holocene lava flows from Mexico, Geoch. Geophys. Geo., v. 6, no. 7,

Michalk D. M., Bönhel H. N., Nowaczyk N. R., Aguírre-Diaz G. J., López-Martinez M., Ownby S., and Negendak J. F. W. 2013, Evidence for geomagnetic excursions recorded in Brunhes and Matuyama Chron lavas from the Trans-Mexican volcanic Belt, J. Geophys, R., v. 118, p. 2648-2669.

Morales J., Goguitchaichvili A., y Urrutia-Fucugauchi J., 2001, A rock-magnetic and paleointensity study of some Mexican volcanic lava flows during the latest Pleistocene to the Holocene. Earth Planets and Space, v. 53(9), p. 893-902.

Morales J., Goguichaichvili A., Acosta G., Gonzáles-Moran T., Alva-Valdivia L., Robles-Camacho J., Hérnandez-Bernal Ma. S., 2009, Magnetic Properties and archeointensity determination on Pre-Columbian pottery from Chiapas, Mesoamerica, Earth Planet Space, v. 61, p. 83-91

Mooser F., 1972, The Mexican volcanic belt, structure and tectonics; Geofís. Internal, v. 12, p. 55-70.

Nagata, T., Kobayashi, K., and Schwarz, E., J., 1965, Archeomagnetic intensity studies of South and Central America, Journal of Geomagnetism and Geolectricity, v. 17, p. 399-405.

Ort M., Carrasco-Nuñez G., 2009, Laterant Vent Migration during Phreatomagmatic and Magmatic Eruptions at Tecuitlapa Maar, East-Central Mexico, Journal of Volcanology and Geothermal Research, v. 181, p. 67-77

Ownby, S. E., Delgado-Granados H., Lange R. A. And Hall C. M., 2007, Volcan Tancitaro, Michoacán México, 40ar/39ar constraints on its history of sector collapse, J. Volcanology and Geothermal Res., v. 161, no. 1-2, p. 1-4.

Ownby S.E., Lange R. A., and Hall C.M., 2008, The eruptive history of the Mascota volcanic field, western México: Age and volumen constraints on the origin of the andesite among a diverse suite of lamprophyric and calc-alkaline lavas, J. Volcanol. Geotherm. Res., v. 177, p., 1077-1091.

Ownby S. E., Lange R. A., Hall C. M., y Delgado-Granados H., 2010, Origin of andesite in the deep crust and eruption rates in the Tancítaro-Nueva Italia Region of the central Mexican arc., Geological Society of American Bulletin, v. 123, no. 1-2, p. 274-294.

Ownby S. E., Lange R. A., Hall C. M., y Delgado-Granados H. 2011, Origin of andesite in the deep crust and eruption rates in the Tancitaro-Nueva Italia region of central Mexican arc, Geol. Soc., Amer. Bull., v. 123, p. 274-294.

Petronille M., Goguitchaichvili A., Henry B., Alva-Valdivia L. M., Rosas-Elguera J., Urrutia-Fucugauchi J., Rodriguez Ceja M., y Calvo-Rathert M., 2005, Paleomagnetic of Ar-Ar dated lava flows from the Ceboruco-San Pedro volcanic field (western Mexico): Evidence for the Matuyama-Brunhes transition precursor and a fully reversed geomagnetic even in the Brunhes chron, J. Geophys. Res., v. 110, no. B08101.

Pétronille M., Goguitchaichvili A., Morales J., Carvallo C., Hueda-Tanabe Y., 2012, Absolute geomagnetic intensity determinations on Formative potsherds (1400-700 B.C.) from the Oaxaca Valley, Southwestern Mexico, Quaternary Research, v.. 78, p. 442-453.

Pavón-Carrasco F. J., Osete M. L., Miquel T. J., and De Santis A., 2014, A geomagnetic field model for the Holocene based on archaeomagnetic and lava flow data. Earth and Planetary Science Letters, v. 388, p. 98-109.

Romero-Hernández E., 2008, Fechamientos Arqueomagnéticos de pisos con control estratigrafíco de la excavación Teopancazco 2005, Teotihuacán. Tesis Licenciatura Física, Fac., de Ciencias, UNAM, México, p. 51.

Ruiz-Martínez V.C., Urrutia-Fucugauchi J., y Osete M.L., 2010, Paleomagnetism of the Western and Central sectors of the Trasn-Mexican volcanic belt-implications for tectonics rotations and palaeosecular variation in the past 11 Ma, Geophysical Journal International, v. 180, p. 577-595.

Saavedra-Cortes S. P., 2010, Estudio arqueomagnético en el área de Tecamac, Estado de México, Tesis Licenciatura Física. Fac., Ciencias, UNAM, México, p. 85.

Sánchez F., 2005, Nuevos fechamientos arqueomagnéticos en Xalla y Teopancazco, zonas habitacionales de Teotihuacán. Tesis Licenciatura Física, Fac. Ciencias, UNAM, México, p. 90.

Steele, W. K., 1971, Paleomagnetic directions from the Iztaccihuatl volcano, Mexico, Earth and Planetary Science Letters, v. 11, p. 211-218.

Steele, W. K., 1985, Paleomagnetic constraints on the volcanic history of iztaccihuatl, Geofísica Internacional, v. 24, no. 1,

Tema E., y Kondopolou D., 2011, Secular variation of the Earths's magnetic field in the Balkan region during the last eigth millennia based on archaeomagnetic data, Geophys. J. Int, v. 186, p. 603-614,

Thellier E., and Thellier O., 1959, Sur L'intensité du champ magnétic terrestre dans le paseé historique et géolique. Ann. Géophysique., v. 15, p. 285-376.

Urrutia J., Maupome L., Brosche P., 1981, Archaeomagnetic research programme, I. An introduction to the knowledge of magnetism in pre-Columbian Mesoamerica. Int. Rep., Inst. Geofis., UNAM, México y Obs. Hoher List der Univ. Sternwarte, Bonn, Germany, p. 25.

Urrutia J., Maupome L., Brosche P., 1986, El compás magnético en China y Mesoamérica, Bol. GEOS, v. 6, no. 3, p. 5-7.

Van Helden A., and Burr E., 1995, Gellibrand, Henry, The Galileo Project, *Rice University, http://galileo.rice.edu/Catalog/NewFiles/gelibrnd.html.*

Wolfman, D., 1990, Mesoamerica chronology and archeomagnetic dating, AD 1-1200. Archaeomagnetic dating Eghmy, J. L. And R. S., Sternberg editors, University of Arizona Press, Tucson.